The quantum-jump approach to dissipative dynamics in quantum optics

M. B. Plenio and P. L. Knight

Optics Section, Blackett Laboratory, Imperial College, London SW7 2BZ, United Kingdom

Dissipation, the irreversible loss of energy and coherence, from a microsystem is the result of coupling to a much larger macrosystem (or reservoir) that is so large that one has no chance of keeping track of all of its degrees of freedom. The microsystem evolution is then described by tracing over the reservoir states, which results in an irreversible decay as excitation leaks out of the initially excited microsystems into the outer reservoir environment. Earlier treatments of this dissipation used density matrices to describe an ensemble of microsystems, either in the Schrödinger picture with master equations, or in the Heisenberg picture with Langevin equations. The development of experimental techniques to study single quantum systems (for example, single trapped ions, or cavity-radiation-field modes) has stimulated the construction of theoretical methods to describe individual realizations conditioned on a particular observation record of the decay channel. These methods, variously described as quantum-jump, Monte Carlo wave function, and quantum-trajectory methods, are the subject of this review article. We discuss their derivation, apply them to a number of current problems in quantum optics, and relate them to ensemble descriptions. [S0034-6861(98)00601-1]

CONTENTS

I. INTRODUCTION

Quantum mechanics is usually introduced as a theory of ensembles. However, the invention of ion traps, for example, offers the possibility to observe and manipulate single particles, where the observability of quantum jumps, which are not directly observable in the ensemble, lead to conceptual problems of how to describe single realizations of these systems. Usually Bloch equations or Einstein rate equations are used to describe the time evolution of ensembles of atoms or ions driven by light. New approaches via conditional time evolution, given say when no photon has been emitted, have been developed to describe single experimental realizations of quantum systems. This leads to a description of the system via wave functions instead of density matrices. This conditional ''quantum trajectory'' approach is still an ensemble description, but only for a subensemble where we know when photons have been emitted.

The jumps that occur in this description can be considered as due to the increase of our knowledge of the system represented by the wave function (or the density operator) describing the system. In the formalism presented in this review, it is assumed that the gedanken measurements are performed in rapid succession, for example, on the emitted radiation field. The result will be that either a photon has been found in the environment or that no photon has been found. A sudden change in our information about the radiation field (for example, through the detection of a photon emitted by the system into the environment) leads to a sudden change of the wave function of the system. However, not only does the detection of a photon lead to an increase of information, but the failure to detect a photon does as well. From these experiments, new insights have been obtained into atomic dynamics and dissipative processes, and new powerful theoretical approaches have been developed. Apart from the new insights into physics, these methods also allow the simulation of complicated problems, e.g., in laser cooling, that were completely intractable using the master-equation approach. In general they can be applied to all master equations that are of Lindblad form, which is in fact the most general form of a master equation.

This article reviews the various quantum-jump approaches developed over the past few years. We focus on the theoretical description of basic dynamics and on simple instructive examples rather than the application to numerical simulation methods.

Some of the topics covered here can also be found in earlier summaries (Erber *et al.*, 1989; Cook, 1990; Mølmer and Castin, 1996; Srinivas, 1996) and more recent summer school lectures (Mølmer, 1994; Zoller and Gardiner, 1995; Knight and Garraway, 1996).

II. INTERMITTENT FLUORESCENCE

Quantum mechanics is a statistical theory that makes probabilistic predictions of the behavior of ensembles (ideally an infinite number of identically prepared quantum systems) using density operators. This description was completely sufficient for the first 60 years of the existence of quantum mechanics because it was generally regarded as completely impossible to observe and manipulate single-quantum systems. For example, Schrödinger (1952) wrote

. . . we never experiment with just one electron or atom or (small) molecule. In thought experiments we sometimes assume that we do; this invariably entails ridiculous consequences. . . . . In the first place it is fair to state that we are not experimenting with single particles, any more than we can raise Ichthyosauria in the zoo.

This (rather extreme) opinion was challenged by a remarkable idea of Dehmelt, which he first made public in 1975 (Dehmelt, 1975, 1982). He considered the problem of high-precision spectroscopy, where one wants to measure the transition frequency of an optical transition as accurately as possible, e.g., by observing the resonance fluorescence from that transition as part (say) of an optical-frequency standard. However, the accuracy of such a measurement is fundamentally limited by the spectral width of the observed transition. The spectral width is due to spontaneous emission from the upper level of the transition, which leads to a finite lifetime τ of the upper level. Basic Fourier considerations then imply a spectral width of the scattered photons of the order of τ^{-1}. To obtain a precise value of the transition frequency, it would therefore be advantageous to excite a metastable transition that scatters only a few photons within the measurement time. On the other hand, one then has the problem of detecting these few photons, and this turns out to be practically impossible by direct observation. Dehmelt's proposal, however, suggests a solution to these problems, provided one would be able to observe and manipulate single ions or atoms, which became possible with the invention of single-ion traps (Paul *et al.*, 1958; Paul, 1990) (for a review, see Horvath *et al.*, 1997). We illustrate Dehmelt's idea in its original simplified rate-equation picture. It runs as follows.

Instead of observing the photons emitted on the metastable two-level system directly, he proposed using an optical double-resonance scheme as depicted in Fig. 1. One laser drives the metastable $0\leftrightarrow 2$ transition while a second strong laser saturates the strong $0\leftrightarrow 1$; the lifetime of the upper level 1 is, for example, 10^{-8} s, while that of level 2 is of the order of 1 s. If the initial state of the system is the lower state 0, then the strong laser will start to excite the system to the rapidly decaying level 1, which will then lead to the emission of a photon after a time that is usually very short (of the order of the lifetime of level 1). This emission restores the system to the lower level 0; the strong laser can start to excite the system again to level 1, which will emit a photon on the strong transition again. This procedure repeats until at some random time the laser on the weak transition manages to excite the system into its metastable state 2, where it remains shelved for a long time, until it jumps back to the ground state, either by spontaneous emission or by stimulated emission due to the laser on the $0\leftrightarrow 2$ transition. During the time the electron rests in the metastable state 2, no photons will be scattered on the strong transition, and only when the electron jumps back to state 0 can the fluorescence on the strong transition start again. Therefore, from the switching on and off of the resonance fluorescence on the strong transition (which is easily observable), we can infer the extremely rare transitions on the $0\leftrightarrow 2$ transition. Therefore we have a method to monitor rare quantum jumps (transitions) on the metastable $0\leftrightarrow 2$ transition by observation of the fluorescence from the strong $0\leftrightarrow 1$ transition.

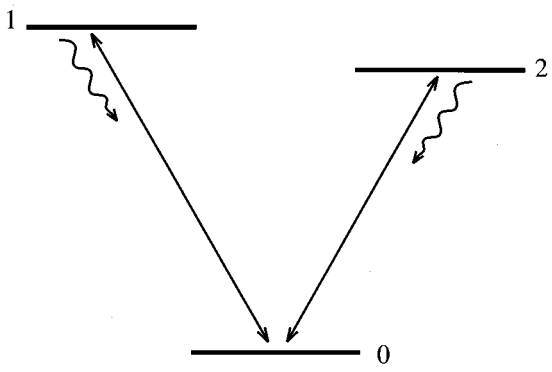

FIG. 1. The V system. Two upper levels 1 and 2 couple to a common ground state 0. The transition frequencies are assumed to be largely different so that each of the two lasers driving the system couples to only one of the transitions. The $1\leftrightarrow 0$ transition is assumed to be strong while the $2\leftrightarrow 0$ transition is weak.

A typical experimental fluorescence signal is depicted in Fig. 2 (Thompson, 1996), where the fluorescence intensity $I(t)$ is plotted. However, this scheme only works if we observe a single quantum system, because if we observe a large number of systems simultaneously, the random nature of the transitions between levels 0 and 2 implies that some systems will be able to scatter photons on the strong transition, while others will not because they are in their metastable state at that moment. From a large collection of ions observed simultaneously, one would then obtain a more or less constant intensity of photons emitted on the strong transition.

The calculation of this mean intensity is a straightforward task using standard Bloch equations. The calcula-

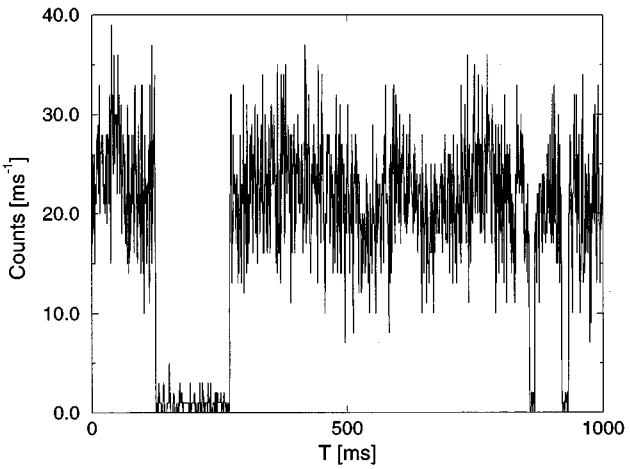

FIG. 2. Recorded resonance fluorescence signal exhibiting quantum jumps from a laser-excited $^{24}Mg^{+}$ ion (Thompson, 1996). Periods of high photon count rate are interrupted by periods with negligible count rate (except for an unavoidable dark-count rate).

tion of single-system properties, such as the distribution of the lengths of the periods of strong fluorescence, required some effort, which eventually led to the development of the quantum-jump approach. Apart from the interesting theoretical implications for the study of individual quantum systems, Dehmelt's proposal obviously has important practical applications. An often-cited example is the realization of a new time standard using a single atom in a trap. The key idea here is to use either the instantaneous intensity or the photon statistics of the emitted radiation on the strong transition (the statistics of the bright and dark periods) to stabilize the frequency of the laser on the weak transition. This is possible because the photon statistics of the strong radiation depends on the detuning of the laser on the weak transition (Kim, 1987; Kim and Knight, 1987; Kim *et al.*, 1987; Ligare, 1988; Wilser, 1991). Therefore a change in the statistics of bright and dark periods indicates that the frequency of the weak laser has shifted and has to be adjusted. However, for continuously radiating lasers this frequency shift will also depend on the intensity of the laser on the strong transition. Therefore, in practice, pulsed schemes are preferable for frequency standards (Arecchi *et al.*, 1986; Bergquist *et al.*, 1994).

Due to the inability of experimentalists to store, manipulate, and observe single-quantum systems (ions) at the time of Dehmelt's proposal, both the practical and the theoretical implications of his proposal were not immediately investigated. It was about ten years later that this situation changed. At that time Cook and Kimble (1985) made the first attempt to analyze the situation described above theoretically. Their advance was stimulated by the fact that by that time it had become possible to actually store single ions in an ion trap (Paul trap; Paul *et al.*, 1958; Neuhauser *et al.*, 1980; Paul, 1990).

In their simplified rate-equation approach Cook and Kimble started with the rate equations for an incoherently driven three-level system as shown in Fig. 1 and assumed that the strong $0\leftrightarrow1$ transition is driven to saturation. They consequently simplify their rate equations, introducing the probabilities P_+ of being in the metastable state and P_- of being in the strongly fluorescing $0\leftrightarrow1$ transition. This simplification now allows the description of the resonance fluorescence to be reduced to that of a two-state random telegraph process. Either the atomic population is in the levels 0 and 1, and therefore the ion is strongly radiating (on), or the population rests in the metastable level 2, and no fluorescence is observed (off). They then proceed to calculate the distributions for the lengths of bright and dark periods and find that their distribution is Poissonian. Their analysis, which we have outlined very briefly here, is of course very much simplified in many respects. The most important point is certainly the fact that Cook and Kimble assume incoherent driving and therefore adopt a rate-equation model. In a real experiment coherent radiation from lasers is used. The complications arising in coherent excitation finally led to the development of the quantum-jump approach. Despite these problems, the analysis of Cook and Kimble showed the possibility of direct observation of quantum jumps in the fluorescence of single ions, a prediction that was confirmed shortly afterwards in a number of experiments (Bergquist *et al.*, 1986; Nagourney *et al.*, 1986a, 1986b; Sauter *et al.*, 1986a, 1986b; Dehmelt, 1987) and triggered a large number of more detailed investigations, starting with early works by Javanainen (1986a, 1986b, 1986c). The subsequent effort of a great number of physicists eventually culminated in the development of the quantum-jump approach. Before we present this development in greater detail, we should like to study in slightly more detail how the dynamics of the system determines the statistics of bright and dark periods. Again assume a three-level system as shown in Fig. 1. Provided the $0\leftrightarrow1$ and $0\leftrightarrow2$ Rabi frequencies are small compared with the decay rates, one finds for the population in the strongly fluorescing level 1 as a function of time something like the behavior shown in Fig. 3 (we derive this in detail in a later section). We choose for this figure the values $\gamma_1 \gg \gamma_2$ for the Einstein coefficients of levels 1 and 2, which reflects the metastability of level 2. For times short compared with the metastable lifetime γ_2^{-1}, the atomic dynamics can hardly be aware of level 2 and evolve as a 0–1 *two-level* system with the "steady-state" population $\overline{\rho}_{11}$ of the upper level. After a time γ_2^{-1}, the metastable state has an effect, and the (ensemble-averaged) population in level 1 reduces to the appropriate *three-level* equilibrium values. The "hump" $\Delta\rho_{11}$ shown in Fig. 3 is actually a signature of the telegraphic fluorescence discussed above. To show this, consider a few sequences of bright and dark periods in the telegraph signal as shown in Fig. 4. The total rate of emission R is proportional to the rate in a bright period times the fraction of the evolution made up of bright periods. This gives

$$R=\gamma_1\overline{\rho}_{11}\left(\frac{T_L}{T_L+T_D}\right), \tag{1}$$

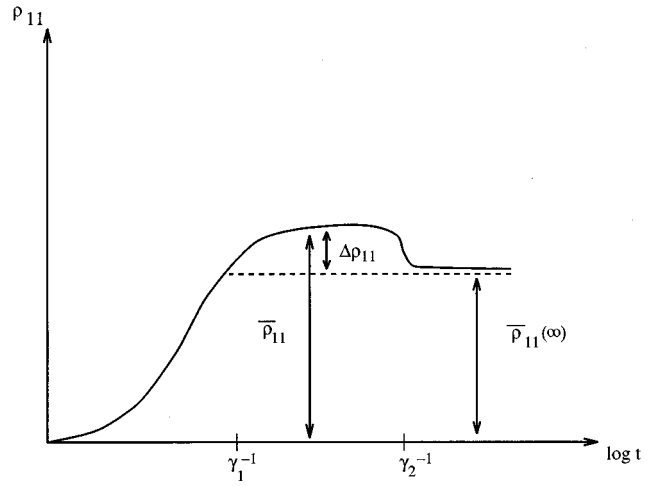

FIG. 3. Time evolution of the population in the strongly fluorescing level 1 of the three-level ion shown in Fig. 1. The lifetimes γ_1^{-1} and γ_2^{-1} are marked on the time axis. What is crucial here is the "hump" $\Delta\rho_{11}$: this is a signature of the telegraphic nature of the fluorescence.

but this has to be equal to the true average,

$$R=\gamma_1\rho_{11}(\infty)\ , \tag{2}$$

so that

$$\frac{T_D}{T_L}=\frac{\overline{\rho_{11}}-\rho_{11}(\infty)}{\rho_{11}(\infty)}=\frac{\Delta\rho_{11}}{\rho_{11}(\infty)}, \tag{3}$$

and the ratio of the period of bright to dark intervals is governed, as we claimed, by the "hump" $\Delta\rho_{11}$.

So far we have concentrated on situations where the Rabi frequencies are small (or for incoherent excitation). What happens for coherent resonant excitation with larger Rabi frequencies? The answer to this question is nothing (Knight *et al.*, 1986): there are essentially no quantum jumps, at least at any significant level, for coherently-driven resonantly excited three-level systems! But this is because the idea of resonance is tricky: the strong Rabi frequency on the $0\leftrightarrow1$ transition dresses the atom, and the ac Stark effect splits the transition (Autler and Towne, 1955; Knight and Milonni, 1980), forcing the system substantially out of resonance. If this is recognized and the probe laser driving the $0\leftrightarrow2$ transition is detuned from the bare resonance until it matches the dressed-atom resonance, then the jumps and telegraphic fluorescence return. We investigate this phenomenon more closely in Sec. V. As far as we know, the dependence of the telegraph fluorescence on detuning for coherently excited transitions has yet to be confirmed experimentally.

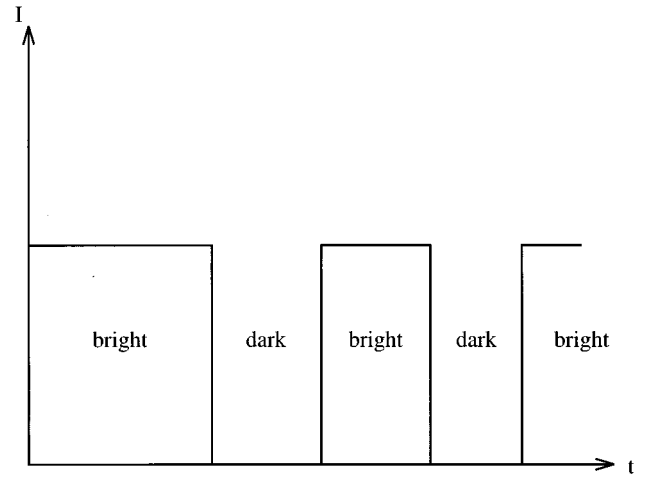

FIG. 4. A few periods of bright and dark sequences in the fluorescence intensity I from a three-level system. The bright periods last on average T_L and the dark periods T_D.

Let us return to the idea of a null measurement. We imagine that we observe the fluorescence from a driven three-level ion over a time scale that is long compared with the strongly fluorescing state lifetime γ_1^{-1} but very short compared with the shelf-state lifetime γ_2^{-1}, so that $\gamma_1^{-1}\ll\Delta t\ll\gamma_2^{-1}$. Pegg and Knight (1988a, 1988b) have shown that the average period of brightness and darkness in the telegraphic fluorescence can be obtained very straightforwardly from considerations of null detection. During such an interval Δt, the population in the shelf state $P_2(t)$ hardly has time to evolve, but population can be rapidly cycled from the ground state $|0\rangle$ to the strongly fluorescing state $|1\rangle$ and back. Detection of a photon at the beginning of a Δt interval implies a survival in the 0–1 sector for the whole interval and a bright period, whereas a null detection is sufficient for us to be confident that the atom is shelved for the whole Δt interval and a dark period ensues.

If we take our origin of time to be after an interval Δt in which we see a photon, then $P_2(0)=0$. We can introduce the "life expectancy" T_L as the time the atom spends in the 0–1 sector continuously. If the atom is still in this sector at a time t_1 (known from an observation of another fluorescence photon just prior to t_1), then the life expectancy will also be T_L. So we can partition the outcomes into the case in which at t_1 it has survived in the 0–1 sector with probability $P_{10}(t_1)$, and the case in which the ion did not survive the whole interval t_1 continuously in the 0–1 sector (Pegg and Knight, 1988a, 1988b)

$$T_L=P_{10}(t_1)(t_1+T_L)+[1-P_{10}(t_1)]ft_1, \tag{4}$$

where f is a fraction (<1). Then for small t_1

$$T_L=\frac{t_1P_{10}(t_1)}{1-P_{10}(t_1)}=\frac{t_1}{1-P_{10}(t_1)}-t_1, \tag{5}$$

and if t_1 is small so we may neglect the possibility of a *return* from state $|2\rangle$ back in to the 0–1 sector, $[1-P_{10}(t_1)]\approx P_2(t_1)$, so that

$$T_L^{-1}=\left.\frac{dP_2}{dt}\right|_{t=0}, \quad \text{given } P_2(0)=0\,. \tag{6}$$

This is finite, so we know that the fluorescence will terminate. To obtain a value for T_L, we merely need to know the evolution equation (not its solution) for the

population in state $|2\rangle$: this would be the Bloch equation for coherent excitation or the Einstein rate equation for incoherent excitation.

The calculation of the mean period of darkness proceeds along similar lines: if no photons are detected in an interval Δt just before $t=0$, we find

$$T_D^{-1}=-\left.\frac{dP_2}{dt}\right|_{t=0}, \quad \text{given } P_2(0)=1 . \tag{7}$$

The analysis presented here obviously also applies for the density-operator equations in exactly the same form, and we obtain

$$T_L^{-1}=(\dot{\rho}_{22})_{t=0} \quad \text{with } \rho_{22}(0)=0, \tag{8}$$

$$T_D^{-1}=-(\dot{\rho}_{22})_{t=0} \quad \text{with } \rho_{22}(0)=1. \tag{9}$$

Here the dot means the *average* gradient of the ρ_{22} versus t curve over a range of order Δt. Because Δt is much smaller than the characteristic change of ρ_{22}, it is very close to the normal derivative at all points.

It is straightforward to use this idea of "collapse by nondetection" to estimate the characteristic time needed to be sure that a quantum jump has occurred (Pegg and Knight, 1988b). There are T_L/t_d times as many short dark periods between photon emissions as there are prolonged dark periods of average length T_D, where t_d ($\approx\gamma_1^{-1}$ for strong transition saturation) is the average length of the short period. Thus the probability that an emission will be followed by a long dark period is approximately t_d/T_L for $T_L \gg t_d$, and the probability that it will be followed by a short dark period is close to unity.

Immediately following a photon emission, a dark period of length at least τ (with $\tau<T_D$) can exist for two complementary reasons: (a) the atom goes to state $|2\rangle$ and therefore does not decay for a time of the order of T_D, or (b) the atom is still in the $|0\rangle\leftrightarrow|1\rangle$ plane but has not yet emitted a photon. The probability of (a) occurring is t_d/T_L and the probability of (b) is approximately $\exp(-\tau/t_d)$. Clearly for $\tau<t_d$ it is much more likely that any observed dark period of length τ is due to (b), but this becomes rapidly less likely as τ increases. The point at which the observation of the dark period is just as likely to involve (a) as (b) is found by equating the two expressions to give

$$\frac{\tau}{T_L}=\frac{t_d}{T_L}\ln(T_L/t_d). \tag{10}$$

It follows that the sampling period Δt must be greater than the τ given by Eq. (10) in order for the observation of darkness during Δt to imply (a) with reasonable certainty.

Further, because we know that immediately following the emission the atom is in $|0\rangle$, the probability of its being in $|2\rangle$ is zero, and because Eq. (10) gives the order of the time of darkness required for the probability of being in $|2\rangle$ to grow to about $\frac{1}{2}$, Eq. (10) gives the characteristic time for the wave-function collapse by nondetection. This characteristic time can be associated with the time necessary for us to be certain that a quantum jump from $|0\rangle$ to $|2\rangle$ has occurred. For completely coherent excitation, Eq. (10) reduces to an expression similar to that for the shelving time found by Porrati and Puterman (1987) and Zoller *et al.* (1987). Note that, while the collapse by nondetection of the system into the metastable state requires a finite time, the collapse of the wave function due to the detection of a photon has to be viewed as practically instantaneous. When we detect a photon our knowledge of the system changes suddenly, and this sudden change of knowledge is reflected by the sudden change of the system state, which, after all, represents our knowledge of the system.

III. ENSEMBLES AND SHELVING

Before we develop detailed theoretical models to describe individual quantum trajectories (i.e., state evolution conditioned on a particular sequence of observed events), it is useful to examine how the entire ensemble evolves. This is in line with the historical development, as initially investigators tried to find quantum-jump characteristics in the ensemble behavior of the system. We do this in detail for the particular three-level V configuration (shown in Fig. 1) appropriate for Dehmelt's quantum-jump phenomena. For simplicity, we examine the case of incoherent excitation. Studies for coherent excitation using Bloch equations can be found, for example, in other publications (Kimble *et al.*, 1986; Schenzle and Brewer, 1986; Kim, 1987; Nienhuis, 1987; Ligare, 1988). The Einstein rate equations for the V system are (Pegg *et al.*, 1986b)

$$\frac{d}{dt}\rho_{11}=-(A_1+B_1W_1)\rho_{11}+B_1W_1\rho_{00}, \tag{11}$$

$$\frac{d}{dt}\rho_{22}=-(A_2+B_2W_2)\rho_{22}+B_2W_2\rho_{00}, \tag{12}$$

$$\frac{d}{dt}\rho_{00}=-(B_1W_1+B_2W_2)\rho_{00}+(A_1+B_1W_1)\rho_{11}+(A_2+B_2W_2)\rho_{22}, \tag{13}$$

where A_i, B_i are the Einstein A and B coefficients for the relevant spontaneous and induced transitions, W_i the applied radiation-field energy density at the relevant transition frequency, and ρ_{ii} is the relative population in state i ($\rho_{00}+\rho_{11}+\rho_{22}=1$ for this closed system). In shelving, we assume that both B_1W_1 and A_1 are much larger than B_2W_2 and A_2 and furthermore that $B_2W_2 \gg A_2$. The steady-state solutions of these rate equations are straightforward to obtain, and we find

$$\rho_{11}(t\to\infty)=\frac{B_1W_1(A_2+B_2W_2)}{A_1(A_2+2B_2W_2)+B_1W_1(2A_2+3B_2W_2)}, \tag{14}$$

$$\rho_{22}(t\to\infty)=\frac{B_2W_2(A_1+B_1W_1)}{A_1(A_2+2B_2W_2)+B_1W_1(2A_2+3B_2W_2)}. \tag{15}$$

Now, if the allowed $0\leftrightarrow 1$ transition is saturated,

$$\rho_{00}(t\to\infty)\approx\rho_{11}(t\to\infty)\,\frac{A_2+B_2W_2}{2A_2+3B_2W_2}\approx\frac{1}{3} \tag{16}$$

and

$$\rho_{22}(t\to\infty)\approx\frac{B_2W_2}{2A_2+3B_2W_2}\approx\frac{1}{3}. \tag{17}$$

Now we see that a small B_2W_2 transition rate to the shelf state has a major effect on the dynamics. Note that if the induced rates are much larger than the spontaneous rates, the steady-state populations are $\rho_{00}=\rho_{11}=\rho_{22}=\frac{1}{3}$: the populations are evenly distributed amongst the constituent states of the transition.

However, the dynamics reveal a different story from that suggested by the steady-state populations. Again, if the allowed transition is saturated, then the time-dependent solutions of the excited-state rate equations tell us that for $\rho_{00}(0)=1$ we have

$$\rho_{11}(t)=\frac{B_2W_2}{2(2A_2+3B_2W_2)}e^{-(A_2+3B_2W_2/2)t}-\frac{1}{2}e^{-(2B_1W_1+A_1+B_2W_2/2)t}+\frac{A_2+B_2W_2}{2A_2+3B_2W_2}, \tag{18}$$

and

$$\rho_{22}(t)=\frac{B_2W_2}{2A_2+3B_2W_2}\{1-e^{-(A_2+3B_2W_2/2)t}\}. \tag{19}$$

Note that these expressions are good only for strong driving of the $0\leftrightarrow 1$ transition. This especially means that for short times ρ_{00} is of the order of 1/2, which results in Eq. (19). Then, for a very long-lived shelf state 2, we see that for saturated transitions ($B_iW_i\gg A_i$)

$$\rho_{11}(t)\approx\frac{1}{3}\left\{1+\frac{1}{2}(e^{-3B_2W_2t/2}-3e^{-2B_1W_1t})\right\} \tag{20}$$

and

$$\rho_{22}(t)\approx\frac{1}{3}\{1-e^{-3B_2W_2t/2}\}. \tag{21}$$

These innocuous-looking expressions contain a lot of physics. We remember that state 1 is the strongly fluorescing state. On a time scale that is short compared with $(B_2W_2)^{-1}$, we see that the populations attain a quasisteady state appropriate to the two-level ($0\leftrightarrow 1$) dynamics,

$$\rho_{11}(t\ \text{ short})\sim\frac{1}{2}\{1-e^{-2B_1W_1t}\}\to\frac{1}{2}. \tag{22}$$

This can of course be confirmed in an experiment (Finn *et al.*, 1986; 1989). For truly long times the third, shelving state makes its effect, and

$$\rho_{11}(t\ \text{ long})\sim\frac{1}{3}, \tag{23}$$

as we saw qualitatively in Fig. 3. As we saw earlier in the discussion of Eq. (3), the change from two-level to three-level dynamics already gives us a signature of quantum jumps and telegraphic fluorescence, provided we are wise enough to recognize the signs. Figure 3 illustrates the change from two- to three-level dynamics.

The steady-state populations are sufficient to describe the average level of the fluorescent intensity. But how do quantum jumps and shelving show up in the intensity correlations? For example, let us examine the second-order correlation function

$$g^{(2)}(t,\tau)=\frac{\langle{:}I(t+\tau)I(t){:}\rangle}{\langle I(t)\rangle^2}, \tag{24}$$

where the colons describe normal ordering (Loudon, 1983). This correlation function is straightforward to compute from the Einstein rate equations using the quantum regression theorem (Lax, 1963), which relates one-time to two-time correlations, given that the dynamics are Markovian. Here of course there are two intensities, that of the $1\to 0$ and of the $2\to 0$ fluorescence. We can then correlate the two light fields: "1" with "1" or "1" with "2" and so on, where "1" and "2" represent the fluorescence on the $1\to 0$ and the $2\to 0$ transitions, respectively. So let us concentrate on evaluating $g_{ij}^{(2)}\times(t,\tau)$, which represents the joint probability of detecting a fluorescent photon j ($j=1,2$) on the transition j at time t and some other photon (not necessarily the next photon) from transition i at time $(t+\tau)$. It is straightforward to show (Pegg *et al.*, 1986b) that

$$g_{11}^{(2)}(\tau)=g_{12}^{(2)}(\tau)=1+\frac{B_2W_2}{2(A_2+B_2W_2)}e^{-(A_2+3B_2W_2/2)\tau}-\frac{2A_2+3B_2W_2}{2(A_2+B_2W_2)}e^{-(2B_1W_1+A_1+B_2W_2/2)\tau}, \tag{25}$$

and

$$g_{22}^{(2)}(\tau)=g_{21}^{(2)}(\tau)=1-e^{-(A_2+3B_2W_2/2)\tau}. \tag{26}$$

Using $B_1W_1\gg B_2W_2$ and that the transitions are saturated, we find that these correlation functions simplify to give

$$g_{11}^{(2)}(\tau)=g_{12}^{(2)}(\tau)=1+\frac{1}{2}(e^{-3B_2W_2\tau/2}-3e^{-2B_1W_1\tau}), \tag{27}$$

so that, as expected, the correlation functions obey the same evolutions as the populations. It is worth noting that for short times τ we expect to see antibunching (Loudon, 1983) from this three-level fluorescence, and this has been observed experimentally from trapped ions (Itano *et al.*, 1988; Schubert *et al.*, 1992).

In the mid 1980s, when studies of quantum-jump dynamics of laser-driven three-level atoms began in earnest, a great deal of effort was expended in determining the relationship between joint probabilities of detection of a photon at time t and the next or any photon a time τ later. This was addressed in detail by Cohen-Tannoudji and Dalibard (1986; Reynaud *et al.*, 1988), by Schenzle and Brewer (1986; Schenzle *et al.*, 1986), and others (Cook, 1981; Lenstra, 1982). One attractive approach, advocated by Cohen-Tannoudji and Dalibard, uses a

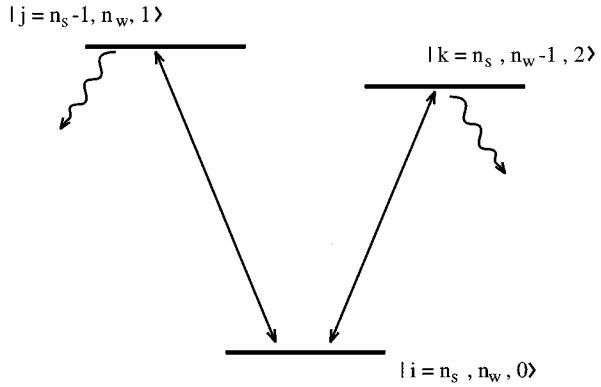

FIG. 5. Atom+field states used to describe the survival of a three-level system in an undecayed state. The numbers n_s,n_w specify photon numbers driving the strongly allowed transitions $0\leftrightarrow 1$ and the weak transition $0\leftrightarrow 2$. Note that fluorescence takes the system out of the three atom+field states.

dressed manifold and from this evaluates the delay function describing the distribution of delay times before the next emission occurs. In Fig. 5 that laser excitation couples together these atom+field states, but fluorescence does not: spontaneous emission is an irreversible loss out of this manifold to states with reduced photon number in the excitation modes, but with photons created in initially unoccupied free-space modes.

We expand our atom+field state vector into the basis states $|l\rangle$ with fixed number of fluorescence photons in the radiation field as shown in Fig. 5 as

$$|\psi(t)\rangle=\sum_l a_l(t)e^{-iE_l t/\hbar}|l\rangle, \tag{28}$$

and solve for the probability amplitudes $a_l(t)$. The probability of remaining without further emission in the n-excitation atom+field manifold up to time τ is

$$P_0(\tau)=\sum_i |a_i(\tau)|^2. \tag{29}$$

The negative differential of this survival probability describes the *delay function* (Cohen-Tannoudji and Dalibard, 1986)

$$I_1(\tau)\equiv -\frac{dP_0}{d\tau}, \tag{30}$$

so that the probability of there being an interval τ between one photon's being emitted (detected) and the next is

$$P_0(\tau)=1-\int_0^\tau I_1(\tau')d\tau'. \tag{31}$$

To evaluate this interval distribution function it is sufficient to calculate the atom+field dressed-state amplitudes. This demonstrates the utility of this approach: there is no need to solve the potentially complicated Bloch equations for the driven three-level atom, although of course this can be done (Schenzle and Brewer, 1986). Kim and co-workers (Kim and Knight, 1987; Kim *et al.*, 1987), Grochmalicki and Lewenstein (1989a), Wilser (1991), and later others have used the delay function to describe shelving in the V system. The conditional probability of an atom's emitting any photon between time τ and $\tau+d\tau$ after emitting a photon at time $\tau=0$ is $I(\tau)d\tau$. The photon emitted at time τ can be the first to be emitted after that at $\tau=0$ or the next after any one at time τ' $(0<\tau'<\tau)$, so that

$$I(\tau)=I_1(\tau)+\int_0^\tau d\tau' I(\tau')I_1(\tau-\tau'), \tag{32}$$

where $I_1(\tau)$ is the interval distribution. If this is expressed in terms of its Laplace transform $\tilde{I}(z)$, then

$$\tilde{I}(z)=\frac{\tilde{I}_1(z)}{1-\tilde{I}_1(z)}. \tag{33}$$

The function $g^{(2)}(\tau)$ is the normalized correlation function for a photon detection at $\tau=0$ followed by the detection of any photon (not necessarily the next) at time τ. It follows that

$$g^{(2)}(\tau)=\frac{I(\tau)}{I(\tau\rightarrow\infty)}, \tag{34}$$

or equivalently in Laplace space

$$\tilde{g}^{(2)}(z)=\frac{\tilde{I}(z)}{\lim\limits_{z\rightarrow 0} z\tilde{I}(z)}, \tag{35}$$

so that

$$\tilde{g}^{(2)}(z)=\left[\lim_{z\rightarrow 0}\frac{1-\tilde{I}_1(z)}{z\tilde{I}_1(z)}\right]\frac{\tilde{I}_1(z)}{1-\tilde{I}_1(z)}. \tag{36}$$

For the case of incoherent, rate-equation excitation of a three-level V-system atom, it is straightforward to calculate the atom+field survival probability, differentiate this to generate the delay function, and then from Eq. (36) deduce $g^{(2)}(\tau)$. If this is done, precisely the same form is obtained as that from the quantum regression theorem. The merit of this approach is easier to appreciate for the case of coherent excitation, where the regression theorem requires the solution of the three-level Bloch equations and the solution of eighth-order polynomial characteristic equations, compared with the need to solve three coupled equations when using the delay-function route. In Sec. V we further illustrate the connection between the next-photon probability density and the any-photon rate in Eqs. (182)–(193).

Rather than examine the correlation functions, it may be useful to examine other properties of the photon statistics and in particular the variance in the photon numbers in the detected fluorescence (Kim, 1987; Kim and Knight, 1987; Kim *et al.*, 1987; Jayarao *et al.*, 1990). For a Poissonian field $(\Delta n)^2=\langle n\rangle$, but for a sub-Poissonian field $(\Delta n)^2<\langle n\rangle$, and for a super-Poissonian field $(\Delta n)^2>\langle n\rangle$. To characterize the deviation from pure Poissonian fluctuations, Mandel (1979) defined the parameter

$$Q_M(\tau)\equiv\frac{(\Delta n)^2-\langle n\rangle}{\langle n\rangle}, \tag{37}$$

which can be written in terms of the mean intensity $\langle I\rangle$ and the second-order correlation function $g^{(2)}(t)$ as

$$Q_M(\tau)=\frac{\langle I\rangle}{\tau}\left\{\int_0^\tau dt_2\int_0^{t_2}dt_1 g^{(2)}(t_1)\right\}-\langle I\rangle\tau. \tag{38}$$

If this is used to describe the fluorescence from a three-level atom involving shelving (Kim, 1987; Kim and Knight, 1987; Kim *et al.*, 1987), then as $\tau\to\infty$ for saturated transitions,

$$Q_M(\tau\to\infty)=\frac{T_D^2}{T_L}\langle I\rangle, \tag{39}$$

where T_L and T_D are the mean times of bright and dark periods in the telegraphic fluorescence signal from the three-level atom shown in Fig. 1. If a dark period does not occur, $Q_M(\tau\to\infty)\to 0$, whereas, the larger T_D becomes, the larger the Mandel parameter becomes, reflecting the large fluctuations implicit in jumps from dark to bright periods. These macroscopic fluctuations are manifested in the photon-counting distributions studied in detail by Schenzle and Brewer (1986) using Bloch equations. They showed that the count distribution of photons detected from the strongly allowed transition were Poissonian except for an excess of zero counts. In an interval T of the order of the lifetime of the shelving state one either counts a large number of photons (a bright period) or one counts nothing (a dark period). The probability of counting n photons in time T is Poissonian except again for an excess of zeros (Schenzle and Brewer, 1986) and is evaluated from the Mandel counting formula [or its quantum equivalent derived by Kelley and Kleiner (1964)],

$$W(n,T)=\frac{1}{n!}\left(\frac{\gamma_1\eta T}{2}\right)^n e^{-\gamma_1\eta T/2}, \tag{40}$$

except for $n=0$. Here γ_1 is the decay rate of the strongly fluorescing state and η is the detector efficiency. So in an interval $T\sim\gamma_2^{-1}$, where γ_2^{-1} is the lifetime of the shelving state, we count either $n\sim\frac{1}{2}\gamma_1\eta\gamma_2^{-1}\approx 10^8$ for typical transitions, or we find $n=0$. Note we essentially do not see $n=1,2,3,\ldots$ as $W(n=1,T=\gamma_2^{-1})\sim 10^8 e^{-10^8}\cong 0$, as shown in Fig. 6. Schenzle and Brewer (1986) interpret these macroscopic intensity fluctuations in terms of quantum jumps. Imagine the fluorescent intensity to be jumping from dark (off) states to bright (on) states with probability distribution

$$P(I)=A\,\delta(I)+(1-A)\,\delta(I-I_0); \tag{41}$$

then we find for the probability of counting n photons in a time T

$$W(n,T)=A\,\delta_{n,0}+(1-A)\frac{(HI_0T)^n}{n!}e^{-HI_0T}, \tag{42}$$

where H is the counting efficiency. The zero count is $W(n=0,T)=A\cong 1/3$ for saturated transitions. The behavior of Eq. (42) is schematically shown in Fig. 6, where we see the excess probability for no counts (dark period) together with a high probability for a large number of jumps (bright period).

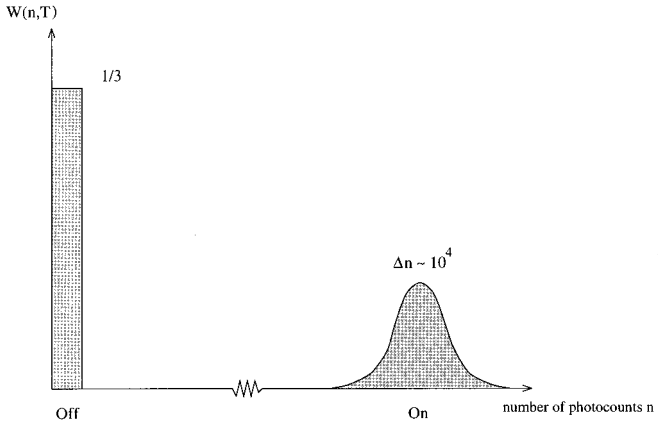

FIG. 6. Macroscopic photocount fluctuations revealed in photocount distribution $W(n,T)$ of counts of the allowed $0\leftrightarrow 1$ transition fluorescence from a saturated V configuration. One either registers a large number of counts in the time interval $[0,T]$ (On), which is a sign of a bright period, or one registers no counts at all (Off), which shows that one is in a dark period. After Schenzle and Brewer (1986).

In the past two sections we have discussed the initial attempts toward a theoretical description of single-ion resonance fluorescence. However, these attempts did not yield a satisfying approach to the problem, as the single-system properties described, e.g., by the delay function, were deduced from equations of motion describing the whole ensemble. In the next section we shall explain and summarize a number of methods using the quantum-jump approach, which allows the most natural description of many properties of resonance fluorescence and time evolution of single-quantum systems.

IV. DISCUSSION OF DIFFERENT DERIVATIONS OF THE QUANTUM-JUMP APPROACH

A. Quantum jumps

Prior to the development of quantum-jump methods, all investigations of photon statistics started out from the ensemble description via optical Bloch equations or rate equations as presented above, which were used to calculate nonexclusive "probability densities" for the emission of one or several photons at time $t_1,\ldots,t_n$ in the time interval $[0,t]$. It is important to note that only the probability of emission of *any* photon was asked for. Therefore many more photons might have been emitted in between the times t_i. An example of such a function, which we discussed in Sec. III, is the intensity correlation function $g^{(2)}(t)$, which gives the normalized rate at which one can expect to detect photons (any photon rather than the next) at time t when one has been found at $t=0$.

Efforts were made to use nonexclusive "probability densities" to deduce the photon statistics of the single three-level ion, and the aim was to show that a single ion exhibits bright and dark periods in its resonance fluorescence on the strong transition (Schenzle and Brewer, 1986; Pegg and Knight, 1988a). This approach is, however, not very satisfying, as it requires the solution of the full master equation and the inversion of a Laplace transformation. Furthermore, this approach is very indirect, as we first calculate the ensemble properties and then try to derive the single-particle properties. It would be much more elegant to have a method that enabled us to calculate the photon statistics of the single ion directly. This goal was discussed widely at a workshop at NORDITA in Copenhagen in December 1985, following a paper at that meeting by Javanainen (1986b), and the goal was finally realized with the development of the quantum-jump approach. Its development essentially started when Cohen-Tannoudji and Dalibard (1986), and at much the same time Zoller, Marte, and Walls (1987), derived the *exclusive* probability $P_0(t)$ that, after an emission at time $t=0$, no other photon has been emitted in the time interval $[0,t]$ (Cohen-Tannoudji and Dalibard, 1986) or the exclusive n-photon probability density $p_{[0,t]}(t|t_1,\ldots,t_n)$ that in $[0,t]$ n photons are emitted exactly at the times $t_1,\ldots,t_n$ (Zoller *et al.*, 1987), without going back to the master equation of the full ensemble. Both quantities are intimately related for two reasons: first, the probability density $I_1(t)$ for the emission of the first photon after a time t is given by

$$I_1(t)=-\frac{d}{dt}P_0(t), \tag{43}$$

and second because it turns out that the exclusive n-photon probability density essentially factorizes into next-photon probability densities $I_1(t)$

$$p_{[0,t]}(t|t_1,\ldots,t_n)=P_0(t-t_n)I_1(t_n-t_{n-1})\cdot\ldots\cdot I_1(t_1). \tag{44}$$

This factorization property was initially assumed and then justified by physical arguments by Cohen-Tannoudji and Dalibard (1986) while Zoller *et al.* (1987) calculated first the exclusive n-photon probability $p_{[0,t]}(t|t_1,\ldots,t_n)$ and subsequently its decomposition into next-photon probabilities. Before we discuss the above approaches, we point out that, although the exclusive (next photon at time t) $I_1(t)$ and nonexclusive (a photon at time t) $I(t)$ distributions are very different, they are related by a simple integral equation (Kim *et al.*, 1987). As discussed in Eq. (32) in Sec. III,

$$I(t)=I_1(t)+\int_0^t dt' I_1(t-t')I(t'), \tag{45}$$

which becomes especially simple when one considers the Laplace transform of that equation, as we have a convolution on the right-hand side of Eq. (45). This relationship enables us in principle to obtain the exclusive probability density $I_1(t)$ from the nonexclusive quantity $I(t)$. In practice, however, this is exceedingly difficult to do, as one has to know all the eigenvalues of the corresponding Bloch equations. Therefore a direct approach is needed.

1. Derivations of the quantum-jump approach

The idea put forward by Zoller *et al.* (1987) was not to calculate the complete density operator ρ irrespective of the number of photons that have been emitted, but to discriminate between density operators corresponding to different numbers of emitted photons in the quantized radiation field. The quantity of interest is therefore

$$\rho_A^{(n)}(t)=\mathrm{Tr}_F\{\mathbb{P}_n\rho(t)\}, \tag{46}$$

where $\rho(t)$ is the density operator of atom and quantized radiation field, $\mathrm{Tr}_F\{\cdot\}$ the partial trace over the modes of the quantized radiation field, and $\mathbb{P}_n$ the projection operator onto the state of the quantized radiation field that contains n photons. This method of calculating the density operator for a given number of photons in the quantized radiation field was first used by Mollow (1975) to investigate the resonance fluorescence spectrum of two-level systems. However, as at that time the investigation of single ions was completely beyond experimental capability, he did not extend his conclusions to single-quantum systems. This was only made possible later by the experimental realization of single ions in ion traps.

In the following we discuss the approach of Zoller *et al.* (1987) for the case of a three-level system in the V configuration (see Fig. 1), rather than, as in the original paper, for the two-level case. Following Mollow (1975) and Blatt *et al.* (1986) one obtains for Eq. (46) the equations of motion

$$\frac{d}{dt}\rho_A^{(0)}(t)=-i[H_{eff}\rho_A^{(0)}(t)-\rho_A^{(0)}(t)H_{eff}^\dagger], \tag{47}$$

and

$$\frac{d}{dt}\rho_A^{(n)}(t)=-i(H_{eff}\rho_A^{(n)}(t)-\rho_A^{(n)}(t)H_{eff}^\dagger)+\sum_{i=1}^{2}2\Gamma_{ii}|0\rangle\langle i|\rho_A^{(n-1)}(t)|i\rangle\langle 0|, \tag{48}$$

where the effective Hamiltonian operator H_{eff} is given by

$$H_{eff}=-\sum_{i=1}^{2}\left\{\hbar(\Delta_i+i\Gamma_{ii})|i\rangle\langle i|+\frac{\hbar\Omega_i}{2}(|0\rangle\langle i|+|i\rangle\langle 0|)\right\}, \tag{49}$$

with the detunings $\Delta_i=\widetilde{\omega}_i-\omega_{i1}$, $\widetilde{\omega}_i$ the laser frequency, Ω_i the Rabi frequency, and $2\Gamma_{ii}$ the Einstein coefficient on the $i\leftrightarrow 1$ transition. It is now important to note that the effective Hamilton operator H_{eff} is a non-Hermitian operator. The real part of $-i\,H_{eff}$ is negative, which implies that the trace of the density operator $\rho_A^{(0)}(t)$ decreases in time. This is not surprising because $\rho_A^{(0)}(t)$ describes the conditional time evolution under the assumption that no photon has been emitted into the

quantized radiation field. The probability that an excited atom has not emitted a photon decreases in time, and therefore the trace of $\rho_A^{(0)}(t)$ describing this probability should decrease in time. This decrease is necessary for the trace of the density operator $\rho(t)$, disregarding the number of emitted photons,

$$T(t,0)\rho(0)=\rho(t)=\sum_{n=0}^{\infty}\rho_A^{(n)}(t), \tag{50}$$

to be preserved under the time evolution. The equations of motion, Eqs. (47) and (48), have the solution

$$\rho_A^{(0)}(t)=S(t,t_0)\rho_A^{(0)}(t_0), \tag{51}$$

where

$$S(t,t_0)\rho_A^{(0)}(t_0)=e^{-i\,H_{eff}(t-t_0)}\rho_A^{(0)}(t_0)e^{iH_{eff}^{\dagger}(t-t_0)} \tag{52}$$

and

$$\rho_A^{(n)}(t)=\int_0^t dt' S(t,t')R\rho_A^{(n-1)}(t'), \tag{53}$$

with

$$R\rho_A^{(n)}(t)=\sum_{i=1}^{2}2\Gamma_{ii}|0\rangle\langle i|\rho_A^{(n)}(t)|i\rangle\langle 0|. \tag{54}$$

From this result it is now possible to deduce the probability that exactly n photons have been emitted in the time interval $[0,t]$. The probability that no photon has been found should then be given by

$$P_0(t)=\mathrm{Tr}_A\{S(t,0)\rho_A(0)\} \tag{55}$$

and

$$P_n(t)=\int_0^t dt_n\ldots\int_0^{t_2}dt_1\mathrm{Tr}_A\{S(t,t_n)R\cdots RS(t_1,0)\rho_A(0)\} \tag{56}$$

is the probability that exactly n photons have been emitted. Zoller, Marte, and Walls then realized that the structure of these expressions coincides with that derived from an abstract theory of continuous measurement constructed by Srinivas and Davies (Davies, 1969, 1970, 1971, 1976; Srinivas and Davies 1981, 1982). This theory supports the interpretation of

$$p_n(t_1,\ldots,t_n)=\mathrm{Tr}_A\{S(t,t_n)R\ldots RS(t_1,0)\rho_A(0)\} \tag{57}$$

as the probability density that exactly n photons have been emitted at times $t_1,\ldots,t_n$ and no photons in between. From the general theory of measurement, they interpreted the quantity

$$P_0(t_1-t_0)=\frac{\mathrm{Tr}_A\{RS(t_1,t_0)RT(t_0,0)\rho_A(0)\}}{\mathrm{Tr}_A\{RT(t_0,0)\rho_A(0)\}} \tag{58}$$

as the probability density that after an emission of a photon at time t_0 the *next* photon will be emitted at t_1. It should be stressed that, although in the work of Zoller *et al.* (1987) the super-operator $T(t,0)$ is identified with the time evolution of the ensemble, irrespective of how many photons have been emitted in $[0,t]$, for the following it should always be chosen to be the time evolution if a given number of emissions have taken place at the times $t_1,\ldots,t_n$. Assuming this [as is also implicitly done later in (Zoller *et al.*, 1987)], one obtains for the probability density that photons are emitted exactly at times $t_1,\ldots,t_n$,

$$\begin{aligned}p_{[0,t]}(t_1,\ldots,t_n)&=\mathrm{Tr}_A\{S(t,t_n)R\ldots RS(t_1,0)\rho_A(0)\},\\&=\frac{\mathrm{Tr}_A\{S(t,t_n)R\ldots RS(t_1,0)\rho_A(0)\}}{\mathrm{Tr}_A\{RS(t,t_{n-1})\ldots RS(t_1,0)\rho_A(0)\}}\cdots\frac{\mathrm{Tr}_A\{RS(t_1,0)\rho_A(0)\}}{\mathrm{Tr}_A\{\rho_A(0)\}},\\&=P_0(t,t_n)I_1(t_n,t_{n-1})\ldots I_1(t_1,0).\end{aligned} \tag{59}$$

Here we have factorized $p_{[0,t]}(t_1,\ldots,t_n)$ into products of $I_1(t_l,t_{l-1})$. In principle these functions can depend on the atomic state at time t_{l-1} (after the emission). However, in most cases this state will be the ground state of the system and will be the same after each emission. Having found that the knowledge of $P_0(t)$ is sufficient [$I_1(t)$ can be obtained via Eq. (43)], Zoller *et al.* then continue to discuss the photon statistics of the three-level V system. Their results may also be used to implement a simulation approach for the time evolution of a single three-level system (Hegerfeldt and Wilser, 1991; Dalibard *et al.*, 1992; Dum, Zoller, and Ritsch, 1992). However, the application of the quantum-jump approach in numerical simulations will be discussed later in this section.

The approach of Zoller, Marte, and Walls already reveals many features of the quantum-jump approach. However, there is a slight complication in their approach, as they rely on the abstract theory of continuous measurement of Srinivas and Davies to give interpretations to their equations (57) and (58). The reason that they need the support of the theory of Srinivas and Davies is that they never talk about the way the photons are measured. In fact only the emission of photons is mentioned and not the detection of photons. From a quantum-mechanical point of view, however, one has to be very careful, as the emission of a photon is *not* well defined. It is the detection of a photon in the radiation field which is a real event. Of course the treatment of Zoller *et al.* (1987) already implies some properties of the measurement process, e.g., they implicitly assume time-resolved photon counting. However, they gave no explicit treatment of such measurements. This problem

was addressed in greater detail by several authors, and in the following we discuss these ideas.

2. The detection and nondetection of photons

Porrati and Putterman (1989) were the first to explicitly include the result of quantum-mechanical measurements into their calculation. They, as well as others (Pegg and Knight, 1988a), noticed that the failure to detect a photon in a measurement leads to a state reduction, as information is gained through that null measurement. Essentially we can be increasingly confident that the ion is in a nonradiating state (examples of this will be shown in Sec. V). Porrati and Putterman assume that at some large time t a measurement on the whole quantized radiation field is performed. Assuming the result of this measurement is the detection of no photons, they calculate all Heisenberg operators at that time projected onto the null-photon subspace of the complete Hilbert space, i.e., operators of the form

$$(\mathbb{P}_0\hat{O}_A\mathbb{P}_0)(t). \tag{60}$$

Although not mentioned explicitly by Porrati and Putterman (1987, 1989), the calculation of this operator turns out to be closely related to the projector formalism (Nakajima, 1958; Zwanzig, 1960; Haake, 1973; Agarwal, 1974), a connection that was elaborated on by Reibold (1992). Although their approach can in principle lead to the quantum-jump method, there are some conceptual problems in the actual execution of the use of the null-measurements idea. The main problem is that Porrati and Putterman only talk about a single measurement at a large time t, performed on the complete quantized radiation field. This does not seem to be a very realistic model of measurements performed by a broadband counter, which informs us immediately whether a photon is detected. Also the calculation of the state after the detection of a photon was not elaborated on by Porrati and Putterman (1987, 1989), where it was merely stated that the system is reset back to its ground state on photodetection, which is of course a physically correct picture. These conceptual concerns to this approach were later addressed in the work of Hegerfeldt and Wilser (1991; Wilser, 1991), of Carmichael (1993a), and of Dalibard *et al.* (1992; Mølmer *et al.*, 1993; Mølmer, 1994). In the following we give a more detailed account of their approach.

We shall follow closely the presentation given by the Hegerfeldt group (Hegerfeldt and Wilser, 1991; Wilser, 1991), as it directly leads to the delay function that was also found in earlier papers (Cohen-Tannoudji and Dalibard, 1986; Zoller *et al.*, 1987). The physical ideas, however, are very similar to those presented elsewhere (Dalibard *et al.*, 1992; Mølmer *et al.*, 1993; Mølmer, 1994). We treat the same three-level system as in the discussion of Zoller *et al.* (1987).

In Hegerfeldt and Wilser (1991) and Wilser (1991) [as well as in Dalibard *et al.* (1992), Mølmer *et al.* (1993); and Mølmer (1994)], the following simple model of how the photons are detected was proposed. It was assumed that the radiating ion is surrounded by a 4π photodetector that detects photons irrespective of their frequency and that the efficiency of the detector is unity. Efficiencies less than unity may be treated in a slightly different way using the same physical ideas (Plenio, 1994; Hegerfeldt and Plenio, 1996) and leads to a natural connection between the next-photon probability density $I_1(t)$ and the any-photon rate (intensity correlation function) $g^{(2)}(t)$ (Kim *et al.*, 1987; Plenio, 1994). We shall return to this point later. As truly continuous measurements in quantum mechanics are not possible without freezing the time evolution of the system through the Zeno effect (Misra and Sudarshan, 1977; Reibold, 1993; Mahler and Weberruß, 1995), it was instead assumed that measurements are performed in rapid succession, where the time difference Δt between successive measurements should be much larger than the correlation time of the quantized radiation field. This means that

$$\Delta t \gg \omega_{10}^{-1}. \tag{61}$$

If successive measurements are more frequent than ω_{10}^{-1}, we enter the regime of the quantum Zeno effect and significantly inhibit the possibility of spontaneous emissions (Reibold, 1993). On the other hand Δt should be much smaller than all time constants of the atomic time evolution to ensure that one finds the photons one by one, so that the time evolution can be found using perturbation theory. Therefore

$$\Gamma_{ii}^{-1}, \Delta_i^{-1}, \Omega_i^{-1} \ll \Delta t. \tag{62}$$

For optical transitions it is easy to satisfy both inequalities, Eqs. (61) and (62), simultaneously.

Now the density operator at time t under the condition that no photons have been detected in all measurements that took place at time $s_1,\ldots,s_n$ has to be calculated. Although the result of each measurement was negative, in the sense that no photon was found, this still has an impact on the wave function of the system, as it represents an increase of knowledge about the system (Dicke, 1981; Porrati and Putterman, 1987; Pegg and Knight, 1988a). Using the projection operator $\mathbb{P}_0$ onto the vacuum state of the quantized radiation field and the time-evolution operator $U(t,t')$ of system and radiation field in a suitable interaction picture, we find

$$|\psi(s_n)\rangle = \mathbb{P}_0 U(s_n, s_{n-1}) \mathbb{P}_0 \ldots \mathbb{P}_0 U(s_1,0)|\psi(0)\rangle, \tag{63}$$

as, after each measurement that has failed to detect a photon, we have to project the quantized radiation field onto the vacuum state according to the von Neumann-Lüders postulate (Lüders, 1951; von Neumann, 1955). As $s_j - s_{j-1}$ obeys Eqs. (61) and (62), it is possible to calculate the time-evolution operator $U(s_j, s_{j-1})$ in second-order perturbation theory to obtain

$$\mathbb{P}_0 U(s_j, s_{j-1}) \mathbb{P}_0 \approx \left(1 - \frac{i}{\hbar} H_{eff}(s_{i-1})(s_i - s_{i-1})\right)\mathbb{P}_0 \tag{64}$$

with the effective Hamiltonian operator given by Eq. (49). In the quantum-jump method presented by Dalibard *et al.* (1992), Mølmer *et al.* (1993), and Mølmer (1994) the Weisskopf-Wigner approach (Weisskopf and

Wigner, 1930) was used to find a formula equivalent to Eq. (64). Inserting this equation into Eq. (63) and changing from a coarse-grained time scale to a continuous one, we obtain for the atomic part of the wave function (the radiation field is in its vacuum state), where no photons have been detected in all measurements in the interval $[0,t]$,

$$|\psi_A^{(0)}(t)\rangle = e^{-iH_{eff}t/\hbar}|\psi_A(0)\rangle. \tag{65}$$

One should note that the effective time evolution does not preserve the norm of the state and that it maps pure states onto pure states. In fact the square of the norm of Eq. (65) is just

$$P_0(t) = \langle \psi_A^{(0)}(t)|\psi_A^{(0)}(t)\rangle \tag{66}$$

and coincides with $P_0(t)$ given in Eq. (55). The function $P_0(t)$ will become important in applications of the method in simulations (Dalibard *et al.*, 1992; Dum, Zoller, and Ritsch, 1992). It should be noted here in passing that if we consider the normalized version of the time evolution Eq. (65) for a two-level system, we find that it is identical to the time evolution according to the neoclassical radiation theory of Jaynes (Bouwmeester *et al.*, 1994). The reason for this is claimed by Bouwmeester *et al.* to be that H_{eff} contains all contributions from virtual photons (i.e., all radiation reaction terms) but does not include the real photons, as their detection leads to state reduction according to the projection postulate. However, neoclassical theory predicts quantum beats from a three-level system in the Λ configuration, while it is easily seen that an analysis of the problem using the quantum-jump approach does not predict quantum beats, a result in accordance with experiment (Milonni, 1976, and references therein).

Eventually the photodetector will find a photon, and the state after this detection can be determined by the projection postulate. We write the state after the detection of a photon as a density operator, as the state after the emission can be a mixture, e.g., as in the three-level Λ configuration (Javanainen, 1992; Hegerfeldt, 1993; Hegerfeldt and Plenio, 1995a; Hegerfeldt and Sondermann, 1996), although in the case of the three-level V system it is not:

$$\begin{aligned}\tilde{\rho}_R(s_n) = &(\mathbb{1}-\mathbb{P}_0)U(s_n,s_{n-1})\mathbb{P}_0\rho_A^{(0)}(s_{n-1}) \\ &\times \mathbb{P}_0 U(s_n,s_{n-1})(\mathbb{1}-\mathbb{P}_0).\end{aligned} \tag{67}$$

At this point the additional assumption is made that the photodetector absorbs the photon (which it does in reality) and that the state after the detection is simply obtained by removing the photons from the radiation field. This can be done by tracing over the quantized radiation field and multiplying with $\mathbb{P}_0$

$$\begin{aligned}\rho_R &= \mathrm{Tr}_F\{\tilde{\rho}_R(s_n)\}\otimes\mathbb{P}_0 \\ &= \sum_{i=1}^{2} 2\Gamma_{ii}|0\rangle\langle i|\rho_A^{(0)}(s_{n-1})|i\rangle\langle 0|(s_n - s_{n-1}).\end{aligned} \tag{68}$$

It should be noted that the assumption that the state, after the detection of a photon in the counter, is given by Eq. (68) is not included in the projection postulate but enters as a physically justified additional assumption. However, using slightly different mathematical methods it is possible to show that the procedure of Eq. (68) is not really necessary. Ideal quantum-mechanical measurements in which the photon is not absorbed lead to the same results (Plenio, 1994; Hegerfeldt and Plenio, 1996). This is a consequence of the intuitively obvious fact that in free space photons emitted by the system will never return to it and is implicit in the treatment of Zoller *et al.* (1987).

3. The quantum-jump approach from classical photoelectron-counting distributions

A different approach towards the quantum-jump method was presented earlier by Carmichael and coworkers (Carmichael *et al.*, 1989; Carmichael, 1993a). They derive the quantum-jump method from a discussion of photoelectron-counting distributions that are found in experiments. A quantum-mechanical theory for photoelectron-counting distributions was developed in 1964 by Kelley and Kleiner (1964), who derived the quantum-mechanical expressions for nonexclusive multicoincidence rates. For the probability to have n photoelectron counts in the time interval $[t,t+T]$, they find

$$\begin{aligned}p(n,t,T) = \Bigg\langle :\Bigg\{ &\frac{\xi\int_t^{t+T} dt'\,\hat{E}^{(-)}(t')\hat{E}^{(+)}(t')}{n!}\Bigg\} \\ &\times \exp\Bigg\{-\xi\int_t^{t+T} dt'\,\hat{E}^{(-)}(t')\hat{E}^{(+)}(t')\Bigg\}:\Bigg\rangle,\end{aligned} \tag{69}$$

where $\hat{E}$ is the electric field operator and ξ is the product of detector efficiency and a factor to convert field intensity into photon flux. The notation $\langle:...:\rangle$ means that all operators have to be normally ordered and time ordered in such a way that times decrease from the center towards the left and right. Expanding Eq. (69), one can write $p(n,t,T)$ as a complicated series of integrals over the nonexclusive multicoincidence rates

$$\begin{aligned}I(t_1,\ldots,t_m) = \xi^m\langle &\hat{E}^{(-)}(t_1)\ldots\hat{E}^{(-)}(t_m) \\ &\times \hat{E}^{(+)}(t_m)\ldots\hat{E}^{(+)}(t_1)\rangle,\end{aligned} \tag{70}$$

which gives the rate for the joint detection of photons at times $t_1,\ldots,t_m$. It is a nonexclusive rate, as there may be more detections in between the times $t_1,\ldots,t_m$. That these possible events are included in Eq. (70) is obvious, as the Heisenberg operators are calculated with respect to the total Hamiltonian of the system, which describes a time evolution in which arbitrarily many photons may be created. The analysis of the photon statistics by means of the coincidence rate Eq. (70) has long been the standard way of investigation. It was, however, realized that this is not the only possibility, and for certain problems it is not even the most natural way. In fact Eq. (69),

for example, can be expressed very easily by the exclusive probability density to find photon counts at exactly the times $t_1,\ldots,t_n$ and at no other time in $[t,t+T]$. One finds for this the expression

$$p(n,t,T)=\int_t^{t+T}dt_n\int_t^{t_n}dt_{n-1}\ldots\int_t^{t_2}dt_1 p_{[t,t+T]}(t_1,\ldots,t_n). \tag{71}$$

Carmichael and co-workers (Carmichael *et al.*, 1989; Carmichael, 1993a) then undertook the step to express the exclusive probability density in terms of the intensity operators. They find

$$p_{[t,t+T]}(t_1,\ldots,t_n)=\sum_{r=0}^{\infty}\frac{(-1)^r}{r!}\int_t^{t+T}dt'_r\ldots\int_t^{t+T}dt'_1 \times\langle:\hat{I}(t'_r)\ldots\hat{I}(t'_1)\hat{I}(t_m)\ldots\hat{I}(t_1):\rangle, \tag{72}$$

where

$$\hat{I}(t)=\xi\hat{E}^{(-)}(t)\hat{E}^{(+)}(t). \tag{73}$$

This can be checked by inserting Eqs. (72) and (73) into Eq. (71) and showing that the result coincides with Eq. (69) (Stratonovitch, 1963; Saleh, 1978). The aim now is to rewrite Eq. (72) in terms of (super)-operators that only act in the atomic space, as these are much easier to handle than the Heisenberg operators $\hat{I}(t)$. It turns out that the resulting equations are quite simple. To this end it is important to note that the electric-field operator in the Heisenberg picture can be decomposed into a free-field part and a source-field part

$$\hat{E}^{(-)}(t)=\hat{E}_f^{(-)}(t_i)+\hat{E}_s^{(-)}(t_i). \tag{74}$$

In the Markov approximation the free field commutes with all electric-field operators at earlier times (Cohen-Tannoudji *et al.*, 1992) and vanishes when acting onto the vacuum state. It is therefore possible to replace the intensity operators $\hat{I}(t_i)$ for $i=1,\ldots,m$ by $\hat{E}_s^{(-)}(t_i)\hat{E}_s^{(+)}(t_i)$ in Eq. (72). All other intensity operators remain unchanged. Carrying out the time ordering in Eq. (72) explicitly and after tedious calculations [for details we refer the reader to Carmichael *et al.* (1989) and Carmichael (1993a)], one obtains for an overall counter efficiency ξ

$$p_{[t,t+T]}(t_1,\ldots,t_n)=\xi^n\mathrm{Tr}_A\{e^{(\mathcal{L}-\xi\mathcal{R})(t+T-t_m)}\mathcal{R}\ldots\mathcal{R}e^{(\mathcal{L}-\xi\mathcal{R})(t_1-t)}\rho(t)\}, \tag{75}$$

where $\mathcal{L}$ is the super-operator given by

$$\mathcal{L}\rho=-\frac{i}{\hbar}[H_{eff}(\xi)\rho-\rho H_{eff}(\xi)], \tag{76}$$

where $H_{eff}(\xi)$ is obtained from H_{eff} for perfect efficiency $\xi=1$ by substituting $\Gamma\to(1-\xi)\Gamma$. $\mathcal{R}$ is the reset operator giving the state after a photon has been detected. Assuming unit efficiency ($\xi=1$) of the detection process, we recover Eq. (49).

4. A formulation as a stochastic differential equation

So far we have discussed a number of approaches to the quantum-jump description of dissipation. These approaches can be formulated somewhat differently in the language of quantum stochastic differential equations (Gardiner, 1992). This formulation is certainly rather formal at first glance, but it has the advantage that certain operations that use the Markov approximation become simpler. On the other hand, one has to use the somewhat unintuitive Ito formalism (Gardiner, 1992; Gardiner *et al.*, 1992), when a more physically oriented derivation would sometimes help to interpret the resulting equations.

To illustrate the idea of this formalism, we consider a laser-driven two-level atom in a quantized radiation field that is in the vacuum state. We follow the description in Sondermann (1995b). The Hamiltonian operator in a suitable interaction picture is given by

$$\begin{aligned}H&=-\hbar\Delta_1|1\rangle\langle1|+\frac{\hbar\Omega}{2}(|0\rangle\langle1|+|1\rangle\langle0|)\\&\quad+\sum_{\mathbf{k}\lambda}(i\hbar g_{\mathbf{k}\lambda}\sigma_{10}a_{\mathbf{k}\lambda}e^{-i(\omega_{\mathbf{k}\lambda}-\omega_{10})t}+\mathrm{H.c.})\\&=H_A+\sigma_{10}\mathbf{D_{10}}\mathbf{E}^{(+)}(t)+\mathbf{D}_{\mathbf{10}}^{\dagger}\mathbf{E}^{(-)}(t)\sigma_{01},\end{aligned} \tag{77}$$

where $\sigma_{ij}=|i\rangle\langle j|$ is an operator annihilating an electron in level j and creating an electron in level i and where

$$\mathbf{D_{10}}\mathbf{E}^{(+)}(t)=\mathbf{D_{10}}\sum_{\mathbf{k}\lambda}i\hbar\left(\frac{e^2\omega_{\mathbf{k}\lambda}}{2\epsilon_0\hbar V}\right)^{(1/2)}\times\boldsymbol{\epsilon}_{\mathbf{k}\lambda}\sigma_{10}a_{\mathbf{k}\lambda}e^{-i(\omega_{\mathbf{k}\lambda}-\omega_{10})t} \tag{78}$$

is the interaction energy between the electric-field operator $E^{\dagger}(t)$ in the Schrödinger picture (or more precisely in the chosen interaction picture) and the atomic dipole moment $\mathbf{D}_{21}$ of the transition. The time-discretized Schrödinger equation then reads

$$\begin{aligned}i\hbar\Delta|\psi(t)\rangle&=H|\psi(t)\rangle\Delta t\\&=\{H_A\Delta t+\sigma_{10}\Delta A^{\dagger}(t)-\sigma_{01}\Delta A(t)\}|\psi(t)\rangle,\end{aligned} \tag{79}$$

where

$$\begin{aligned}\Delta A(t)&=\int_t^{t+\Delta t}dA(t)\\&=\int_t^{t+\Delta t}dt\ \mathbf{D_{10}}\sum_{\mathbf{k}\lambda}i\hbar\left(\frac{e^2\omega_{\mathbf{k}\lambda}}{2\epsilon_0\hbar V}\right)^{(1/2)}\times\boldsymbol{\epsilon}_{\mathbf{k}\lambda}\sigma_{10}a_{\mathbf{k}\lambda}e^{-i(\omega_{\mathbf{k}\lambda}-\omega_{10})t}.\end{aligned} \tag{80}$$

We assume in the following that $\Delta t\gg\omega_{10}^{-1}$, which is crucial to justify the Markov approximation. The idea is now to perform the Markovian limit directly in the Schrödinger equation instead of performing this limit on the results. This is the step where we have to introduce the notion of quantum stochastic differential equations, as in performing this limit we cannot subsequently interpret the resultant Schrödinger equation as an ordinary

differential equation (Gardiner, 1992; Gardiner *et al.*, 1992). Under the Markov assumption we have

$$[\Delta A(t),\Delta A^\dagger(s)]=\begin{cases}0 & \text{if } |t-s|\geq\Delta t,\\ \Gamma\Delta t & \text{otherwise,}\end{cases} \tag{81}$$

which in the limit $\Delta t\to 0$ results in

$$[dA(t),dA^\dagger(s)]=\begin{cases}0 & \text{if } t\neq s,\\ \Gamma dt & \text{otherwise.}\end{cases} \tag{82}$$

We also need to know that if we assume that the initial state of the quantized radiation field is the vacuum, then

$$dA(t)dA(t)=0=dA^\dagger(t)dA^\dagger(t), \tag{83}$$

where this equation is defined in the mean-square-topology sense, i.e., one applies both sides on an initial vector and takes the absolute square of the result afterwards (Gardiner, 1992; Gardiner *et al.*, 1992). Taking the limit $\Delta t\to 0$ in Eq. (80), we have assumed the ordinary rules of calculus and therefore generated a stochastic differential equation in the sense of Stratonovitch

$$i\hbar d|\psi(t)\rangle|_S=\{H_A dt+\sigma_{10}dA^\dagger(t)-\sigma_{01}dA(t)\}|\psi(t)\rangle. \tag{84}$$

Since a Stratonovitch equation is not easy to integrate, we would like to put it in Ito form, using Eqs. (81)–(83) (Gardiner, 1992; Gardiner *et al.*, 1992). We then find

$$i\hbar d|\psi(t)\rangle|_I=\{H_A dt+dA^\dagger(t)\sigma_{01}-\Gamma\sigma_{11}dt\}|\psi(t)\rangle, \tag{85}$$

where the $\Gamma\sigma_{11}dt$ arises from a $dA(t)dA^\dagger(t)$ contribution. As the $dA(t)$ commute with all earlier $dA(s)$ upon which $|\psi(t)\rangle$ depends, it can be commuted to the right until it operates on the initial state and therefore the vacuum. Therefore the contribution of the $dA(t)$ vanishes, and only the $dA^\dagger(t)$ contribution survives.

What we are in fact interested in here is the rederivation of the quantum-jump approach. Therefore we are interested in the time evolution when no photon is present in the field, i.e., we are interested in the state vector

$$\mathbb{P}_0|\psi(t)\rangle=|\psi(t)\rangle_0, \tag{86}$$

where $\mathbb{P}_0$ is the projector onto the vacuum state of the quantized radiation field. We find

$$d|\psi(t)\rangle_0=\mathbb{P}_0 d|\psi(t)\rangle=(-iH_A/\hbar-\Gamma\sigma_{11})\mathbb{P}_0|\psi(t)\rangle dt. \tag{87}$$

The $dA^\dagger(t)$ now vanishes because, when acting on a vacuum state to its left, it gives zero contribution. The norm of the conditional state vector $|\psi(t)\rangle_0$ is just the probability to find no photon until t if there was no photon at $t=0$. This is just the reduced time evolution found in the previously discussed derivations. The probability density $I_1(t)$ for an emission at time t is just the rate of decrease of the norm of the emission free-time evolution, i.e.,

$$\begin{aligned}d_0\langle\psi(t)|\psi(t)\rangle_0|_I&=(d_0\langle\psi(t)|)|\psi(t)\rangle_0+{}_0\langle\psi(t)|(d|\psi(t)\rangle_0)\\&\quad+(d_0\langle\psi(t)|)(d|\psi(t)\rangle_0)\\&={}_0\langle\psi(t)|iH_A/\hbar-\Gamma\sigma_{11}|\psi(t)\rangle_0\\&\quad+{}_0\langle\psi(t)|-iH_A/\hbar-\Gamma\sigma_{11}|\psi(t)\rangle_0\\&=-2\Gamma_0\langle\psi(t)|\sigma_{11}|\psi(t)\rangle_0.\end{aligned} \tag{88}$$

In this way we have recovered the time evolution of the no-photon probability $P_0(t)$. What happens when a photon has been detected? Then we need to calculate the contribution to the state of the system projected onto the one-photon subspace at time t, i.e., $\mathbb{P}_1|\psi(t)\rangle$, that originates from systems where no photon has been emitted so far. It can easily be seen that this contribution comes from an atom in the ground state because only an operator of the form $dA^\dagger\sigma_{01}$ in Eq. (85) survives. Therefore, using this formulation, we have recovered the quantum-jump approach; we observe that this formalism, although not delivering new insights into physics different from those of previous derivations of the quantum-jump approach, is very elegant from a formal point of view. To understand the formalism a little better, we now show how one may obtain Eq. (87) without referring to the formalism of stochastic differential equations (Zoller and Gardiner, 1995). We consider a finite time step for the state vector $\mathbb{P}_0|\psi(t)\rangle$, using the Hamiltonian operator Eq. (77) and first-order perturbation theory. We obtain

$$\begin{aligned}\Delta\mathbb{P}_0|\psi(t)\rangle&=\mathbb{P}_0(-iH_A/\hbar\Delta t-\sigma_{10}\Delta A(t))|\psi(t)\rangle\\&=\mathbb{P}_0U(t,0)U^\dagger(t,0)(-iH_A/\hbar\Delta t\\&\quad-\sigma_{10}\Delta A(t))U(t,0)U^\dagger(t,0)|\psi(t)\rangle\\&=-iH_A/\hbar\Delta t\mathbb{P}_0|\psi(t)\rangle\\&\quad+\mathbb{P}_0U(t,0)\sigma_{10}(\Delta A(t)-\Gamma\sigma_{01}(t))|\psi(0)\rangle,\end{aligned} \tag{89}$$

where in the last line we have used the well-known expression for the Heisenberg operator of the electric-field operator, which can be written as a free-field contribution and a source term (the dipole of the atom radiates the outgoing field) (Loudon, 1983). Note that $\sigma_{01}(t)$ is now a Heisenberg operator. Eliminating $A(t)$ in the last row of Eq. (89), as it operates on the initial vacuum state, we obtain

$$\Delta\mathbb{P}_0|\psi(t)\rangle=\Delta t(-iH_A/\hbar-\Gamma\sigma_{11})\mathbb{P}_0|\psi(t)\rangle. \tag{90}$$

Now we may easily perform the limit $\Delta t\to 0$ to obtain the same result as in Eq. (87), however, without the explicit use of the quantum stochastic differential calculus.

B. Quantum-state diffusion and other approaches to single-system dynamics

1. Quantum-state diffusion

So far we have discussed the quantum-jump approach for the description of single radiating quantum systems. The main ingredient in the derivation was the assumption of time-resolved photon-counting measurements on the quantized radiation field. The resulting time evolution could be divided into a coherent time evolution

governed by a non-Hermitian Hamiltonian operator that is interrupted by instantaneous jumps caused by the detection of a photon and the consequent gain in knowledge about the system. One could ask whether this description is unique, that is, it represents the only possibility. From the emphasis we put on the importance of the measurement process in the derivation of the quantum-jump approach, one can already guess that other measurement prescriptions will yield different kinds of quantum trajectories. In the following we shall discuss an important example (Gisin and Percival, 1992) of a different kind of quantum trajectory, quantum state diffusion, which in fact can be derived from a very important measurement method in quantum optics, namely, the balanced heterodyne detection. Before we show the connection of quantum-state diffusion to balanced heterodyne detection, let us point out that quantum-state diffusion was originally derived independently from a measurement context. Steps in this direction were made when several authors became interested in alternative versions of quantum mechanics (Pearle, 1976; Ghirardi *et al.*, 1986; Diosi, 1988, 1989; Ghirardi *et al.*, 1990) and the investigation of the wave function collapse, i.e., the projection postulate (Gisin 1984, 1989). In these investigations stochastic differential equations for the time evolution of the state vector of the system were studied. Again there is a multitude of possible equations; however, Gisin and Percival (1992) provided a natural symmetry condition under which it is possible to derive a unique diffusion equation, which is referred to as the quantum-state diffusion model (QSD). Given a Bloch equation in Lindblad form (Lindblad, 1976)

$$\dot{\rho}=-\frac{i}{\hbar}[H_{sys},\rho]+\sum_m (2L_m\rho L_m^\dagger - L_m^\dagger L_m\rho-\rho L_m^\dagger L_m), \tag{91}$$

with the system Hamiltonian H_{sys}, and the Lindblad operators L_m, the quantum-state diffusion equation for the state vector is

$$\begin{aligned}|d\psi\rangle=&-\frac{i}{\hbar}(H_{sys}-i\hbar L_m^\dagger L_m)|\psi\rangle dt\\&+\sum_m (2\langle L_m\rangle L_m-\langle L_m^\dagger\rangle\langle L_m\rangle)|\psi\rangle dt\\&+\sum_m (L_m-\langle L_m\rangle)|\psi\rangle d\xi_m .\end{aligned} \tag{92}$$

The $d\xi_m$ represent independent complex normalized Wiener processes whose averages, denoted by $M(...)$, satisfy

$$\begin{aligned}&M(d\xi_m)=0,\\&M(\mathrm{Re}(d\xi_m)\mathrm{Re}(d\xi_n))=M(\mathrm{Im}(d\xi_m)\mathrm{Im}(d\xi_n))\\&\qquad\qquad=\delta_{mn}dt,\\&M(\mathrm{Re}(d\xi_m)\mathrm{Im}(d\xi_n))=0.\end{aligned} \tag{93}$$

Equation (92) has to be interpreted as an Ito stochastic differential equation, see, for example, Stratonovitch (1963) and Gardiner (1992). It is easy to check that averaging Eq. (92) over the stochastic Wiener process yields the density operator equation, Eq. (91), and that therefore (in the mean) normalization is preserved. For numerical studies, often a somewhat simpler equation is used that does not preserve normalization even under the mean. This is given by

$$\begin{aligned}|d\psi\rangle=&-\frac{i}{\hbar}H|\psi\rangle dt+\sum_m (2\langle L_m^\dagger\rangle L_m-L_m^\dagger L_m)|\psi\rangle dt\\&+\sum_m L_m|\psi\rangle d\xi_m .\end{aligned} \tag{94}$$

It should be noted that Eq. (93) is a nonlinear equation as it also depends on the expectation values of the Lindblad operators L_m. This makes the analytical treatment of this equation very difficult, and there are only a few cases for which an analytic solution is known (Gisin, 1984, 1989; Salama and Gisin, 1993; Carmichael, 1994; Wiseman and Milburn, 1994). However, it was found by Goetsch, Graham, and Haake (Goetsch and Graham, 1993, 1994; Goetsch *et al.*, 1995) and later for non-Markovian systems by Strunz (1996a, 1996b), that it is possible to find linear stochastic differential equations that also reproduce the ensemble average. Stochastic differential equations for the wave function have also been derived by Barchielli (1986, 1993; Barchielli and Belavkin, 1991) (see also Zoller and Gardiner, 1995 for a good summary of these approaches) from a more abstract mathematical point of view. The approach of Barchielli also gives a common mathematical basis for both diffusion and jump processes.

However, we do not intend to elaborate further on the mathematical side of the theory. Instead we would like to show that it is possible to derive quantum-state diffusion from the quantum-jump approach in a certain limiting case, i.e., the case of infinitely many jumps, where each jump has an infinitesimal impact on the wave function. In fact it turns out that quantum-state diffusion can be related to an explicit and well-known physical measurement process in quantum optics, namely, the method of balanced heterodyne detection (see, for example, Castin *et al.*, 1993; Carmichael, 1993a; Wiseman and Milburn, 1993a, 1993b; Mølmer, 1994; Knight and Garraway, 1996; Wiseman, 1996). In the following we would like to show this explicitly for the specific example of a decaying cavity, and we follow a similar path to that used in the approach of Garraway and Knight (Castin *et al.*, 1993; Garraway and Knight, 1994b; Knight and Garraway, 1996). To be specific, we shall illustrate the method for the case of balanced heterodyne detection of the output of an undriven optical cavity. We have in mind the situation given in Fig. 7.

2. Quantum-state diffusion as a quantum-jump description of heterodyne detection

The left-hand cavity A (with mode operators a_{cav}) is the source of a weak output field (mode operators $a_{\mathbf{k}\lambda}$) that we want to analyze, while the lower cavity (mode

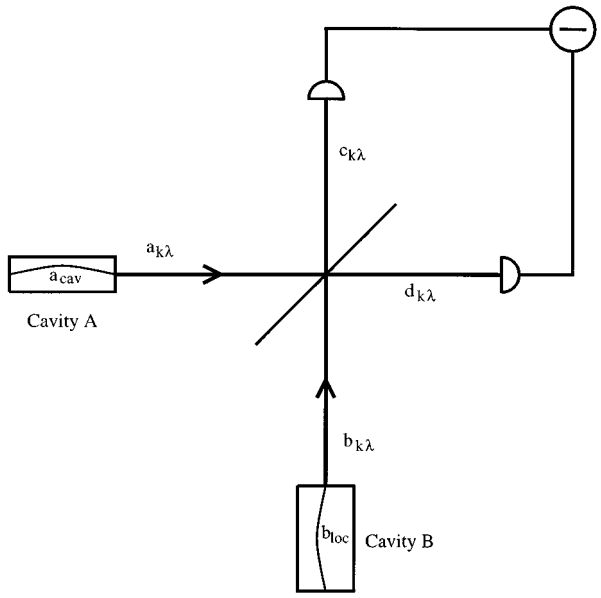

FIG. 7. Schematic picture of the heterodyne-detection scheme. Cavity A emits a weak signal that we mix with the signal from the local oscillator cavity B. We measure the difference in the counts in the two counters that detect the photons that leave the beamsplitter.

operators b_{loc}) is assumed to be in a coherent state $|\beta\rangle$ with a very large amplitude β for all times, so that the radiated field (with mode operators $b_{\mathbf{k}\lambda}$) of that cavity is very large. The Hamiltonian operator describing this situation is

$$\begin{aligned} H=&\hbar\omega_{cav}a_{cav}^{\dagger}a_{cav}+\sum_{\mathbf{k}\lambda}\hbar\omega_{\mathbf{k}\lambda}a_{\mathbf{k}\lambda}^{\dagger}a_{\mathbf{k}\lambda}\\ &+\sum_{\mathbf{k}\lambda}\{i\hbar g_{\mathbf{k}\lambda}a_{cav}^{\dagger}a_{\mathbf{k}\lambda}+\text{H.c.}\}+\hbar\omega_{loc}b_{loc}^{\dagger}b_{loc}\\ &+\sum_{\mathbf{k}\lambda}\hbar\omega_{\mathbf{k}\lambda}b_{\mathbf{k}\lambda}^{\dagger}b_{\mathbf{k}\lambda}+\sum_{\mathbf{k}\lambda}\{i\hbar f_{\mathbf{k}\lambda}b_{loc}^{\dagger}b_{\mathbf{k}\lambda}+\text{H.c.}\}, \end{aligned} \tag{95}$$

where the $g_{\mathbf{k}\lambda}$ and $f_{\mathbf{k}\lambda}$ are the coupling constants between the cavity and the outside world and ω_{cav} and ω_{loc} the frequencies of the cavity A and the local oscillator cavity, respectively. The action of the beamsplitter is to mix the two incoming modes. Assuming a 50% beamsplitter, we find for the new mode operators (Loudon and Knight, 1987)

$$\begin{aligned} c_{\mathbf{k}\lambda}&=\frac{1}{\sqrt{2}}(a_{\mathbf{k}\lambda}+b_{\mathbf{k}\lambda}),\\ d_{\mathbf{k}\lambda}&=\frac{1}{\sqrt{2}}(-a_{\mathbf{k}\lambda}+b_{\mathbf{k}\lambda}). \end{aligned} \tag{96}$$

Now going over to an interaction picture with respect to

$$\begin{aligned} H_0=&\hbar\omega_{cav}a_{cav}^{\dagger}a_{cav}+\sum_{\mathbf{k}\lambda}\hbar\omega_{\mathbf{k}\lambda}a_{\mathbf{k}\lambda}^{\dagger}a_{\mathbf{k}\lambda}+\hbar\omega_{loc}b_{loc}^{\dagger}b_{loc}\\ &+\sum_{\mathbf{k}\lambda}\hbar\omega_{\mathbf{k}\lambda}b_{\mathbf{k}\lambda}^{\dagger}b_{\mathbf{k}\lambda} \end{aligned} \tag{97}$$

and subsequently changing the basis via a displacement operator such that the initial state of the local oscillator is the vacuum (Mollow, 1975; Pegg, 1980), we obtain, using $\Omega=\omega_{loc}-\omega_{cav}$,

$$\begin{aligned} H=&\sum_{\mathbf{k}\lambda}\frac{i\hbar}{\sqrt{2}}[g_{\mathbf{k}\lambda}a_{cav}^{\dagger}e^{-i\Omega t}+f_{\mathbf{k}\lambda}(b_{loc}^{\dagger}+\beta^{*})]\\ &\times c_{\mathbf{k}\lambda}e^{-i(\omega_{\mathbf{k}\lambda}-\omega_{loc})t}+\text{H.c.}\\ &+\sum_{\mathbf{k}\lambda}\frac{i\hbar}{\sqrt{2}}[-g_{\mathbf{k}\lambda}a_{cav}^{\dagger}e^{-i\Omega t}+f_{\mathbf{k}\lambda}(b_{loc}^{\dagger}+\beta^{*})]\\ &\times d_{\mathbf{k}\lambda}e^{-i(\omega_{\mathbf{k}\lambda}-\omega_{loc})t}+\text{H.c.} \end{aligned} \tag{98}$$

Now applying the methods that we used to derive the quantum-jump approach, we easily obtain the two jump operators

$$\begin{aligned} J_c&=\frac{1}{\sqrt{2}}(\sqrt{\gamma_{cav}}a_{cav}e^{i\Omega t}+\sqrt{\gamma_{loc}}\beta),\\ J_d&=\frac{1}{\sqrt{2}}(-\sqrt{\gamma_{cav}}a_{cav}e^{i\Omega t}+\sqrt{\gamma_{loc}}\beta), \end{aligned} \tag{99}$$

where γ_{cav} and γ_{loc} are the decay rates of the cavity and the local oscillator. Within a short time interval Δt, i.e., such that $(\omega_{cav}-\omega_{loc})\Delta t\ll 1$, we will count on average

$$\langle J_c^{\dagger}J_c\rangle=\frac{\beta^2\gamma_{loc}}{2}\left(1+\sqrt{\frac{4\gamma_{cav}}{\gamma_{loc}\beta^2}}\,\langle x_{\Omega t}\rangle\right) \tag{100}$$

counts in mode c, and

$$\langle J_d^{\dagger}J_d\rangle=\frac{\beta^2\gamma_{loc}}{2}\left(1-\sqrt{\frac{4\gamma_{cav}}{\gamma_{loc}\beta^2}}\,\langle x_{\Omega t}\rangle\right) \tag{101}$$

counts in mode d, where

$$\langle x_{\phi}\rangle:=\langle a_{cav}^{\dagger}e^{i\phi}+a_{cav}e^{-i\phi}\rangle. \tag{102}$$

These are average values around which the actual number of counts in the two counters fluctuates. We can approximate this number of counts $m(t)$ by the stochastic process

$$m(t)=\langle J^{\dagger}J\rangle\Delta t+\langle J^{\dagger}J\rangle^{1/2}\Delta W, \tag{103}$$

such that $\langle(\Delta W)^2\rangle=\Delta t$. For the powers of the jump operators we find

$$\begin{aligned} J_c^{m_1}&=\beta^{m_1}\left(\frac{\gamma_{loc}}{2}\right)^{m_1/2}\left(1+\frac{m_1}{\beta}\sqrt{\frac{\gamma_{cav}}{\gamma_{loc}}}\,a_{cav}e^{i\Omega t}\right),\\ J_d^{m_2}&=\beta^{m_2}\left(\frac{\gamma_{loc}}{2}\right)^{m_2/2}\left(1-\frac{m_2}{\beta}\sqrt{\frac{\gamma_{cav}}{\gamma_{loc}}}\,a_{cav}e^{i\Omega t}\right). \end{aligned} \tag{104}$$

As we normalize after each emission, the prefactors are not really important, and we can divide the jump opera-

tors by these. One should note that the phase of these prefactors is fixed due to the fact that in the limit of infinite β the jump operators have to become the unit operator. Therefore there is no freedom in the choice of the sign of the prefactors. It is now easy to derive the effective Hamiltonian operator H_{eff}, for which we find

$$H_{eff}=-i\hbar\frac{\gamma_{cav}}{2}\left(a^{\dagger}a+\frac{\gamma_{loc}}{\gamma_{cav}}\beta^2\right). \tag{105}$$

Using this together with Eq. (104), we obtain

$$|\tilde{\psi}(t+\Delta t)\rangle=\left(1-\frac{i}{\hbar}H_{eff}\Delta t+e^{-i\Omega t}a_{cav}\left(2\gamma_{cav}\langle x_{\Omega t}\rangle+\sqrt{\frac{\gamma_{cav}}{2}}(\Delta W_1-\Delta W_2)\right)\right)|\tilde{\psi}(t)\rangle. \tag{106}$$

Adding together the two Wiener noises $\Delta W=(\Delta W_1-\Delta W_2)/\sqrt{2}$, taking the limits $\Delta t\to dt$ and $\Delta W\to dW$, and defining

$$d\xi=e^{-i\Omega t}dW, \tag{107}$$

we obtain, after dropping a counter-rotating term of the form $e^{-2i\Omega t}$,

$$|d\tilde{\psi}\rangle=\left[-\frac{\gamma_{cav}}{2}\left(a^{\dagger}_{cav}a_{cav}+\frac{\gamma_{loc}}{\gamma_{cav}}\beta^2\right)dt+\gamma_{cav}a_{cav}\langle a^{\dagger}_{cav}\rangle dt+\sqrt{\gamma_{cav}}a_{cav}d\xi\right]|\tilde{\psi}\rangle. \tag{108}$$

This is the unnormalized diffusion equation, given, for example, by Gisin and Percival (1992). One should note that if we had considered homodyne detection, i.e., the case $\Omega=0$, then we would have found a different diffusion equation, as there would not have been a counter-rotating term that we could have dropped. Therefore an additional term in Eq. (108) would appear (Carmichael, 1993a; Mølmer, 1994).

To yield the normalized equations for quantum-state diffusion as they are given by Gisin and Percival (1992), we have to normalize the wave function, and we have to include a stochastic phase factor $\alpha(t)$ into the wave function (Garraway and Knight, 1994b), i.e., we look for a diffusion equation for

$$|\psi(t)\rangle=\frac{e^{i\alpha(t)}|\tilde{\psi}\rangle}{\langle\tilde{\psi}|\tilde{\psi}\rangle}. \tag{109}$$

The reason we have to include this seemingly unmotivated phase factor is that in the derivation of the quantum-state diffusion equation by Gisin and Percival (1992), a term is added to the diffusion equation to give it the simplest possible form. This term in fact gives rise to a random phase change. To yield quantum-state diffusion we choose $\alpha(t)$ as

$$\alpha(t)=\frac{i\gamma}{2}\langle a_{cav}\rangle d\xi-\frac{i\gamma}{2}\langle a^{\dagger}_{cav}\rangle d\xi^*. \tag{110}$$

This choice has the effect of removing $d\xi^*$ that would appear in the diffusion equation of the normalized wave function without the additional phase factor. Using Eq. (110) in Eq. (108) and assuming $d\xi d\xi^*=dt$, we finally obtain

$$|d\psi\rangle=-\frac{\gamma}{2}a^{\dagger}_{cav}a_{cav}+\gamma\left(a_{cav}\langle a^{\dagger}_{cav}\rangle+\frac{1}{2}\langle a^{\dagger}_{cav}a_{cav}\rangle-\frac{1}{2}\langle a^{\dagger}_{cav}\rangle\langle a_{cav}\rangle\right)|\psi\rangle dt+\sqrt{\gamma}(a_{cav}-\langle a_{cav}\rangle)d\xi. \tag{111}$$

We have therefore shown that the quantum-state diffusion equation Eq. (111) [or Eq. (92)] can be regarded as a limiting case of the quantum-jump approach. In Sec. V we will illustrate the transition from the quantum-jump behavior to the quantum-state-diffusion behavior that takes place when we increase the amplitude of the local oscillator (Granzow, 1996). It should be noted that it is also possible to obtain a jumplike behavior from quantum-state diffusion equations. However, this procedure is much less satisfying than the above derivation of quantum-state diffusion from quantum jumps. The reason is that one has to modify the quantum-state diffusion equation by adding an additional operator, the localization operator. The amplitude with which this localization operator appears in the equations is arbitrary and has to be adjusted according to the experimental situation (Gisin *et al.*, 1993). This is not particularly satisfying, at least in cases in which we deal with single-ion resonance fluorescence. Here the quantum-jump approach appears to be much more natural. In fact it can be shown that one can not associate the jumps occurring in the quantum-state-diffusion picture with photon emissions, as such an interpretation can lead to more than one emission from an undriven two-level system (Granzow, 1996). Taking these considerations into account, one could be tempted to say that the quantum-jump approach is more fundamental than quantum-state diffusion. However, both approaches have the same justification, as they were both derived from a particular measurement situation. Depending on the experimental situation and the measurement scheme employed, we have to choose either the quantum-jump approach or the quantum-state diffusion model to obtain the correct description of the experimental situation. Quantum-state diffusion was, as mentioned before, not originally introduced to describe a specific experimental situation. It was rather seen as an attempt to formulate alternative versions of quantum mechanics, and there are attempts to derive diffusion equations from fundamental ideas, such as, for example, decoherence induced by gravitational fluctuations (Percival, 1994b, 1995, 1997; Percival and Strunz, 1997). Although the quantum-state diffusion model can not be regarded as the proper description of quantum jumps in single-photon counting experiments but rather as the description of heterodyne detection, it is nevertheless useful in the investigation of single-system behavior. Interesting phenomena such as localization in phase and position space (Gisin and Percival, 1993a, 1993b; Percival, 1994a; Herkommer *et al.*, 1996) are found. These can be used to improve the perfor-

mance of simulation procedures using a "moving-basis" approach (Schack *et al.*, 1995; Schack *et al.*, 1996), where only a time-dependent subset of all basis states is used in the simulation. A similar method is also possible for a variant of the quantum-jump approach (Holland *et al.*, 1996). Note also that one can obtain diffusion equations when one applies the quantum-jump approach to mesoscopic systems (Brun *et al.*, 1997). Again one obtains a quantum-state-diffusion description, as it represents the mathematical limit of a system experiencing numerous jumps that individually have small effect on the system.

3. Other approaches

So far, we have discussed the evolution of *open* systems, that is of microsystems in contact with Markovian reservoirs such as the bath of vacuum-field modes responsible for spontaneous emission. The quantum-jump concept within an open-system context has to do with the gain in information about the microsystem that is accessible from the record available in the dissipative environment. Such jump processes do not require an extension or modification of conventional quantum mechanics, and we refer to these as "extrinsic" jumps. A very different jump mechanism has been studied by a number of authors (Ghirardi *et al.*, 1986; Diosi, 1989; Ghirardi *et al.*, 1990; Percival, 1994b; Percival and Strunz, 1997). In these approaches the Schrödinger equation is modified in such a way that quantum coherences are automatically destroyed in a closed system by an intrinsic stochastic-jump mechanism. This should be distinguished from the extrinsic mechanisms we are concerned with in the bulk of this review.

To see how an intrinsic jump mechanism works, we need a concrete realization that we can apply to a specific time evolution. Milburn (1991) has proposed just such a realization, in which standard quantum mechanics is modified in a simple way to generate intrinsic decoherence. He assumes that on sufficiently short time steps, the system does not evolve continuously under normal unitary evolution, but rather in a stochastic sequence of identical unitary transformations. This assumption leads to a modification of the Schrödinger equation that contains a term responsible for the decay of quantum coherence in the energy-eigenstate basis, without the intervention of a reservoir and therefore without the usual energy dissipation associated with normal decay (Moya-Cessa *et al.*, 1993). The decay is entirely of phase dependence only, akin to the dephasing decay of coherences produced by impact-theory collisions or by fluctuations in the phase of a laser in laser spectroscopy.

It is interesting to apply Milburn's model of intrinsic decoherence to a problem of dynamical evolution: that is, the interaction of two subsystems and the coherences that establish themselves as a consequence of their interaction. The interaction between a single two-level atom and a quantized cavity mode was considered by Moya-Cessa *et al.* (1993), and they showed how the intrinsic decoherence affects the long-time coherence characteristics of the entangled atom-field system. In particular it could be shown how the revivals (a signature of long-time coherence) are removed by this intrinsic decoherence. The quantum-jump approach as we have discussed it so far only treats systems (atoms) interacting with a Markovian bath (the quantized multimode radiation field). However, one might be interested in applying the quantum-jump approach to non-Markovian interactions. Examples are electrons interacting with phonons or, in quantum optics, an atom in a cavity interacting with a mode that loses photons to the outside world (Garraway, Knight, and Steinbach, 1995). The second example already suggests a possible way one could model such systems. Here the atom sees a cavity mode with finite width, i.e., a spectral function that is not flat but a Lorentzian (Piraux *et al.*, 1990, and references therein). However, one does not need to solve a non-Markovian master equation, as the width of the mode is produced by its coupling to the outside world. Taking this coupling explicitly into account, by describing a coupled atom-cavity field mode with a dissipative-field coupling to the environment, one again obtains a Markovian master equation. This is also the recipe for the treatment of an interaction of a bath with a general spectral function $R(\omega)$ (Imamoglu, 1994). One has to decompose $R(\omega)$ into a sum (or integral) of Lorentzians with positive weights. Each Lorentzian can then be modeled by a mode interacting with both the system and a Markovian reservoir. This method is practical only if the number of additional modes that one has to take into account is not too large. One should also note that in this case the meaning of a jump in the simulation can become obscure, as the excitation of the system is transferred to the Markovian bath in two steps via the additional mode (Garraway, Knight, and Steinbach, 1995). However, if one is only interested in a simulation method to obtain the master equation for non-Markovian interactions, this is not important.

We have discussed a number of derivations of the quantum-jump approach so far. A different approach towards the description of single-system dynamics has been proposed by Teich *et al.* (1989) and Teich and Mahler (1992). In their method the dynamics described by the master equation is split into two distinct parts. One part smoothly changes the instantaneous basis of the density operator (coherent evolution), while the other part causes jumps between the basis states according to a rate equation. The instantaneous basis can be viewed as a generalization of the dressed-state basis. For a stationary state the basis states are fixed so that only jump processes occur. However, the approach is analytically quite complicated for nonstationary processes, and in addition there are interpretational problems (Wiseman and Milburn, 1993a).

4. Decoherent histories

At this point we would like to explain briefly a recently proven connection (Yu, 1996; Brun, 1997) between the quantum-jump approach and a totally differ-

ent concept, the decoherent-histories formulation of quantum mechanics. A similar connection, although mathematically more involved, between the quantum-state diffusion model and the decoherent-histories approach has also been established (Diosi *et al.*, 1995). The decoherent-histories formulation of quantum mechanics was introduced by Griffiths (1984), Omnès (1988, 1989, 1994), and Gell-Mann and Hartle (1990, 1993). In this formalism, one describes a quantum system in terms of an exhaustive set of possible histories that must obey a decoherence criterion that prevents them from interfering, so that these histories may be assigned classical probabilities.

In ordinary nonrelativistic quantum mechanics, a set of histories for a system can be specified by choosing a sequence of times $t_1,\ldots,t_N$ and a complete set of projections $\{\mathbb{P}^j_{\alpha_j}(t_j)\}$ at each time t_j that represent different exclusive possibilities, i.e., they obey

$$\sum_{\alpha_j} \mathbb{P}^j_{\alpha_j}(t_j)=\mathbb{1}, \tag{112}$$

$$\mathbb{P}^j_{\alpha_j}(t_j)\mathbb{P}^j_{\alpha_j'}(t_j)=\delta_{\alpha_j\alpha_j'}\mathbb{P}^j_{\alpha_j}(t_j). \tag{113}$$

Note that the projection operators $\mathbb{P}^j_{\alpha_j}$ are Heisenberg operators; one could represent them in the Schrödinger picture by

$$\mathbb{P}^j_{\alpha_j}(t_j)=e^{-iHt}\mathbb{P}^j_{\alpha_j}e^{iHt}. \tag{114}$$

The Schrödinger-picture projection operators are assumed to be operators in the system space.

A particular history is given by choosing one $\mathbb{P}^j_{\alpha_j}$ at each point in time, specified by the sequence of indices $\{\alpha_j\}$, denoted α for short. The *decoherence functional* on a pair of histories α and α' is then given by

$$D[\alpha,\alpha']=\mathrm{Tr}\{\mathbb{P}^N_{\alpha_N}(t_N)\cdots\mathbb{P}^1_{\alpha_1}(t_1)\rho(t_0)\mathbb{P}^1_{\alpha_1'}(t_1)\cdots\mathbb{P}^N_{\alpha_N'}\}, \tag{115}$$

where $\rho(t_0)$ is the initial density matrix of the system. The decoherence criterion is now given by this decoherence functional $D[h,h']$. Two histories h and h' are said to *decohere* if they satisfy the relationship

$$D[h,h']=p(h)\delta_{hh'}, \tag{116}$$

where $p(h)$ is the probability of history h. A set of histories $\{h\}$ is said to be exhaustive and decoherent if all pairs of histories satisfy the criterion Eq. (116) and the probabilities of all the histories sum to 1.

To establish a connection between quantum jumps and decoherent histories, one uses a system that interacts with the outside world in one direction. An example of such a system is a cavity. The counter outside the cavity is now modelled by a two-level system that is strongly coupled to a bath so that both its coherence and its excitation is damped much faster than all time constants of the evolution of the system. One then defines the two projection operators

$$\mathbb{P}_0=\mathbb{1}\otimes|0\rangle\langle 0|, \quad \mathbb{P}_1=\mathbb{1}\otimes|1\rangle\langle 1|. \tag{117}$$

These projections model the presence or absence of photons outside the system. It would be more general to consider more than one mode of the radiation field, and the proof can be generalized to that case. We now space these projections a short time δt apart, and each history is composed of N projections representing a total time $T=N\delta t$. A single history is a string $\{\alpha_1,\alpha_2,\ldots,\alpha_N\}$, where $\alpha_j=0,1$ represents whether or not a photon has been emitted at time $t_j=(j-1)\delta t$. Using this, it is possible to write the decoherence functional as

$$D[h,h']=\mathrm{Tr}\{\mathbb{P}_{\alpha_N}e^{\mathcal{L}\delta t}(\mathbb{P}_{\alpha_{N-1}}e^{\mathcal{L}\delta t}(\ldots e^{\mathcal{L}\delta t}(\mathbb{P}_{\alpha_1}|\psi\rangle \times\langle\psi|\mathbb{P}_{\alpha_1'})\ldots)\mathbb{P}_{\alpha_N'})\}, \tag{118}$$

where $\mathcal{L}$ is the superoperator describing the time evolution according to the Bloch equations for the system (cavity) coupled to the two-level system. It is now possible to show that the decoherence functional in fact obeys Eq. (116) to a very good approximation. It should be noted that the construction of the decoherent histories using the two operators in Eq. (117) closely resembles the derivation of the quantum-jump approach as given by Hegerfeldt and Wilser (1991) and Wilser (1991).

The crucial point in the quantum-jump approach is the fact that we assume that we perform time-resolved measurements on the photons that are emitted by the atom. These photons may be mixed with a local oscillator in a heterodyne detection as we did for the derivation of quantum-state diffusion but even there we assume time-resolved measurements. A nice feature of the quantum-jump approach has been that it allows us to describe the radiating system by a wave function instead of a density matrix. However, one may ask the question whether this is the only possible way to reach a wave-function description of radiating systems. In fact it turns out that in some sense there is a complementary approach that also yields a wave-function description. This method was proposed by Holland and Cooper (1996) and uses frequency-resolved measurements instead of time-resolved measurements. It turns out that again it is possible to decompose the density operator into pure states (Mollow, 1975), which, however, are now characterized by the number of photons that have been detected and for which the frequency instead of their precise emission time is known.

C. Simulation of single trajectories

After we have introduced and discussed different derivations of the quantum-jump approach, we will now briefly explain how the quantum-jump approach is used to simulate single-quantum systems. We will describe the simulation approach for a decaying undriven cavity. The generalization to an arbitrary system should then be obvious. Carmichael (1993a) has given a precise relationship between the conditioned density operator contingent on a precise sequence of detection events (a "record") and the ensemble-averaged density operator.

He shows, for example, that if the zero-temperature boson-damping master equation is written in Liouvillian form

$$\frac{d\rho}{dt}=\mathcal{L}\rho \tag{119}$$

and we split the Liouvillian action $\mathcal{L}$ as a sum of two terms, an anticommutator and a "sandwich" term,

$$\mathcal{L}\rho=-\frac{\gamma}{2}[\hat{a}^\dagger\hat{a},\rho]_+ +\gamma\hat{a}\rho\hat{a}^\dagger=(\mathcal{L}-\mathcal{S})+\mathcal{S}, \tag{120}$$

then we may identify the "sandwich" term $\mathcal{S}$ as a jump operator. Equation (119) can be integrated formally as

$$\begin{aligned}\rho(t)&=\exp\{[(\mathcal{L}-\mathcal{S})+\mathcal{S}]t\}\rho(0)\\&=\sum_{m=0}^{\infty}\int_0^t dt_m\int_0^{t_m}dt_{m-1}\cdots\int_0^{t_2}dt_1\\&\quad\times\{e^{(\mathcal{L}-\mathcal{S})(t-t_m)}\mathcal{S}e^{(\mathcal{L}-\mathcal{S})(t_m-t_{m-1})}\\&\quad\times\mathcal{S}\cdots\mathcal{S}e^{(\mathcal{L}-\mathcal{S})t_1}\rho(0)\},\end{aligned} \tag{121}$$

where the quantity in curly brackets in Eq. (121) is labeled $\overline{\rho_c(t)}$ by Carmichael and is the conditioned density operator describing a specific "trajectory" or detection sequence. We can write $\overline{\rho_c(t)}$ in terms of the conditioned pure-state projectors

$$\overline{\rho_c(t)}=|\overline{\Psi_c(t)}\rangle\langle\overline{\Psi_c(t)}|. \tag{122}$$

The component $\exp[(\mathcal{L}-\mathcal{S})\Delta t]$ propagates $\overline{\rho_c(t)}$ for a time Δt without a decay being recorded: for the conditioned state $|\overline{\Psi_c(t)}\rangle$,

$$|\overline{\Psi_c(t+\Delta t)}\rangle=\exp[-iH_{eff}\Delta t/\hbar]|\overline{\Psi_c(t)}\rangle, \tag{123}$$

where the non-Hermitian effective Hamiltonian

$$H_{eff}=H-i\hbar\frac{\gamma}{2}\hat{a}^\dagger\hat{a} \tag{124}$$

derives from the anticommutator in Eq. (120). Once a decay is registered, the gain in information is responsible for the jump

$$|\overline{\Psi_c(t)}\rangle\rightarrow\hat{a}|\overline{\Psi_c(t)}\rangle. \tag{125}$$

The procedure adopted in quantum-jump simulations can then be summarized as follows (Dalibard *et al.*, 1992; Dum, Zoller, and Ritsch, 1992):

(1) Determine the current probability of an emission

$$\Delta P=\gamma\Delta t\langle\Psi|\hat{a}^\dagger\hat{a}|\Psi\rangle. \tag{126}$$

(2) Obtain a random number r between zero and one, compare with ΔP, and decide on emission as follows:

(3) If $r<\Delta P$ there is an emission, so that the system jumps to the renormalized form

$$|\Psi\rangle\rightarrow\frac{\hat{a}|\Psi\rangle}{\sqrt{\langle\Psi|\hat{a}^\dagger\hat{a}|\Psi\rangle}}. \tag{127}$$

(4) If $r>\Delta P$ no emission takes place, so the system evolves under the influence of the non-Hermitian form

$$|\Psi\rangle\rightarrow\frac{\{1-(i/\hbar)\,H\Delta t-(\gamma/2)\Delta t\hat{a}^\dagger\hat{a}\}|\Psi\rangle}{(1-\Delta P)^{1/2}}. \tag{128}$$

(5) Repeat to obtain an individual trajectory, or history.

(6) Average observables over many such trajectories.

To reassure ourselves that this is all true, we note that the history splits into two alternatives in a time Δt:

$$|\Psi\rangle=\begin{cases}|\Psi_{\text{emit}}\rangle & \text{with probability } \Delta P,\\ |\Psi_{\text{no emission}}\rangle & \text{with probability } 1-\Delta P.\end{cases} \tag{129}$$

Then in terms of the density matrix, the evolution for a step Δt becomes a sum of the two possible outcomes,

$$\begin{aligned}|\Psi\rangle\langle\Psi|&\rightarrow\Delta P|\Psi_{\text{emit}}\rangle\langle\Psi_{\text{emit}}|+(1-\Delta P)\\&\quad\times|\Psi_{\text{no emit}}\rangle\langle\Psi_{\text{no emit}}|\end{aligned} \tag{130}$$

$$\begin{aligned}&=\gamma\Delta t\hat{a}|\Psi\rangle\langle\Psi|\hat{a}^\dagger+\left\{1-\frac{i}{\hbar}H\Delta t\right.\\&\quad\left.-\frac{\gamma}{2}\Delta t\hat{a}^\dagger\hat{a}\right\}|\Psi\rangle\langle\Psi|\left\{1+\frac{i}{\hbar}H\Delta t-\frac{\gamma}{2}\Delta t\;\hat{a}^\dagger\hat{a}\right\}\\&\sim|\Psi\rangle\langle\Psi|-\frac{i}{\hbar}\Delta t[H,|\Psi\rangle\langle\Psi|]\\&\quad+\frac{\gamma}{2}\Delta t\{2\,\hat{a}|\Psi\rangle\langle\Psi|\hat{a}^\dagger-\hat{a}^\dagger\hat{a}|\Psi\rangle\langle\Psi|\\&\quad-|\Psi\rangle\langle\Psi|\hat{a}^\dagger\hat{a}\},\end{aligned} \tag{131}$$

so that

$$\frac{\Delta\rho}{\Delta t}=-\frac{i}{\hbar}[H,\rho]+\frac{\gamma}{2}\{2\,\hat{a}\rho\hat{a}^\dagger-\hat{a}^\dagger\hat{a}\rho-\rho\hat{a}^\dagger a\} \tag{132}$$

as in the original master equation (119). We have now seen how the quantum-jump approach can be used to simulate a master equation. In Sec. V we will see some examples of such simulations and also of single realizations of quantum trajectories. After this simple approach to simulating the master equation, we give a brief exposition of the idea of higher-order unravellings of the master equation (Steinbach *et al.*, 1995a). To see the motivation, we have to realize that the quantum-jump approach is based on the simulation of the conditioned evolution of either a density operator or a state vector. However, at a certain level it is not a rigorous implementation of the trajectory concept. Because this method discretizes time into small steps δt, a quantum jump in the simulation takes a finite time δt, whereas in a simulation of quantum trajectories the information gained from detection should instantaneously be used in conditioning the quantum state of the system. This pinpoints the subtle difference between conditioned trajectories and the slightly simpler idea of evaluating the probability of decay quanta at discrete timesteps. One way to remedy the fact that conditioning takes time in the simulation is to add evolution with the effective Hamiltonian to the projection step that has to be per-

formed when a photon is detected. Having said this, the question arises as to when during the time interval δt do we need to condition the quantum state according to the result of the detection process. First, it is worth noting that, wherever we decide to do this, it would not change the accuracy of integrating the master equation in first order. Second, we may try to increase the accuracy by choosing a specific point in the interval δt. Let us integrate the master equation to second order in δt:

$$\rho_S(t+\delta t)=\rho_S(t)+\frac{1}{2}\,\delta t([\mathcal{L}\rho_S]_t+[\mathcal{L}\rho_S]_{t+\delta t})+O(\delta t^3). \tag{133}$$

Here $\mathcal{L}$ is the Liouville operator describing the evolution of the complete master equation. The terms that result from evaluating the right-hand side of this equation can be cast into the following form (for details, see Steinbach *et al.* (1995a). By C we denote the reset operator that has to be applied after the detection of a photon.

$$\begin{aligned}\rho_S(t+\delta t)= &\quad U\rho_S(t)U^\dagger \\ &+\frac{1}{2}\delta t \quad UC\rho_S(t)C^\dagger U^\dagger \\ &+\frac{1}{2}\delta t \quad CU\rho_C(t)U^\dagger C^\dagger \\ &+\frac{1}{2}\delta t^2 \quad UCC\rho_C(t)C^\dagger C^\dagger U^\dagger+O(\delta t^3).\end{aligned} \tag{134}$$

Here U denotes evolution under the influence of the effective Hamiltonian

$$U=\exp\left(-\frac{i}{\hbar}H_{eff}\delta t\right), \tag{135}$$

which we call the "no-jump" evolution. The four terms on the right-hand side of Eq. (134) represent four specific conditioned evolutions or mini-trajectories that the system might follow. An expansion into mini-trajectories is important because only then can the density-matrix evolution, Eq. (134), be simulated with pure states. The first mini-trajectory in Eq. (134) represents evolution without any jump, and the second and the third represent a jump followed by evolution without jumps and vice versa, respectively, and the fourth includes two successive jumps followed by no-jump evolution.

We see that it is not sufficient to specify one point in the interval δt at which to condition the density operator due to the quantum jump. We have to consider two points, at the beginning and at the end of δt, and also the possibility of two immediately successive quantum jumps in order to increase the accuracy in δt by one order.

One can pursue this idea to obtain results that are accurate up to fourth order (in δt). The master equation has to be integrated along the lines of a fourth-order Runge-Kutta method for ordinary differential equations (Steinbach *et al.*, 1995a).

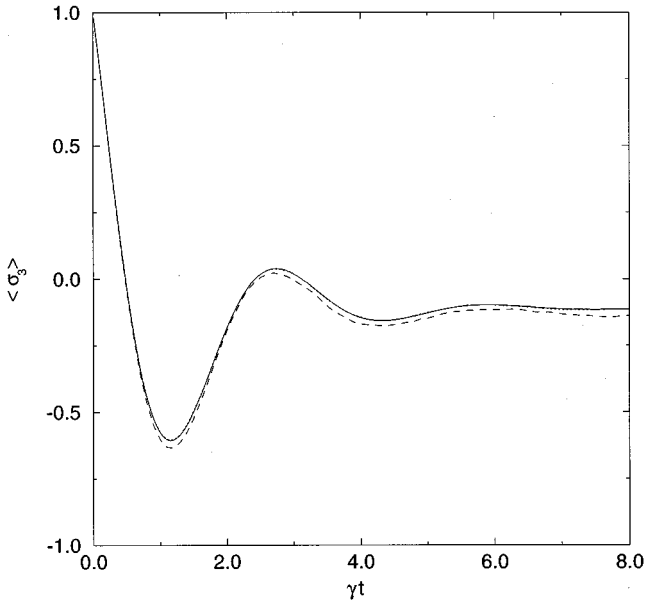

FIG. 8. Ensemble-averaged time evolution for the expectation value $\langle\sigma_3\rangle=\langle(|1\rangle\langle 1|-|0\rangle\langle 0|)\rangle/2$ (inversion in the two-level system). The dotted line shows a sample of 250,000 trajectories obtained by the fourth-order Monte Carlo method ($\Omega=A$, $\gamma\delta t=0.1A^{-1}$, and zero detuning). It is hard to distinguish the dotted line from the solid line showing the analytical result. The dashed line shows a sample of 250,000 trajectories obtained by the first-order Monte Carlo method for the same parameters. From Steinbach *et al.*, 1995a.

The way in which Eq. (134) is turned into a Monte Carlo simulation is clear: each mini-trajectory defines the conditioned evolution of the system and is assigned a specific probability with which it occurs, analogous to the jump and no-jump probabilities in the standard method. Just as in the standard procedure, a random number uniformly distributed between 0 and 1 is drawn to choose at random which of the mini-trajectories will govern the system evolution in the next time step δt. The no-jump evolution is tested first as this, for small δt, is the most likely mini-trajectory. We note that the probability for evolution without detection remains unchanged as compared with the standard method. Because the no-jump evolution is most probable, the diversity of the mini-trajectories hardly influences the necessary computing time. However, if the no-jump mini-trajectory is not selected, then one of the alternative trajectories in Eq. (134) must be chosen.

To illustrate the improvement the method of higher-order unravellings presents (Steinbach *et al.*, 1995a), one can simulate a laser-driven two-level system using the ordinary first-order integration and compare the result to the same simulation using the method of higher-order unravellings. In Fig. 8 the simulation results of the inversion $\langle\sigma_3\rangle=\langle|1\rangle\langle 1|-|0\rangle\langle 0|\rangle/2$ of the two-level system are plotted after 250000 runs for a Rabi frequency $\Omega=A$, the Einstein coefficient of the transition, zero detuning, and a time step $\delta t=0.1A^{-1}$. We clearly see that the first-order quantum-jump approach (dashed line) devi-

ates from the exact result (solid line), while the dotted line obtained from a fourth-order unravelling is much closer to the exact result.

The problem that the simulation algorithm in Eqs. (119)–(132) is given for discrete time steps and is therefore equivalent to a first-order Euler scheme can also be overcome in a different way. With the use of the delay function one can construct the quantum-jump evolution in the limit $\Delta t \to 0$, that is, in a manner that does not rely on the discretization. The simulation then runs as follows.

(1) At the t_0 at which the last jump has occurred a random number r between 0 and 1 is obtained.
(2) The time τ to the next jump is then obtained by solving numerically

$$P_0(\tau)=|e^{-iH_{eff}\tau/\hbar}|\psi(t_0)\rangle|^2=r. \tag{136}$$

This solution can be obtained using, for example, a fourth-order Runge-Kutta integration or other more sophisticated methods.
(3) If needed $|\psi(t)\rangle$ is calculated numerically in the time interval $[t_0, t_0+\tau]$ from

$$|\psi(t)\rangle=e^{-iH_{eff}(t-t_0)/\hbar}|\psi(t_0)\rangle. \tag{137}$$

(4) Proceed with the quantum jump at time $t_0+\tau$. Go to point 1.

The advantage of the procedure above is that effectively no time discretization is imposed. Therefore one can implement the most efficient time-evolution algorithm for the particular problem of interest to compute $e^{-iH_{eff}(t-t_0)/\hbar}$. For example, a fourth-order Runge-Kutta method with adjustable step size, operator-splitting techniques, or predictor-corrector schemes can be implemented straightforwardly. The delay function can be used when it can be calculated analytically. This situation occurs, for example, in the dynamics of two- and three-level systems (this method has in fact been used in the examples given in Sec. V) and in dark-state laser cooling (VSCPT) (Bardou *et al.*, 1994).

D. A quantum system driven by another quantum system

The next problem we want to investigate is that of a quantum system B driven by the radiation emitted from another quantum system A (Carmichael, 1993b; Gardiner, 1993). In the following we closely follow Carmichael (1993b). One could try to solve the problem by determining the dynamics of the driving system A first and from that the statistics of the emitted light. However, in general an infinite number of correlation functions is required to characterize the state of the light emitted from A. In semiclassical theory one could instead simulate the properties of the light by implementing a suitable stochastic process. Unfortunately, this is not possible in the quantum case. Therefore it is better not to divide the problem in two, but to determine the dynamics of the composite system $A \oplus B$. To obtain the broken time symmetry, one uses an interaction between

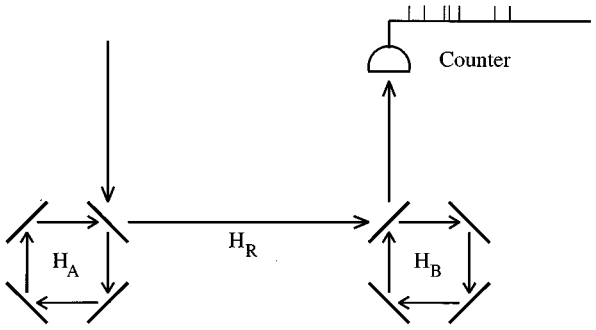

FIG. 9. Schematic picture of the experimental situation envisaged in the theory of "cascaded" quantum systems. System B is driven by the quantum system A. The counter registers a superposition of both fields, one emitted from system A and the other emitted from system B. After Carmichael (1993b).

A and B that is mediated by a reservoir R and assumes the Born-Markoff approximation. A simplified version of the problem is illustrated in Fig. 9, where it is assumed that only one mode of each cavity needs to be considered. The cavities have three perfectly reflecting mirrors and one with transmission coefficient $T \ll 1$. The Hamiltonians H_A and H_B describe the free-cavity modes and any interactions that take place inside the cavities. H_R is the free Hamiltonian of a travelling-wave reservoir R that couples the cavities in one direction only. The fields $\mathcal{E}(0)$ and $\mathcal{E}(l)$ that couple to the cavities are written in photon-flux units. The complete Hamiltonian for $A \oplus B \oplus R$ is

$$H=H_A+H_B+H_R+H_{AR}+H_{BR}, \tag{138}$$

with

$$H_{AR}=i\hbar(2\kappa_A)^{1/2}[a\mathcal{E}^\dagger(0)-\mathcal{E}(0)a^\dagger],$$
$$H_{BR}=i\hbar(2\kappa_B)^{1/2}[b\mathcal{E}^\dagger(l)-\mathcal{E}(l)b^\dagger], \tag{139}$$

where κ_A and κ_B are the cavity linewidths and a and b are annihilation operators for the cavity modes. H describes two systems interacting with the same reservoir. It should be noted that A and B couple to that reservoir at different positions in space. Usually spatially separated reservoir fields are treated as independent, an assumption that cannot be valid for the geometry shown in Fig. 9, where the output from cavity A appears a time $\tau=l/c$ later at the input of cavity B. The spatial separation of the two cavities can in fact be eliminated using the Born-Markoff approximation in the Heisenberg picture to relate $\mathcal{E}^\dagger(0)$ and $\mathcal{E}^\dagger(l)$. One obtains

$$U_A(\tau)\mathcal{E}^\dagger(l)U_A^\dagger(\tau)=\mathcal{E}^\dagger(0)+\frac{1}{2}(2\kappa_A)^{1/2}a, \tag{140}$$

where

$$U_A(\tau)=e^{i(H_A+H_R+H_{AR})\tau/\hbar}. \tag{141}$$

If $\chi(t)$ is the density operator of system $A \oplus B \oplus R$, we may define the retarded density operator of the system $A \oplus B \oplus R$ as

$$\chi'(t)=U_A(\tau)\chi(t)U_A^\dagger(\tau) \tag{142}$$

and can easily show that $\chi'(t)$ satisfies the Liouville equation with the Hamiltonian

$$H'=H_S+H_R+H_{SR}, \tag{143}$$

where

$$H_S=H_A+H_B+i\hbar(\kappa_A\kappa_B)^{1/2}(a^\dagger b-ab^\dagger),$$
$$H_{SR}=i\hbar\{[(2\kappa_A)^{1/2}a+(2\kappa_B)^{1/2}b]\mathcal{E}^\dagger(0)-\text{H.c.}\}. \tag{144}$$

Now A and B couple to the reservoir at the same spatial location and in addition couple directly with coupling constant $(\kappa_A\kappa_B)^{1/2}$. Now one can easily derive the master equation for the density operator of $A\oplus B$ $\rho'=\mathrm{Tr}_R\{\chi'\}$ and obtain

$$\dot\rho'=\frac{1}{i\hbar}[H_S,\rho']+C\rho' C^\dagger-\frac{1}{2}C^\dagger C\rho'-\frac{1}{2}\rho' C^\dagger C, \tag{145}$$

with

$$C=(2\kappa_A)^{1/2}a+(2\kappa_B)^{1/2}b. \tag{146}$$

Having found the master equation, one can easily find the conditional time evolution that then allows one to unravel the dynamics of the composite system $A\oplus B$. The time evolution of the conditional wave function $|\psi_c(t)\rangle$ between photodetections is governed by the Hamiltonian operator

$$H=H_A+H_B-i\hbar[\kappa_A a^\dagger a+\kappa_B b^\dagger b+2(\kappa_A\kappa_B)^{1/2}ab^\dagger]. \tag{147}$$

After a photodetection we have to reset the system using the operator C, i.e., $|\psi_C(t)\rangle\rightarrow C|\psi_C(t)\rangle$. Now we are in a position to simulate individual trajectories of two coupled quantum systems. For applications of the theory, for example, to an atom driven by squeezed light or by antibunched light emitted from another atom, see Carmichael (1993b), Gardiner (1993), Gardiner and Parkins (1994), and Kochan and Carmichael (1994). An early example of an investigation of atoms driven by antibunched light was discussed by Knight and Pegg (1982).

E. Spectral information and correlation functions

Until now we have discussed the quantum-jump approach only in connection with quantities of the system or its resonance fluorescence that require a temporal resolution; no frequency information has been obtained, as only broadband photon counting has been assumed. However, it would be nice to be able to use the quantum-jump approach for spectral properties of the resonance fluorescence of the system. Of special interest are, for example, the power spectrum of resonance fluorescence or the absorption spectrum of a weak probe laser. It turns out that it is in fact possible to use the quantum-jump approach (Dum, Parkins, *et al.*, 1992; Gardiner *et al.*, 1992; Mølmer *et al.*, 1993; Mu, 1994; Plenio, 1994; 1996; Hegerfeldt and Plenio, 1996) and also quantum-state diffusion (Gisin, 1993; Sondermann, 1995a; Brun and Gisin, 1996; Schack *et al.*, 1996) to calculate those spectra. There are several different ways to derive quantum-jump equations that enable us to calculate spectral information. In the following we will discuss three of them.

One possible approach can be made via the method of quantum stochastic differential equations (QSDE) (Dum, Parkins, *et al.*, 1992; Gardiner *et al.*, 1992). We already outlined the spirit of their approach in Eqs. (77)–(90). Following, essentially, Gardiner *et al.* (1992), but using the notation used in Eqs. (77)–(90), one defines an output mode operator

$$dM(t)=\int_t^{t+dt}ds\,\mathbf{D_{10}}\sum_{\mathbf{k}\lambda}i\hbar\left(\frac{e^2\omega_{\mathbf{k}\lambda}}{2\epsilon_0\hbar V}\right)^{(1/2)}\times\boldsymbol{\epsilon}_{\mathbf{k}\lambda}\sigma_{10}a_{\mathbf{k}\lambda}e^{-i(\omega_{\mathbf{k}\lambda}-\omega_{21})s} \tag{148}$$

and then the spectrum in the Schrödinger picture as

$$S(\omega)=\lim_{t\rightarrow\infty}\frac{\langle\phi(t)|r^\dagger(\omega,t)r(\omega,t)|\phi(t)\rangle}{t-t_0}, \tag{149}$$

where we defined

$$r(\omega,t)=\int_{t_0}^t dM(s)e^{-i\omega(t-s)}. \tag{150}$$

We can now introduce the auxiliary wave function

$$|\beta(t)\rangle=r(\omega,t)|\phi(t)\rangle. \tag{151}$$

For these two wave functions one then obtains a Stratonovitch stochastic differential equation that can then be transformed into the Ito form. One then obtains

$$d\begin{pmatrix}|\phi(t)\rangle\\|\beta(t)\rangle\end{pmatrix}=\begin{pmatrix}-i\,H_{eff}/\hbar & 0\\ \sqrt{A}\sigma_{01} & -iH_{eff}/\hbar-i\omega\end{pmatrix}\begin{pmatrix}|\phi(t)\rangle\\|\beta(t)\rangle\end{pmatrix}. \tag{152}$$

The spectrum is now obtained by averaging

$$S(\omega)=\lim_{t\rightarrow\infty}\frac{\langle\beta(t)|\beta(t)\rangle}{t-t_0} \tag{153}$$

over many realizations. Note that Eq. (152) for $|\phi(t)\rangle$ is just the conditional time evolution when no photons have been emitted. This equation is used to determine the jump times. The equation for $|\beta(t)\rangle$ has a free evolution similar to $|\phi(t)\rangle$ except for an additional rotation with frequency ω. In addition it is driven by $|\phi(t)\rangle$. This driving can be interpreted as a process where a photon is emitted into the modes described by $dM(t)$ and therefore the atom is de-excited. The approach given here can be used to simulate spectra in a number of situations (Dum, Zoller, and Ritsch, 1992; Marte, Dum, Taieb, Lett, and Zoller, 1993; Marte, Dum, Taieb, and Zoller, 1993). This approach is in fact similar in spirit to the approach of Schack *et al.* (1996), who also assume the interaction of the system with one mode of the quantized radiation field. Schack *et al.* then derive the quantum-state diffusion equations that allow the calculation of the spectrum. It should be noted that using Eq.

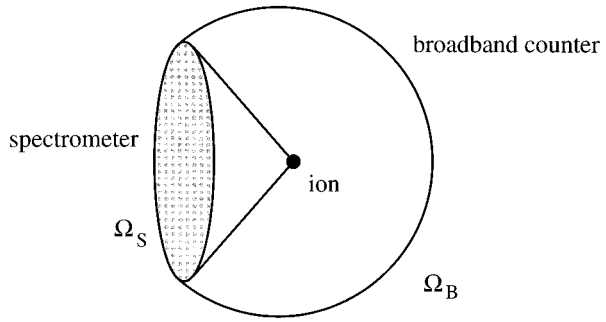

FIG. 10. A schematic representation of a possible experimental setup for the measurement of conditional spectra. The spectrometer occupies a solid angle Ω_S, while the broadband counter occupies Ω_B. The broadband counter performs frequent measurements, while in the spectrometer only one measurement at a late time T is performed.

(152) and then following our derivation of quantum-state diffusion from quantum jumps would have led to the same result.

A slightly different approach to the problem more in the spirit of the derivation of the quantum-jump approach of Hegerfeldt and Wilser (1991) and Wilser (1991) was undertaken by Plenio (1994) and Hegerfeldt and Plenio (1996). Their starting point is the photon number operator, and they define the spectrum via the number of photons that have been emitted into certain narrow frequency intervals (Agarwal, 1974), or, to be more precise, the number of photons in a certain mode of the quantized radiation field [an approach using the electric-field operator that follows similar lines is also possible and is essentially equivalent to the approach of (Gardiner *et al.*, 1992)]. To remain close to a physical picture, they envisaged an experimental situation as depicted in Fig. 10. A part of the quantized radiation field (in a solid angle Ω_B) is observed by a broadband counter, while in the rest of the space (solid angle Ω_S) a spectrometer (for example, a Fabry-Perot) is situated.

The broadband counter performs time-resolved observations on the quantized radiation field. It is again assumed that the time-resolved measurements can be modeled by a sequence of gedanken measurements that are performed in rapid succession, as in the derivation of the quantum-jump approach (Hegerfeldt and Wilser, 1991; Wilser, 1991). At a large time T, we then perform a spectrally resolved measurement of those photons that have entered the spectrometer. In that way one has measured a spectrum with a spectral resolution $\sim 1/T$, which is conditioned on the particular detection sequence one has found in the broadband counter. The derivation of the relevant set of differential equations to calculate the spectrum follows similar ideas, as they were developed in the work of Hegerfeldt and Wilser (1991) and Wilser (1991). The outline of the derivation presented here seems to be more complicated than the one in Eqs. (148)–(153). The reason is that in Eqs. (148)–(153) an infinitesimally small spectrometer was assumed and extensive use of the formalism of quantum stochastic differential equations was made. In the following neither of these assumptions is made. (For a more detailed exhibition of the ideas, see Plenio, 1994; Hegerfeldt and Plenio, 1996). The aim is to calculate differential equations for the conditional photon number in the mode $\mathbf{k}\lambda$, which is given by

$$\mathrm{Tr}\{a^\dagger_{\mathbf{k}\lambda}(0)a_{\mathbf{k}\lambda}(0)\rho(t|t_1,t_2,\ldots,t_n)\}, \tag{154}$$

where $\omega=|\mathbf{k}|/c$, $\hat{\mathbf{k}}=\mathbf{k}/|\mathbf{k}|$, and we assume that $\mathbf{k}$ is a vector pointing into the solid angle Ω_S of the spectrometer. The conditional spectrum of resonance fluorescence is now obtained by summing over all vectors $\mathbf{k}$ in Ω_S. For the calculation of Eq. (50) we need the state $\rho(t|t_1,t_2,\ldots,t_n)$, where photons were detected at times $t_1,\ldots,t_n$ only. With $\mathbb{P}_{0\Omega_B}$ the projection operator onto the vacuum state for all modes with $\hat{\mathbf{k}}\in\Omega_B$ and with the abbreviation

$$\mathcal{A}\equiv\mathbb{P}_{0\Omega_B}U(t,s^n_{m_n})\prod_{k=1}^{m_n}\mathbb{P}_{0\Omega_B}U(s^n_k,s^n_{k-1}), \tag{155}$$

where s^n_k are the times of measurements where no photon was found, we find, for $t_n<t<t_{n+1}$,

$$\rho(t|t_1,t_2,\ldots)=\mathcal{A}\rho(t_n+0|t_1,\ldots,t_{n-1})\mathcal{A}^\dagger, \tag{156}$$

where $\rho(t_n+0|t_1,\ldots,t_{n-1})$ is the state right after the detection of a photon in Ω_B; it is recursively given by

$$\begin{aligned}&\rho(t_n+0|t_1,\ldots t_{n-1})\\&\quad\equiv\mathrm{Tr}_{\Omega_B}\{(1-\mathbb{P}_{0\Omega_B})U(t_n,s^{n-1}_{m_{n-1}})\rho(s^{n-1}_{m_{n-1}}|t_1,\ldots,t_{n-1})\\&\qquad\times U^\dagger(t_n,s^{n-1}_{m_{n-1}})(1-\mathbb{P}_{0\Omega_B})\}\otimes\mathbb{P}_{0\Omega_B}.\end{aligned} \tag{157}$$

Here $\mathrm{Tr}_{\Omega_B}\{\cdot\}$ denotes the partial trace over all modes with a $\mathbf{k}$ vector that points into the solid angle Ω_B. As in the usual quantum-jump approach, at this point the assumption enters that the photons detected in the broadband detector are absorbed during the measurement as in a real counter. One can show, however, that this assumption is not necessary for obtaining the equations of motion used in this section (Plenio, 1994). In fact one can just as well assume ideal quantum-mechanical measurements instead and obtain the same results (Plenio, 1994). This is of course a manifestation of the intuitive physical idea that photons emitted by the atom will not be reabsorbed as long as there are no reflecting mirrors close to the atom. Mathematically it is essentially a consequence of the Markov approximation, which is incorporated elegantly in the formalism of Gardiner *et al.* (1992). The general principle is to first find the Heisenberg-Langevin equations for operators of the form

$$Q^0(t)\equiv U_I^\dagger(t,0)\mathbb{P}_{0\Omega_B}Q\mathbb{P}_{0\Omega_B}U_I(t,0), \tag{158}$$

where $U_I(t,0)$ is the interaction-picture time-evolution operator. With the abbreviation

$$\mathcal{P}_n:=\prod_{j=0}^{m_n}\mathbb{P}_{0\Omega_B}(s^n_j)\prod_{k=0}^{n-1}\left\{C(s^{k+1}_0)\prod_{i=0}^{m_k}\mathbb{P}_{0\Omega_B}(s^k_i)\right\}, \tag{159}$$

where $\mathbb{P}_{0\Omega_B}(t)$ and $C(t)$ are defined similar to Eq. (74) without $\mathbb{P}_{0\Omega_B}$, we then find for Eq. (154)

$$\mathrm{Tr}\{a_M^\dagger(0)\boldsymbol{\sigma}(0)a_M(0)\rho(t|t_1,t_2,\ldots)\}$$
$$=\langle\mathcal{P}_n^\dagger(a_M^\dagger\boldsymbol{\sigma}a_M)^0(t)\mathcal{P}_n\rangle. \tag{160}$$

The next step is to calculate the time derivative of the right-hand side of Eq. (160). Quite similar to the derivation of the quantum regression theorem one can then obtain the final set of differential equations (Plenio, 1994; Hegerfeldt and Plenio, 1996). As long as the solid angle covered by the broadband counter is not equal to 4π, the resulting equations still describe mixtures, since the photons emitted into the spectrometer are not observed in a time-resolved way. For the explicit form of the equations of motion, see Plenio (1994) and Hegerfeldt and Plenio (1996). In the limit of a 4π broadband counter, the resulting equations map pure states into pure states and are actually the same as those derived by Gardiner *et al.* (1992). The main ingredients in this derivation are that the initial state of the quantized radiation field is the vacuum state and that the Markov approximation is valid. Using this approach it is straightforward to derive the quantum-jump approach for the calculation of the absorption spectrum of a weak probe beam by an atom. The idea is to assume that the probe beam consists of a mode that is in a coherent state.

$$|\alpha_{\mathbf{k}\lambda}\rangle=D(\alpha_{\mathbf{k}\lambda})|0\rangle, \tag{161}$$

where

$$D(\alpha_{\mathbf{k}\lambda})=e^{\alpha_{\mathbf{k}\lambda}a_{\mathbf{k}\lambda}^\dagger-\alpha_{\mathbf{k}\lambda}^*a_{\mathbf{k}\lambda}}. \tag{162}$$

One then performs a unitary transformation that maps this coherent state onto the vacuum state. This leads to additional oscillating fields in the Hamiltonian operator and to an initial state in the probe mode which is now the vacuum. Therefore the approach outlined above may be used again. Without further complicated calculations one obtains the spectrum as the change in the photon number in the probe mode. It is possible to show that this definition of the absorption spectrum reduces to the stationary absorption spectrum for sufficiently long times (Plenio, 1994, 1996).

The approaches exhibited so far enable us to simulate spectral information (e.g., the spectrum of resonance fluorescence). They were derived for both a definition of the spectrum via the electric-field operator (Gardiner *et al.*, 1992) and via the photon-number operator (Plenio, 1994; Hegerfeldt and Plenio, 1996). The physically motivated derivation of the formalism by Hegerfeldt and Plenio (1995b; Plenio, 1994) with a finite-size spectrometer yields, as a byproduct, equations of motion for a system that is observed by a counter that does not cover the whole solid angle and/or has below unit efficiency. These equations of motion will later be used to illustrate the connection between the next-photon and the any-photon probability and to show that an inefficient photon counter will not measure the next-photon probability but the any-photon probability, which is proportional to the intensity correlation function $g^{(2)}(t)$.

The approaches discussed so far gave equations that enabled us to calculate the spectrum of resonance fluorescence directly from the norm of a component of a propagated wave function. However, there is a third way to obtain the spectrum of resonance fluorescence, which is via the simulation of the correlation function $\langle\sigma_{10}(t+\tau)\sigma_{01}(t)\rangle$ [where $\sigma_{01}(t)$ is the Heisenberg operator corresponding to $|0\rangle\langle 1|$] and subsequent Fourier transformation of the simulation results. Indeed this is the way in which Dalibard, Castin, and Mølmer (Mølmer *et al.*, 1993; Mølmer, 1994) and others (Mu, 1994; Garraway, Kim, and Knight, 1995) employed the quantum-jump approach to obtain simulations of the spectrum of resonance fluorescence. The simulation procedure for a correlation function of the form $C(t+\tau)=\langle A(t+\tau)B(t)\rangle$ runs as follows. First one evolves using the Monte Carlo wave-function approach a wave function $|\phi(0)\rangle$ towards $|\phi(t)\rangle$. Then one forms the auxiliary wave functions

$$|\chi_\pm(0)\rangle=\frac{1}{\sqrt{\mu_\pm}}(1\pm B)|\phi(t)\rangle, \tag{163}$$

$$|\chi'_\pm(0)\rangle=\frac{1}{\sqrt{\mu'_\pm}}(1\pm iB)|\phi(t)\rangle, \tag{164}$$

where the $\mu_\pm,\mu'_\pm$ are normalization constants. Now one has to evolve each of these four wave functions according to the Monte Carlo wave-function procedure and then to form

$$c_\pm(\tau)=\langle\chi_\pm(\tau)|A|\chi_\pm(\tau)\rangle, \tag{165}$$

$$c'_\pm(\tau)=\langle\chi'_\pm(\tau)|A|\chi'_\pm(\tau)\rangle, \tag{166}$$

from which one obtains

$$C(t,\tau)=\frac{1}{4}[\mu_+\overline{c_+}(\tau)-\mu_-\overline{c_-}(\tau)-i\mu'_+\overline{c'_+}(\tau)$$
$$+i\mu'_-\overline{c'_-}(\tau)]. \tag{167}$$

It can be shown that this procedure produces the correct ensemble averages (Dalibard *et al.*, 1992). A subsequent Fourier transform of the simulation results yields a spectrum. This procedure has been used, for example, to simulate the spectrum of a three-level system in a V configuration (Garraway, Kim, and Knight, 1995). However, care has to be taken in this procedure because, if one only performs a single Fourier transform to obtain the stationary spectrum

$$S_1(\omega):=2\,\mathrm{Re}\int_0^\infty d\tau\, e^{i\Delta\tau}\langle\sigma_{10}(\tau)\sigma_{01}(0)\rangle_{ss}, \tag{168}$$

one inevitably runs into difficulties, as one can only simulate finite times. Then, however, the Fourier transformation yields spurious negativities in the power spectrum that are due to finite-time effects. This problem can be circumvented by using a finite-time double integral of the correlation function, as required in the definition of the time-dependent spectrum.

$$S_T(\omega):=\frac{1}{T}\int_0^T dt'\int_0^T dt''e^{i\Delta(t'-t'')}\langle\sigma_{10}(t')\sigma_{01}(t'')\rangle. \tag{169}$$

This quantity has the advantage that it is manifestly positive for each realization, as it is of the form $\langle A^\dagger A\rangle$. However, this considerably slows down the simulation procedure because the integral transform is now much more complicated.

A different criticism should be mentioned concerning the interpretation of a single run of this simulation procedure. While the derivation of the simulation procedure by Hegerfeldt and Plenio (1996) clearly shows that a physical interpretation of a single run in the schemes derived in Hegerfeldt and Plenio (1996), Plenio (1994), and Gardiner *et al.* (1992) is possible, this is not obviously the case for the simulation procedure of Mølmer *et al.* (1993). A problem lies in the fact that four different wave functions have to be propagated in the procedure, each of which might follow different jump sequences. Furthermore, even if only one jump sequence is followed, it is not clear what the interpretation of the correlation function is. This may be illustrated by the following example. We now would like to simulate a trivial correlation function of the form $\langle 1(t+\tau)A(t)\rangle$. We would expect that in each realization the simulation procedure would give the same result as for the single time-expectation value $\langle A(t)\rangle$. This, however, is not the case, as is easily seen in the following example. We assume a spontaneously decaying two-level system and the initial state

$$|\phi(0)\rangle=\left(\frac{1}{1+e^2}\right)^{1/2}(|0\rangle+e|1\rangle). \tag{170}$$

The emission-free time evolution is given by

$$U_0(t+t',t)=e^{\mathbf{M}t'}, \tag{171}$$

where

$$\mathbf{M}=\begin{pmatrix}0 & 0\\ 0 & -\Gamma_{22}\end{pmatrix}. \tag{172}$$

If we assume that no jump at all occurs until $t+\tau$, we obtain, according to the procedure of Mølmer *et al.* (1993), the single-run result for the correlation function $\langle 1(t+\tau)\sigma_{01}(t)\rangle$ to be

$$\langle 1(t+\tau)\sigma_{01}(t)\rangle=\frac{1}{1+e^{-2\Gamma_{11}\tau}}, \tag{173}$$

while the expectation value of the operator $\sigma_{01}(t)$ at time $t=1/\Gamma_{11}$ is given by

$$\langle\sigma_{01}(t=1/\Gamma_{11})\rangle=\frac{1}{2}. \tag{174}$$

These two expressions obviously differ. Therefore we can conclude that the simulation procedure of Mølmer *et al.* (1993) yields the correct ensemble results; however, if we are interested in questions concerning single runs or spectra conditioned on a given jump statistics, care has to be taken, and it is safer to resort to the approaches of Dum, Parkins, *et al.* (1992), Gardiner *et al.* (1992), and Hegerfeldt and Plenio (1996; Plenio, 1994). Applications to conditioned spectra will be given later in Sec. V.

Here we have only described in detail quantum-jump approaches to calculate spectral information. Of course one can also obtain a quantum-state diffusion simulation of spectral information. One can derive the equations, either by starting out from the quantum-jump equations given above and then following our derivation of the quantum-state diffusion equations as a result of heterodyne detection, or by deducing the equations, given that the system couples to an additional output mode [i.e., similar to (Gardiner *et al.*, 1992) but here literally one mode of the quantized radiation field is chosen] and then writing down the master equation for that enlarged system. From that one can then easily obtain quantum-state-diffusion equations (Brun and Gisin, 1996). However, if one tries to apply the equations to the calculation of time correlation functions of the form $\langle A(t+\tau)B(t)\rangle$, one again encounters interpretational problems similar to those explained for the approach of Mølmer *et al.* described above. It should be noted that the approach to calculate time correlation functions given by Gisin (1993) does not lead to $\langle A(t+\tau)B(t)\rangle$ as usually defined in quantum optics, but to a different correlation quantity that is difficult to interpret (Sondermann, 1995a).

V. APPLICATIONS OF THE QUANTUM-JUMP APPROACH

A. Photon statistics

In the previous sections we have introduced and discussed the quantum-jump approach, illuminating many different approaches to it. After these sometimes formal considerations, we would like to give a number of examples to give a better understanding of the formalism and its physical implications. The examples will be drawn mainly from two physical situations: single trapped ions driven by lasers and electromagnetic fields in cavities, i.e., cavity QED.

We start by illustrating the difference between single realizations and ensemble averages by investigating a laser-driven two-level system damped by a zero-temperature quantized radiation field. The master equation is then given by

$$\dot\rho=-\frac{i}{\hbar}[H_A,\rho]-\Gamma\{\sigma_{11}\rho+\rho\sigma_{11}\}+2\Gamma\sigma_{01}\rho\sigma_{10}, \tag{175}$$

with

$$H_A=-\hbar\Delta|1\rangle\langle 1|+\frac{\hbar\Omega}{2}(|0\rangle\langle 1|+|1\rangle\langle 0|), \tag{176}$$

where 2Γ equals the Einstein coefficient of the observed two-level system, Ω is the Rabi frequency, and Δ is the detuning of the laser.

Assuming standard broadband photodetection, the quantum-jump approach gives for the conditional time evolution between detections

$$|\psi(t)\rangle=e^{-iH_{eff}t/\hbar}|\psi(0)\rangle, \tag{177}$$

with

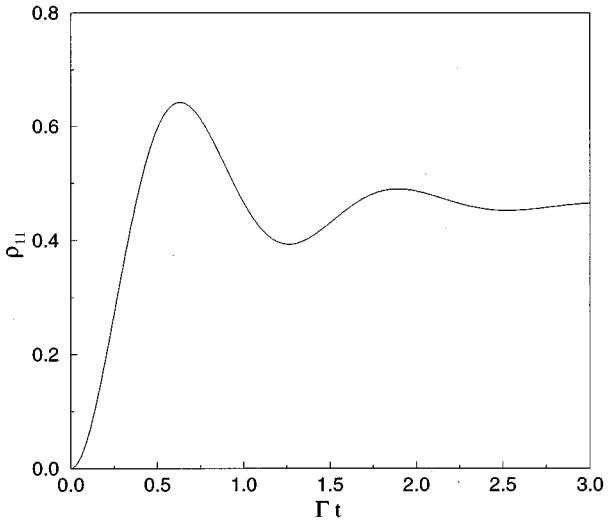

FIG. 11. The upper-state population ρ_{11} of an ensemble of two-level systems, which is driven by a laser with Rabi frequency $\Omega=5\Gamma$ and vanishing detuning $\Delta=0$. The system exhibits some oscillations and then approaches a nonzero steady-state value.

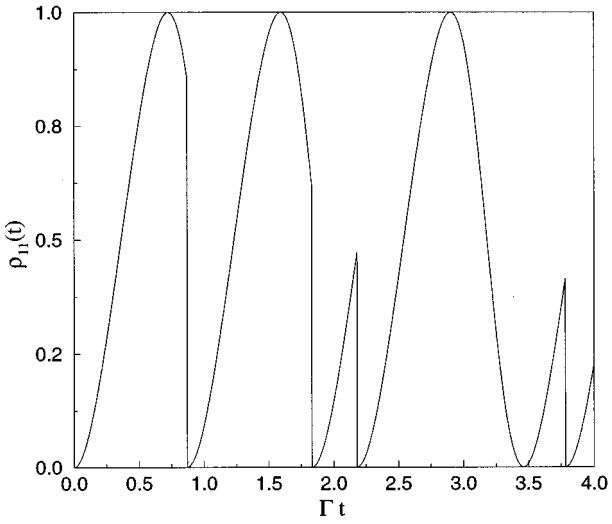

FIG. 12. The time evolution of the upper-state population ρ_{11} of a single driven two-level system. As in Fig. 11 the two-level system is driven by a laser with Rabi frequency $\Omega=5\Gamma$ and vanishing detuning $\Delta=0$. The system starts a Rabi oscillation, which is then interrupted by a quantum jump (detection of a photon). After the jump the system is reset in the ground state and a new Rabi oscillation starts. After Garraway *et al.* (1995).

$$H_{eff}=H_A-i\hbar\Gamma, \tag{178}$$

and for the normalized state after the detection of a photon

$$|\psi(t_+)\rangle=\frac{\sigma_{01}|\psi(t)\rangle}{\|\sigma_{01}\psi(t)\|}=|0\rangle. \tag{179}$$

The probability for not having a jump in the time interval $[0,t]$, if the initial state is the ground state, $|\psi(0)\rangle=|1\rangle$, is given by

$$P_0(t)=\langle\psi_{eff}(t)|\psi_{eff}(t)\rangle=\frac{\lambda_2}{\lambda_2-\lambda_1}e^{\lambda_1 t}-\frac{\lambda_1}{\lambda_2-\lambda_1}e^{\lambda_2 t}, \tag{180}$$

with

$$\lambda_{1/2}=\frac{-\Gamma+i\Delta}{2}\pm\frac{\sqrt{\Gamma^2-\Delta^2-\Omega^2-2i\Delta\Gamma}}{2}. \tag{181}$$

Using the parameters $\Omega=5\Gamma$ and $\Delta=0$, the upper-state population ρ_{11} of the ensemble evolves as shown in Fig. 11, where the initial state is the ground state. The population rises from zero, undergoing some Rabi oscillations, and then tends towards a steady state. Now let us look at individual realizations of the time evolution using the same parameters and initial conditions. The result for one possible realization is shown in Fig. 12. The picture is strikingly different from Fig. 11 in that the time evolution is not smooth, but exhibits jumps, and it does not tend towards a steady state. We rather observe that initially the system starts to perform a Rabi oscillation. As the population in the upper level grows in time so does the probability for the emission of a photon. This oscillation is then terminated by the emission of a photon that brings the atom back to its ground state. Then the whole process starts again. Figures 11 and 12 show little similarity; however, averaging over many individual realizations shown in Fig. 12 leads to a closer and closer approximation of the ensemble average. To illustrate this we have plotted the ensemble result together with the average over $N=100$ and 10000 individual realizations in Fig. 13. It is found that the root-mean-square deviation of the simulated average from the exact ensemble result is of the order of $1/\sqrt{N}$. We have examined the photon statistics of a two-level sys-

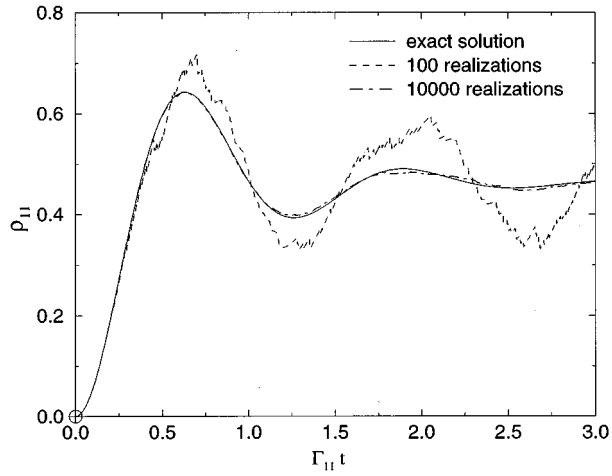

FIG. 13. The ensemble result of Fig. 11 is compared to the average over $N=100$ and $N=1000$ realizations generated using the quantum-jump approach. The fluctuations of the averages become smaller with increasing N, and the ensemble average gets approximated more and more closely. The Rabi frequency is $\Omega=5\Gamma$, and the detuning is $\Delta=0$.

tem by detecting all the photons emitted by the atom with high time resolution, as we assumed that the counter has unit efficiency and covers the whole solid angle. Assuming this, one would be able to measure the next-photon probability density $I_1(t)$. However, in a real experiment the counter efficiency is much less than unity, due to imperfect quantum efficiency and because only a finite solid angle is covered by the counter. Therefore the question is which function we actually measure when we perform a real experiment in which we determine the detection time of the next photon in our imperfect counter.

To answer this question we would like to employ the quantum-jump approach, assuming a perfect photon counter, which, however, does not cover all space. If it covers a solid angle Ω_B, then this is equivalent to a 4π counter of efficiency $\beta=\Omega_B/4\pi$. The equation of motion for this setup up has been derived in Sec. IV in connection with the simulation of spectral information [see Eqs. (154)–(160)]. The efficiency β of the detection process is the fraction of the emitted photons that are actually detected. We obtain the conditional equation of motion for the density operator under the assumption that no photon has been detected in the counter,

$$\dot{\rho}_0=-\frac{i}{\hbar}\{H_{eff}\rho_0-\rho_0 H_{eff}\}+2\Gamma(1-\beta)\sigma_{01}\rho\sigma_{10}. \tag{182}$$

H_{eff} is given by Eq. (178), and one should note that now the conditional time evolution does not map pure states onto pure states. This is of course due to the incomplete information gained from the imperfect counter. Therefore we have to average over all possible events that the counter could not detect, and this leads to a mixture. One observes two familiar limits: for zero counter efficiency we recover the ordinary optical Bloch equations, whereas for unit efficiency $\beta=1$ we find the effective time evolution inferred from the assumption that no photon has been found in the whole solid angle, given a perfect counter.

Having found Eq. (182), we can now calculate the probability that the detector finds no photon in the time interval $[0,t]$

$$P_0(t)=\mathrm{Tr}\{\rho_0(t)\}, \tag{183}$$

which reduces to Eq. (55) or Eq. (66) in the limit $\beta\to 1$. The next-count rate is then the negative time derivative of Eq. (183)

$$I_{1,\beta}(t)=2\Gamma\beta\rho_{11}(t), \tag{184}$$

where ρ_{22} is obtained by solving Eq. (182). Instead of solving this equation analytically, we plot the solution for several different counter efficiencies β. We assume $\Gamma=1$ and $\Omega=5\Gamma$. In Fig. 14 we plot the next-detection probability for counter efficiency $\beta=1$, $\beta=0.1$, and $\beta=0.0049$, where the latter value of β is computed from Mandel's antibunching experiments (Kimble *et al.*, 1977; Dagenais and Mandel, 1978). We observe that, for decreasing counter efficiency, the function Eq. (184) approximates the any-photon probability of the whole ensemble, which becomes more and more closely proportional to the intensity correlation function $g^{(2)}(t)$. So far we have shown how to calculate the next-detection rate for different counter efficiencies from the quantum-jump approach. We have plotted the results numerically. However, it is also possible to derive an analytical expression in a somewhat different way. This was done in Kim *et al.* (1987) and was in fact one earlier approach to the problem. As described earlier one can utilize the fact that there is a very simple relation between the any-photon rate $I_\beta(t)$ of the complete ensemble and the next-detection rate $I_{1,\beta}(t)$ for a counter with efficiency β. This relation can be found using

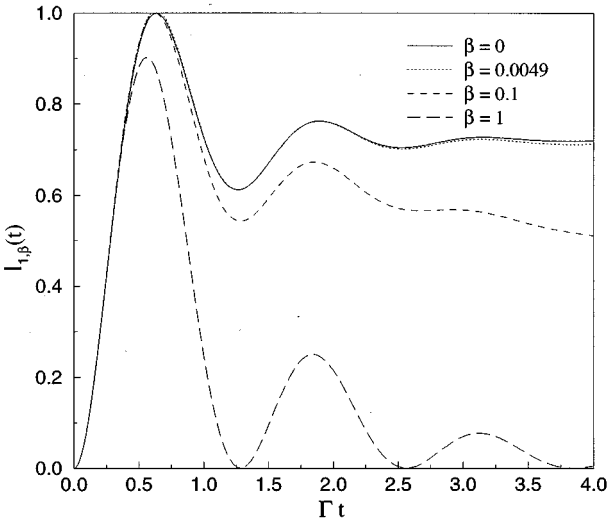

FIG. 14. The next-photon rate for different counter efficiencies $\beta=1$, $\beta=0.1$, and $\beta=.0049$, and the any-photon probability that is obtained in the limit $\beta=0$. The Rabi frequency is $\Omega=5\Gamma$, and the detuning is $\Delta=0$.

$$\rho_{11}(t)=\rho_{11}^{(\beta)}(t)+\int_0^t dt'\,\rho_{11}(t-t')2\Gamma\beta\rho_{11}^{(\beta)}(t'), \tag{185}$$

and

$$I_{1,\beta}(t)=2\Gamma\beta\rho_{11}^{(\beta)}(t), \tag{186}$$

$$I_\beta(t)=2\Gamma\beta\rho_{11}(t), \tag{187}$$

where $\rho_{11}^{(\beta)}(t)$ is calculated from Eq. (182). Inserting this and taking the Laplace transform yields

$$\hat{I}(z)=\frac{1}{\beta}\frac{\hat{I}_{1,\beta}(z)}{1-\hat{I}_{1,\beta}(z)}. \tag{188}$$

The intensity correlation function $g^{(2)}(t)$ is related to the any-photon rate $I_\beta(t)$ for an imperfect counting process by

$$2\Gamma\rho_{11}(\infty)\beta g^{(2)}(t)=I_\beta(t). \tag{189}$$

Therefore we obtain

$$\hat{I}_{1,\beta}(z)=\frac{2\Gamma\rho_{11}(\infty)\beta\hat{g}^{(2)}(z)}{2\Gamma\rho_{11}(\infty)\beta\hat{g}^{(2)}(z)+1}, \tag{190}$$

where $\hat{g}^{(2)}(z)$ is the Laplace transform of the intensity correlation function $g^{(2)}(t)$.

One should note that the intensity correlation function does not depend on the efficiency β, as it is normalized with respect to the stationary detection rate. From Eq. (190) one observes that, up to a normalization factor, the next-photon probability tends towards the intensity correlation function. Inserting the well-known expressions for the stationary state of the two-level system and the intensity correlation function for zero detuning

$$\rho_{22}(\infty)=\frac{\Omega^2}{2\Omega^2+4\Gamma^2} \tag{191}$$

and

$$\hat{g}^{(2)}(z)=\frac{\Omega^2+2\Gamma^2}{z[(z+3\Gamma/2)^2+\Omega^2-\Gamma^2/4]} \tag{192}$$

into Eq. (190), we obtain

$$\hat{I}_{1,\beta}(z)=\frac{\beta\Omega^2\Gamma}{(z+\Gamma)[z(z+2\Gamma)+\Omega^2(z+\beta\Gamma)]}. \tag{193}$$

This Laplace transform can be inverted easily. Plotting this function exactly reproduces Fig. 14 if one normalizes the maximum of $I_{1,\beta}(t)$ to unity.

B. Intermittent fluorescence

After this discussion of the photon statistics of the resonance fluorescence of a two-level system, we now proceed to illustrate the formalism for a more complex system, namely, a three-level system in V configuration as shown in Fig. 1. We assume that the $0\leftrightarrow1$ transition is strongly allowed while the $0\leftrightarrow2$ transition is metastable. In a typical experiment one would have a lifetime of the order of seconds for the metastable level 2, while the unstable level 1 has a lifetime of several nanoseconds. The system is irradiated by two lasers, one on each transition. The Rabi frequency Ω_1 of the laser driving the $0\leftrightarrow1$ transition is assumed to be much larger than the Rabi frequency Ω_2 on the $0\leftrightarrow2$ transition. If one observes the intensity of resonance fluorescence on the strong transition under these conditions one typically obtains a result as shown in Fig. 2, or, in a more schematical representation, in Fig. 4. Long periods of brightness with many photon counts (bright periods) are interrupted by prolonged periods with no photodetections (dark periods). As we discussed previously, a simplified treatment of this situation using rate equations was given by Cook and Kimble (1985; Kimble *et al.*, 1986). However, as the described situation involves lasers, a more detailed treatment is required, as coherences can play a crucial role in the time evolution of the system. Such treatments were initially undertaken using Bloch equations, but this is not the most natural description of the problem. Such a natural description of the problem was provided by the quantum-jump approach. In the following we will use the quantum-jump approach to calculate the photon statistics of the V system, and we will use it to gain interesting and sometimes surprising insights into the single-system dynamics. It will turn out that the rate-equation treatment of Cook and Kimble, while giving a qualitative picture, is insufficient to explain many interesting properties of the system. A similar analysis can be carried out for other systems, such as a Λ configuration (Agarwal *et al.*, 1988b; Plenio, 1994; Hegerfeldt and Plenio, 1995a), and in a system where both upper levels couple strongly to the ground level but are close together (Hegerfeldt and Plenio, 1992, 1993, 1994; Köhler, 1996).

In the following analysis we will always assume that both bright and dark periods are much longer than the lifetime of the unstable level 1. This condition is necessary from a physical point of view, as otherwise one would not be able to distinguish between a dark period and the time interval between two successive emissions in a bright period. Also a bright period consisting of approximately one photon has little meaning. With the detuning Δ_i and Rabi frequencies Ω_i of the lasers on the $0\leftrightarrow i$ transition, we obtain the condition (Hegerfeldt and Plenio, 1995b)

$$\Omega_2^2\ll\frac{1}{4}\frac{16\Delta_2^2\Gamma_{11}^2+(\Omega_1^2+4\Delta_2(\Delta_1-\Delta_2))^2}{\Gamma_{11}^2+(\Delta_1-\Delta_2)^2}, \tag{194}$$

where $2\Gamma_{11}$ equals the Einstein coefficient of level 1. This condition assumes that the Einstein coefficient of level 2 is negligible. Again this can be cast into an analytical form. We require (Hegerfeldt and Plenio, 1995b)

$$\Gamma_{22}\ll\frac{\Omega_1^2\Omega_2^2\Gamma_{11}}{16\Delta_2^2\Gamma_{11}^2+\{\Omega_1^2+4\Delta_2(\Delta_1-\Delta_2)\}^2}, \tag{195}$$

which expresses the fact that spontaneous emissions from level 2 are much less frequent than stimulated transitions. This also implies that there are sufficiently many long dark periods. These conditions can be obtained by first solving the problem for $\Gamma_{22}=0$. Then one has to note that one obtains bright and dark periods only if the waiting-time distribution has two very different decay constants. Two different decay constants are obtained if Eqs. (194) and (195) are satisfied. The conditions Eqs. (194) and (195) take on a simpler form, e.g., when one assumes $\Delta_1=\Delta_2=0$.

To be able to calculate the mean lengths of bright and dark periods, we need to define precisely what we mean by bright and dark periods. To distinguish between bright and dark periods we introduce a time T_0. If our perfect photodetector fails to detect a photon in a time interval $[0,T_D]$, where it has found a photon at time $t=0$, we speak of a dark period of length T_D. If, however, in a time interval $[0,T_L]$ the time between successive photon detections is always less than T_0, we have a bright period of length T_L. Using these definitions and the next-photon probability density $I_1(t)$, we obtain for the mean length of a dark period

$$T_D(T_0)=\frac{\int_{T_0}^{\infty}dt'\,t'I_1(t')}{\int_{T_0}^{\infty}dt'\,I_1(t')}=T_0+\frac{\int_{T_0}^{\infty}dt'\,P_0(t')}{P_0(T_0)}, \tag{196}$$

while the mean length of a bright period is

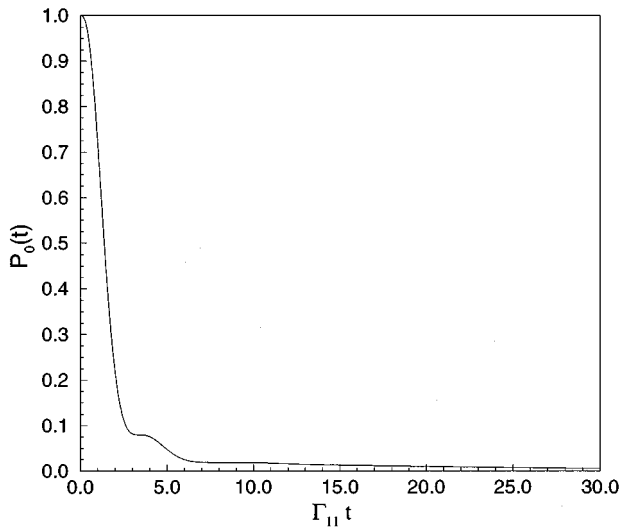

FIG. 15. The waiting-time distribution $P_0(t)$ of the V system describing the probability that after an emission at $t=0$ no other emission has taken place until t. Parameters are $\Omega_1=2\Gamma_{11}$, $\Omega_2=0.35\Gamma_{11}$, $\Delta_1=\Delta_2=0$, and $\Gamma_{22}=0$, where Γ_{ii} are decay constants. One observes a slowly decaying tail of $P_0(t)$, indicating the possibility of dark periods.

$$T_L(T_0)=\frac{1}{P_0(T_0)}\frac{\int_0^{T_0}dt'\,t'I_1(t')}{\int_0^{T_0}dt'I_1(t')}. \tag{197}$$

These expressions appear to be quite complicated, but they can be simplified when we use the assumption that bright and dark periods are long compared to the lifetime of level 1. In that case it is obvious that the time evolution of the system has two widely different time scales, one determining the emission rate during bright periods, the other giving the rate at which dark periods occur. This is reflected in the fact that the probability to find no photon in the interval $[0,t]$ has a slowly decaying tail as we can observe from Fig. 15, where we plot $P_0(t)$ for the parameters $\Omega_1=2\Gamma_{11}$, $\Omega_2=0.35\Gamma_{11}$, $\Delta_1=\Delta_2=0$, and $\Gamma_{22}=0$. If we choose T_0 such that it is much larger than the mean time between photon detections in a bright period while still being much shorter than the mean length of a dark period, we can reliably distinguish between bright and dark periods. The choice of T_0 implies that

$$P_0(T_0)=pe^{-2T_0\,\mathrm{Im}(\lambda_1)}\cong p\ll 1, \tag{198}$$

where λ_1 is the smallest eigenvalue of the effective Hamiltonian of the system

$$H_{eff}=\begin{pmatrix} 0 & -\frac{\Omega_1}{2} & -\frac{\Omega_2}{2} \\ -\frac{\Omega_1}{2} & i\Gamma_{11}+\Delta_1 & 0 \\ -\frac{\Omega_2}{2} & 0 & \Delta_2 \end{pmatrix}. \tag{199}$$

Simplifying Eqs. (196) and (197), we then obtain

$$T_D(T_0)=\frac{1}{-2\ \mathrm{Im}\ \lambda_1} \tag{200}$$

and

$$T_L(T_0)=\frac{\tau_L}{p}, \tag{201}$$

where τ_L is the mean time between successive photodetections in a bright period

$$\tau_L(T_0)=\int_0^{T_0}dt'\,t'I_1(t')\Big/\int_0^{T_0}dt'I_1(t'). \tag{202}$$

The mean time interval between successive emissions in a bright period can be found from Eq. (202), or more easily from

$$\tau_L=\frac{1}{2\Gamma_{11}\rho_{11}^{TLS}}, \tag{203}$$

where ρ_{11}^{TLS} is the population of the upper level 1 of a two-level system driven by a laser of Rabi frequency $\Omega_1=2\Gamma_{11}$ and $\Delta_1=0$. Now it is quite easy to obtain analytical expressions for T_D and T_L. We find

$$T_D=\frac{16\Delta_2^2\Gamma_{11}^2+(\Omega_1^2-4\Delta_2(\Delta_2-\Delta_1))^2}{2\Omega_1^2\Omega_2^2\Gamma_{11}}, \tag{204}$$

$$T_L=\frac{2\Delta_1^2+2\Gamma_{11}^2+\Omega_1^2}{2\Gamma_{11}^2+2(\Delta_1-\Delta_2)^2}T_D. \tag{205}$$

We see that under the conditions of Eqs. (194) and (195) both bright and dark periods are much longer than the lifetime of the unstable $0\leftrightarrow 1$ transition.

Investigating the average rate $1/(T_D+T_L)$ at which we observe quantum jumps, i.e., the onset of dark periods, we see that it depends on the detuning of the laser on the $0\leftrightarrow 2$ transition. If we assume that the strong laser ($\Omega_1\gg\Gamma_1$) is resonant ($\Delta_1=0$), we observe that the ratio $1/(T_D+T_L)$ becomes minimal when $\Delta_2=0$ and maximal for the Autler-Townes or Stark split detunings $\Delta_2=\pm\Omega_1/2$.

$$\frac{1}{T_D+T_L}=\frac{4\Omega_1^2\Omega_2^2\Gamma_{11}}{16\Delta_2^2\Gamma_{11}^2+(\Omega_1^2-4\Delta_2^2)^2}\frac{\Gamma_{11}^2+\Delta_2^2}{4\Gamma_{11}^2+2\Delta_2^2+\Omega_1^2}. \tag{206}$$

This dependence on the detuning Δ_2 reflects the fact that due to the strong driving of the $0\leftrightarrow 1$ transition, the lower level exhibits Autler-Townes splitting. The two effective levels are shifted by $\pm\Omega_1/2$ with respect to the original level 0. To obtain long dark periods one needs to bring the weak laser on the $0\leftrightarrow 2$ transition into resonance with one of the dressed states of the $0\leftrightarrow 1$ transition. The resulting frequency dependence is shown in Fig. 16. Before we proceed with the investigation of the single system behavior, we show again, now quantitatively, that the existence of bright and dark periods in the resonance fluorescence has a visible effect on the ensemble quantities too. To see this, we plot the intensity correlation function $g^{(2)}(\tau)$ in Fig. 17. We observe that there is a slowly decaying contribution for times

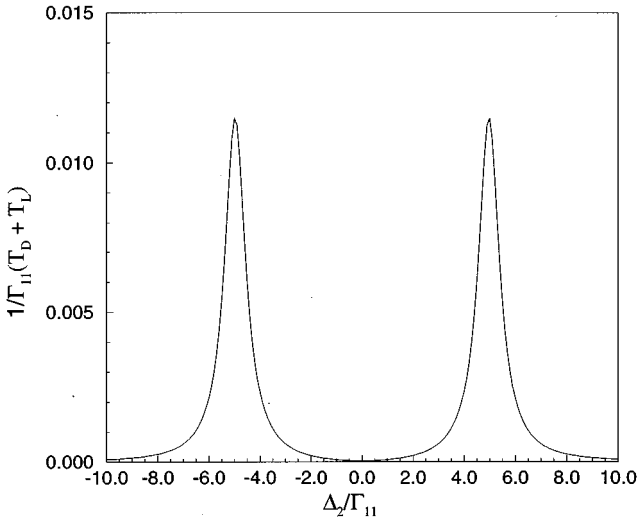

FIG. 16. $1/(T_D+T_L)$, representing the average rate at which quantum jumps will be observed in the three-level V system, as a function of the detuning Δ_2 on the weak transition. The parameters are $\Omega_1=10\Gamma_{11}$, $\Omega_2=0.3\Gamma_{11}$, $\Delta_1=0$, and $\Gamma_{22}=0$. One observes that the maximum quantum-jump rate is achieved for detunings $\Delta_2=\pm\Omega_1/2$, illustrating the Autler-Townes splitting of the ground state.

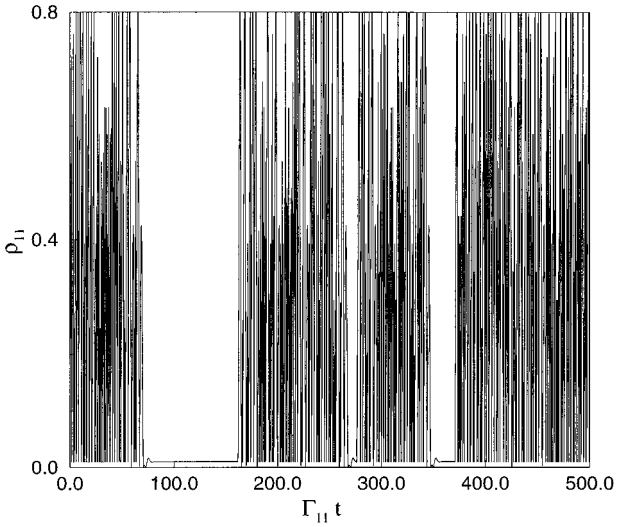

FIG. 18. The time evolution of the population ρ_{11} of the rapidly decaying level in the V system. Periods where the time evolution exhibits rapid Rabi oscillations interrupted by quantum jumps can suddenly stop and lead to periods of no Rabi oscillations and no jumps. The parameters are $\Omega_1=2\Gamma_{11}$, $\Omega_2=0.2\Gamma_{11}$, $\Delta_1=0$, $\Delta_2=0$, and $\Gamma_{22}=0$.

$\tau\gg\Gamma_{22}^{-1}$, quite similar to the behavior of the next-photon probability density $I_1(t)$ shown in Fig. 15. One can show that in this regime we can approximate $g^{(2)}(\tau)$ by

$$g^{(2)}(\tau)\cong 1+\frac{T_D}{T_L}\exp\left\{\left(\frac{1}{T_D}+\frac{1}{T_L}\right)\tau\right\}, \tag{207}$$

where T_D and T_L are given by Eqs. (204) and (205). Therefore, from the measurement of the $g^{(2)}$ function, we can infer the existence of long bright and dark periods, and one can determine their mean lengths. The fact that this information is hidden in the intensity correlation function is not surprising, as it is proportional to the any-photon rate $I(\tau)$, which is related to the next-photon rate $I_1(\tau)$ via

$$I(\tau)=I_1(\tau)+\int_0^\tau d\tau' I(\tau-\tau')I_1(\tau'). \tag{208}$$

Later we will also show that the existence of bright and dark periods also leaves its fingerprints in the spectrum of resonance fluorescence as well as in the absorption spectrum.

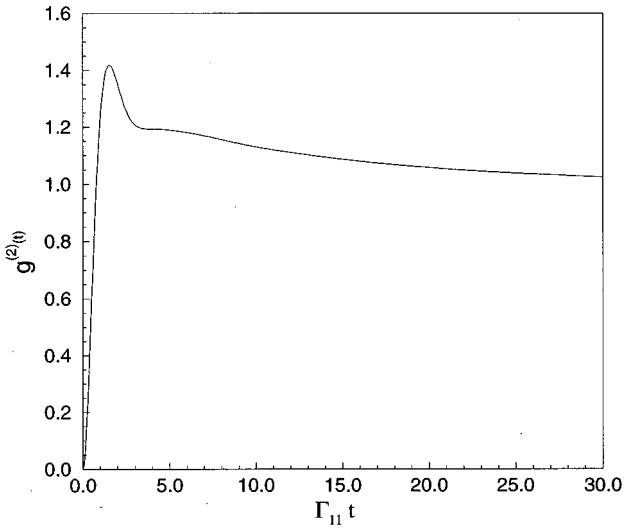

FIG. 17. The intensity correlation function $g^{(2)}(\tau)$ of a V system for the same parameters as in Fig. 15. One clearly observes that $g^{(2)}(t)$ first falls off quickly to a value of around 1.2 for times around $\tau\approx 5\Gamma_{11}^{-1}$ and then starts to fall off slowly towards the stationary value of 1.

After this analytical discussion of the photon statistics of the V system, we will now investigate what the system time evolution for a single realization will typically look like. For the parameters $\Omega_1=2\Gamma_{11}$, $\Omega_2=0.2\Gamma_{11}$, $\Delta_1=0$, $\Delta_2=0$, and $\Gamma_{22}=0$, we have plotted both the time evolution of the population ρ_{11} of the unstable level 1 and population ρ_{22} of the metastable level 2. In Fig. 18 one observes that in some regions a rapid change of ρ_{11} accompanied by many detections takes place. However, there are also regions where no photon is found and most of the population is in level 2 (with a remnant still in level 1). One should note that, as seen in Fig. 19, the population in level 2 grows continuously and does not jump from level 0 into level 2, as one might expect from a rate-equation picture. Nevertheless, there is a jump, not at the beginning of the dark period, but at its end (Wilser, 1991; Garraway, Knight, and Steinbach, 1995), as we can see in Fig. 20, where we have magnified the time evolution of ρ_{11} in a dark period. The jump occurs after a long time and marks the end of the dark period, as after the jump the population is in the ground state,

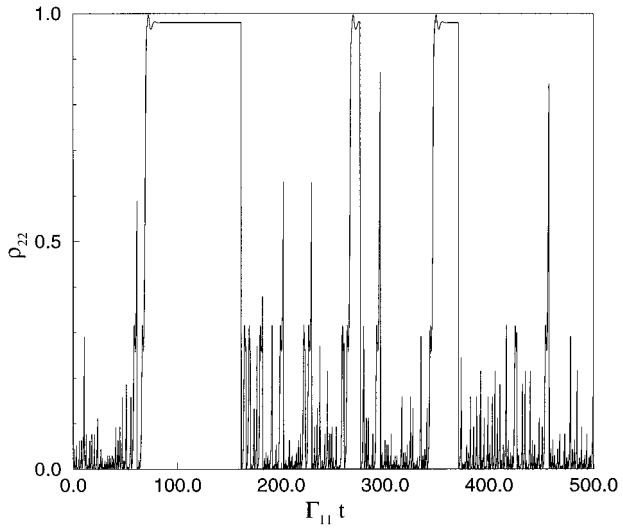

FIG. 19. The population ρ_{22} of the metastable state 2 with the same parameters as in Fig. 18. One clearly observes that during a dark period the population evolves smoothly into the metastable state 2.

which is strongly coupled to state 1. It should be noted that in the simulation shown in Figs. 18–20 the decay rate of the metastable level was assumed to be $\Gamma_{22}=0$, which implies that the dark period always ends with an emission from level 1. The continuous change of population towards the metastable state in a dark period nicely clarifies the importance of the failure to detect photons (null measurements) for the time evolution of the wave function. The failure to detect a photon provides us information about the system state that is described by the wave function. In this case the no-detection event tells us that we are more likely to find the system in the metastable state. Accordingly, the wave function quickly (within several lifetimes of the unstable level) tends towards the metastable state if we have not found a photon during this time. The evolution is continuous, as we assume (in the limit of the Markov approximation) continuous measurements of the radiation field. Therefore the failure to detect a photon in an infinitesimal time interval $[t,t+\delta t]$ leads to an infinitesimal change proportional to δt. Conversely, the detection of a photon leads to a discontinuous change of the wave function because one quantum of energy has leaked out of the system into the environment. Therefore the system has to change discontinuously and jumps back into its ground state. Again this change of the wave function is due to our increased knowledge of the system.

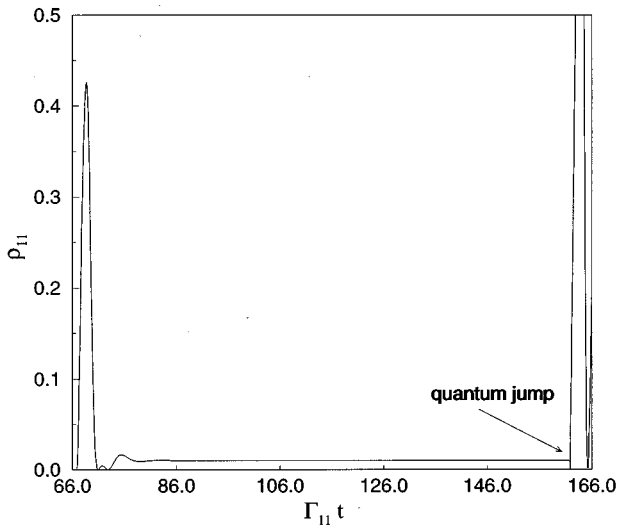

FIG. 20. The population of the unstable state 1 in a dark period for the same parameters as in Fig. 18. The population does not jump out of level 1 but evolves continuously. However, at the end of the dark period a jump occurs that is due to an emission for level 1 because we assumed the shelving level 2 to be stable.

C. From quantum jumps to quantum-state diffusion

So far we have only illustrated the quantum-jump approach to the photon statistics of a single ion. In Sec. IV we have seen that other pictures are possible, namely, the quantum-state-diffusion picture. Instead of presenting a large number of examples of the quantum-state-diffusion model, we rather want to illustrate how the transition from the quantum-jump picture to the quantum-state-diffusion picture takes place. In Sec. IV we have seen how to derive the quantum-state-diffusion equations from a quantum-jump description of a balanced heterodyne-detection experiment. In this derivation we had to assume the limit in which the photon number in the local oscillator tends to infinity. In the following we will illustrate this limit by choosing a number of finite values for the photon number of the local oscillator. To keep the following analysis as simple as possible, we in fact do not consider the case of balanced heterodyne detection but of homodyne detection (Vogel and Welsch, 1994). Instead of a cavity we will investigate the time evolution of a laser-driven two-level system with upper level 1 and lower level 0. We follow the presentation given by Granzow (1996). For the simulations we need to know two quantities. The Lindblad operator for the homodyne-detection scheme is given by

$$L=|0\rangle\langle 1|+\alpha\mathbf{1}, \tag{209}$$

where α is the field amplitude of the local oscillator. As the Lindblad operator is changed and depends on α, so does the effective Hamiltonian operator between photon detections. We have

$$H_{eff}=-\hbar\Delta|1\rangle\langle 1|-\frac{\hbar\Omega}{2}(|1\rangle\langle 0|+|0\rangle\langle 1|) -i\hbar\Gamma_{11}(L^{\dagger}L+\alpha^{*}L+\alpha L^{*}|\alpha|^{2}), \tag{210}$$

where $2\Gamma_{11}$ equals the Einstein coefficient of the upper level 1, Ω is the Rabi frequency on the $0\leftrightarrow 1$ transition, and Δ is the detuning. The probability for a jump in the time interval δt is given by

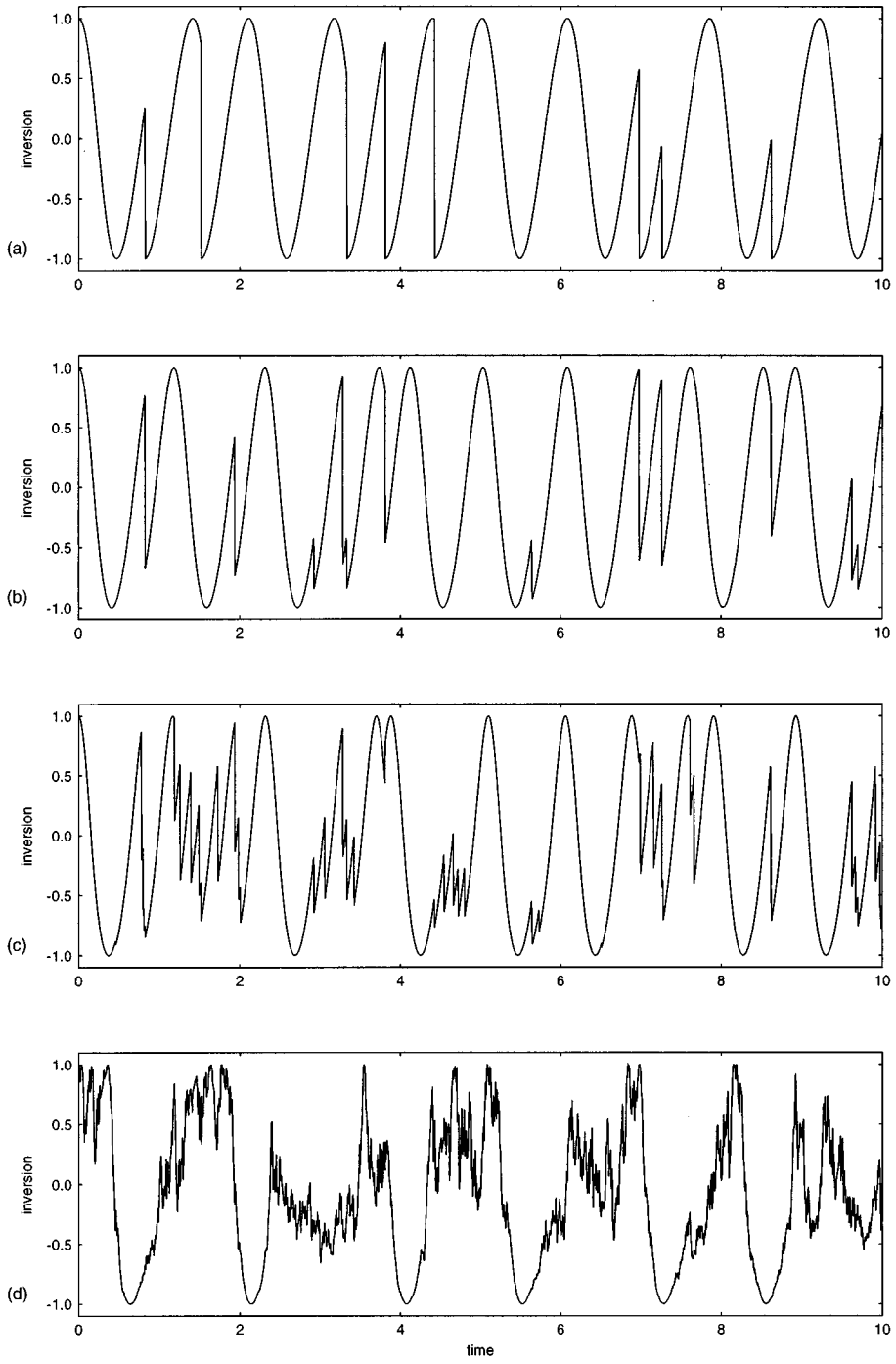

FIG. 21. Single realizations of a driven two-level system whose resonance fluorescence is observed in homodyne detection. The Rabi frequency is $\Omega=4\Gamma_{11}$, and the amplitude of the local oscillator is (a) $\alpha=0$, (b) $\alpha=0.5$, (c) $\alpha=1$, and (d) $\alpha=10$. With increasing α, jumps become more frequent and smaller in amplitude. From Granzow (1996).

$$p_c=2\Gamma_{11}[\langle L^\dagger L\rangle+\alpha^*\langle L\rangle+\alpha\langle L^\dagger\rangle+|\alpha|^2]\delta t. \quad (211)$$

These expressions can be derived analogously to the procedure that we applied in the description of the balanced heterodyne detection. In Fig. 21 we have plotted single realizations of a two-level system with Rabi frequency $\Omega=4\Gamma$ and local oscillator amplitudes (a) $\alpha=0$, (b) $\alpha=0.5$, (c) $\alpha=1$, and (d) $\alpha=10$. One clearly observes that with increasing α the number of jumps increase while their amplitudes decrease. For $\alpha=10$ we already see a behavior very close to that one would obtain in the limiting case $\alpha=\infty$.

D. A decaying cavity

So far we have illustrated the quantum-jump approach in the context of single-ion resonance fluorescence. Now we would like to discuss a different kind of problem, namely, cavity QED (Haroche, 1984). That

means we are interested in the field states inside a cavity as well as the time evolution of an atom interacting with such a cavity (Grochmalicki and Lewenstein, 1989b; Imamoglu, 1993). Again these problems can be formulated in the framework of the quantum-jump theory because both the losses of the cavity to the outside world as well as spontaneous emission of an atom give rise to a master equation of Lindblad form, which can be simulated using wave functions. A derivation of the simulation equations is possible using the physical picture of photon counters surrounding the system. For example, a broadband photon counter outside the cavity will detect photon losses of the cavity. As an initial example to illustrate the physical insight that we gain from the quantum-jump approach, we would like to investigate the time evolution of a field state in a lossy cavity. As an initial state we chose the state

$$|\psi\rangle = \frac{(|0\rangle + |10\rangle)}{\sqrt{2}}. \tag{212}$$

In an appropriate interaction picture, the time evolution under the condition that no photon has been found by the photon counter outside the cavity is given by the effective Hamiltonian

$$H_{eff} = -i\hbar\Gamma a^{\dagger}a, \tag{213}$$

while the normalized state after the detection of a photon is given by

$$|\psi_R\rangle = \frac{a|\psi\rangle}{\sqrt{\langle\psi|a^{\dagger}a|\psi\rangle}}. \tag{214}$$

In Fig. 22 the mean photon number for a single realization is shown. Initially no jump takes place, and the effect of this failure to detect a photon outside the cavity is that the mean photon number inside the cavity decreases; it becomes more and more unlikely to find a photon inside the cavity because, if there was a photon in the cavity, it would leave the cavity, leading to a photon count. However, in the simulation shown in Fig. 22 we finally observe a photon outside the cavity, and at that moment we know that there have been photons in the cavity. Calculating the state after the detection, given that we started with the superposition Eq. (212), we find that the post-detection state is a Fock state containing 9 photons. This implies that the mean photon number after the photon detection is actually higher than before the detection. After this first detection, the cavity continues to decay, and now each detection of a photon outside the cavity decreases the mean number of photons inside the cavity, while now the number of photons remains invariant under the conditional time evolution from the relevant Fock states.

In the previous example we saw that the exponential decay of the field mode in the ensemble average is the result of the superposition of many single realizations in which the cavity excitation changes discontinuously at random times. Coherence between component parts of a superposition state changes in amplitude and is eventually destroyed. However, this is not the only way in

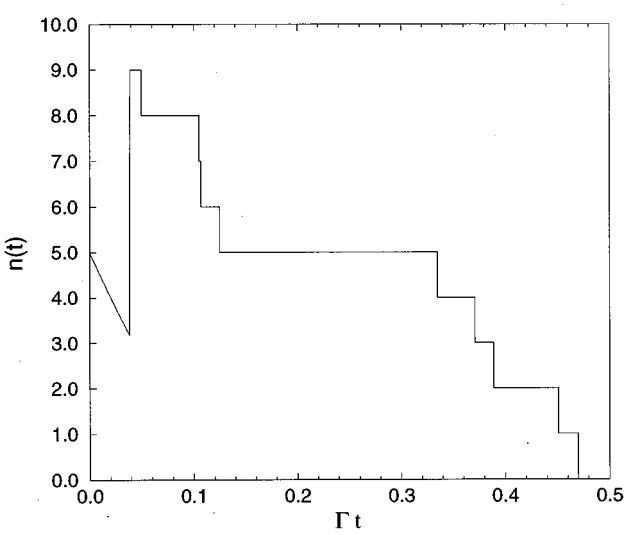

FIG. 22. The expected photon number of the state of a cavity with decay rate 2Γ prepared in an initial state $|\psi\rangle = (|0\rangle + |10\rangle)/2$ as a function of time. Before we observe the first photon outside the cavity, the expected photon number decreases. The first jump increases the expected photon number because we now know that the state has to be $|9\rangle$. Subsequently, each photodetection decreases the expected photon number by one.

which coherence between superposition states is destroyed. In the following example we show that the decay of coherence of a "Schrödinger-cat" state of the form

$$|\psi\rangle = (|\alpha\rangle + |-\alpha\rangle\rangle)/\| \, |\alpha\rangle + |-\alpha\rangle \, \|, \tag{215}$$

where $\|\cdot\|$ is a normalization factor, is due to a randomization of the relative phase between the two coherent states, while the modulus of the relative phase remains invariant under the no-jump evolution (Garraway and Knight, 1994a). In each individual realization the cat state remains a cat state. Although the amplitude of the two coherent states decays, the relative phase between the two coherent states just changes its sign. In fact if the state before the detection is given by Eq. (215), then after the detection of a photon we have the state

$$|\psi_+\rangle = a|\psi\rangle/\|\cdot\| = (|\alpha\rangle - |-\alpha\rangle\rangle)/\|\cdot\|. \tag{216}$$

The conditional time evolution when no photon has been found is given by

$$|\psi(t)\rangle = (|\alpha e^{-\Gamma(t-t')}\rangle - |-\alpha e^{-\Gamma(t-t')}\rangle\rangle)/\|\cdot\|, \tag{217}$$

so that the amplitudes of the coherent states decay exponentially while their relative phase remains unaffected. Averaging over many realizations, however, leads to a decaying relative phase as random phases tend to cancel out. It is interesting to note that the rate of decay for the relative phase of the Schrödinger-cat state is given by $\Gamma|\alpha|^2$, while the amplitude decay rate is given by Γ. Therefore, in the ensemble average, the cat decoheres before the amplitudes of its constituents are significantly affected (Garraway and Knight, 1994b).

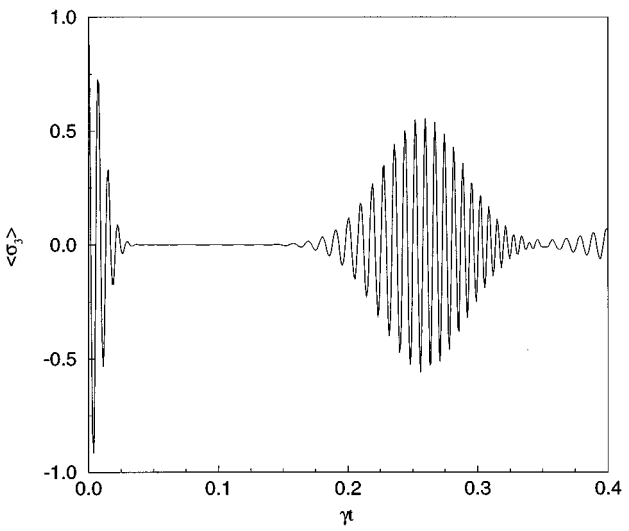

FIG. 23. Revivals in the inversion $\langle\sigma_3\rangle=(|1\rangle\langle 1|-|0\rangle\langle 0|)/2$ of a two-level atom in a cavity with an initial field prepared in a coherent state $|\alpha\rangle$ with $\alpha=4$. The parameters of the simulation were $\Delta=0$, $g/\gamma=100$, where g is the atom-field coupling constant. γ is used to scale time, while in the next figure it is the decay constant of the cavity.

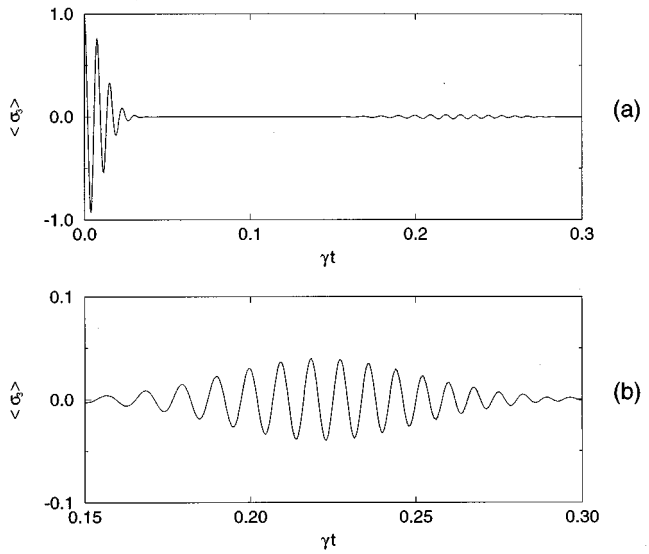

FIG. 24. Revivals in the inversion $\langle\sigma_3\rangle=\langle(|1\rangle\langle 1|-|0\rangle\langle 0|)\rangle/2$ of a two-level atom in a cavity with an initial field prepared in a coherent state $|\alpha\rangle$ with $\alpha=4$. Even a modest decay rate of the cavity leads to a rapid destruction of the revivals. (b) shows the revival. It was obtained by a quantum-jump simulation using 320,000 runs and is indistinguishable from the numerical integration of the master equation. The parameters of the simulation were $\Delta=0$, $g/\gamma=100$, and $\gamma\delta t=5\times10^{-4}$.

Another example that shows that the loss of coherence can be due to phase shifts at random times is the phenomenon of revivals in the Jaynes-Cummings model [Shore and Knight (1993) and references therein]. In this phenomenon a two-level atom is initially in its excited state 1, while the cavity field is in a coherent state with amplitude α,

$$|\psi\rangle=|1\rangle\langle 1|\otimes|\alpha\rangle\langle\alpha|. \tag{218}$$

This initial product state becomes entangled [Ekert and Knight (1995) and references therein], and the average excitation of the atom rapidly tends towards 1/2. The reason for this is that the frequency of Rabi oscillations depends on the number of photons in the field mode (Narozhny *et al.*, 1981). The different Rabi frequencies quickly decohere so that one observes an average excitation of 1/2 of the atom. However, as the frequencies are discrete, they partially rephase after a longer time, and the excitation of the atom rises again. This revival is shown, for example, in Fig. 23. Revivals of this kind have been observed experimentally by Meekhof *et al.* (1996) and Brune *et al.* (1996) and of the micromaser kind by Rempe and Walther (1987). If the cavity is damped, however, these revivals are much weaker and will vanish for strong damping, as shown in Fig. 24, where we have chosen the same parameters as in Fig. 23 but with an additional cavity-damping constant of $\gamma=0.01g$, where g is the atom-field coupling constant. We assumed that the atom does not decay spontaneously. No substantial revivals can be observed (Barnett and Knight, 1986). What will we see for an individual realization? If we assume that the atom does not decay spontaneously, we obtain the effective Hamiltonian

$$H_{eff}=H_{sys}-i\hbar\gamma a^{\dagger}a \tag{219}$$

that generates the conditional time evolution of the atom-cavity system if no photons are detected outside the cavity. H_{sys} generates the free evolution of an undamped atom-cavity-field system, while the second term on the right-hand side describes the damping of the cavity at a rate 2γ. The state after the detection of a cavity photon is

$$|\psi_{+}\rangle=\frac{a|\psi\rangle}{\|\cdot\|}. \tag{220}$$

A single realization for the parameters of Fig. 24 is shown in Fig. 25. Now the revivals persist; however, each jump that occurs at a random time introduces a phase shift. An average taken over many individual realizations then leads to a quick decay of the coherence, and revivals are not observed any more. A similar analysis can be performed for a lossless cavity with an atom that may spontaneously decay (Burt and Gea-Banacloche, 1996).

In these examples we only considered undriven atoms in a cavity. Driven two-state systems inside a cavity can of course also be investigated using the quantum-jump approach (Alsing and Carmichael, 1991; Tian and Carmichael, 1992), but we do not discuss this in detail here.

E. Other applications of the quantum-jump approach

So far we have illustrated the quantum-jump approach for a number of examples in single-ion physics and cavity QED. The quantum-jump approach can and has been applied to a large number of problems, which

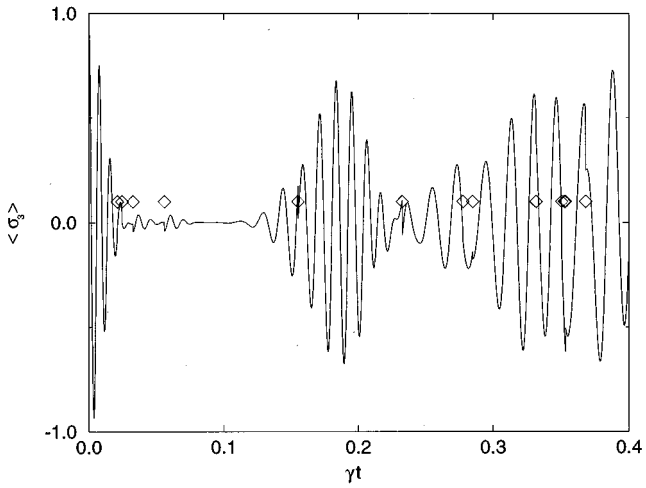

FIG. 25. For the same parameters as in Fig. 24 we plot a single realization of the time evolution. The diamonds mark the instants where a photon was detected outside the cavity. Note that the revivals in a single realization survive. The quantum jumps lead to a phase jump of the time evolution of the inversion of the atom, which leads to a destruction of the revivals in the ensemble average. From Garraway, Knight, and Steinbach (1995).

we cannot discuss in detail here. Amongst these examples are the discussion of correlations between quantum jumps in two stored ions. Such correlations were observed in an experiment (Sauter, Blatt, *et al.*, 1986), in which the intermittent fluorescence of two Ba^+ ions in an ion trap was investigated and correlations were found between the quantum jumps in the two ions which exceeded those expected from independent jumps. However, Itano *et al.* (1988) could not confirm these correlations in their experiment. Theoretical investigations (Lewenstein and Javanainen, 1987; 1988; Agarwal *et al.*, 1988a; Hendriks and Nienhuis, 1988; S. V. Lawande, Jagatap, and Lawande, 1989; Lawande, Lawande, and Jagatap, 1989) predicted that correlations should be small if the ions are separated by many optical wavelengths. If the ions are closer than an optical wavelength together, correlations might be observable. For such small separations even two two-level ions could exhibit quantum jumps (Yamada and Berman, 1990; Kim *et al.*, 1989; Q. V. Lawande *et al.*, 1990).

Another example of the application of the quantum-jump approach is the investigation of the quantum Zeno effect (Misra and Sudarshan, 1977). The quantum Zeno effect was measured in an experiment by Itano *et al.* (1990) that was originally proposed by Cook (1988). The experiment used a two-level system. The ground-state population was measured via coupling the lower level strongly to a rapidly decaying third level. Observation of resonance fluorescence then indicates that the system was in its ground state. This experiment was investigated theoretically independently by Power and Knight (Power, 1995a, 1995b; Power and Knight, 1996), by Beige and Hegerfeldt (1996a, 1996b), and by Mahler and coworkers (Mahler and Weberruβ, 1995) using the quantum-jump approach, and, e.g., by Frerichs and Schenzle (1991) using Bloch equations. The investigations using the quantum-jump approach helped to understand the experiment from the single-particle point of view and will be important in the analysis of future quantum Zeno experiments (Plenio *et al.*, 1996) using single ions instead of around 5000 as in the experiment by Itano *et al.* (1990).

Cohen-Tannoudji and co-workers have applied the quantum-jump approach to the problem of lasing without inversion (Cohen-Tannoudji *et al.*, 1992a, 1992b, 1993) to understand the processes involved from the point of view of single systems and to simulations of dark-state cooling (Bardou *et al.* 1994).

Apart from these more analytical applications of the quantum-jump approach, its numerical usefulness has been demonstrated as well, for example, in numerical simulations of laser-cooling experiments in two or three dimensions (see, for example, Castin and Mølmer, 1995; Marte, Dum, Taieb, Lett, and Zoller, 1993; Marte, Dum, Taib, and Zoller, 1993). The fact that the quantum-jump approach allows the description of the system using a wave function instead of the density operator has made these investigations possible. Both the gain in computational speed and the saving in memory space is considerable, as in a quantum-jump simulation only N differential equations have to be propagated, instead of N^2 in the density-operator simulation.

The quantum-state-diffusion model, apart from its importance in fundamental issues such as the measurement process or intrinsic decoherence, is now widely used to investigate the transition between classical and quantum behavior and in the field of quantum chaos (see, for example, Spiller and Ralph, 1994; Brun *et al.* 1996; Rigo and Gisin, 1996). As we have already mentioned in Sec. IV, the quantum-state-diffusion model also exhibits interesting localization properties in both position and phase space (Gisin and Percival, 1993a, 1993b; Percival, 1994a; Herkommer *et al.*, 1996), which can be used to implement very fast simulation algorithms (Schack *et al.*, 1995, 1996). Similar localization properties exist also for variants of the quantum-jump approach (Holland *et al.*, 1996).

A more exotic application of the quantum-jump approach, or more precisely of the experiments in which quantum jumps were observed, is the fact that these experiments can provide a ''perfect'' random-number generator. This is because these experiments allow the observation of single quantum jumps, which occur at absolutely random times, due to the fundamental indeterminacy of quantum mechanics (Erber and Putterman, 1985; Erber *et al.*, 1989). Whether this idea is useful is, however, doubtful, although in principle there could be applications, e.g., in cryptography.

F. The spectrum of resonance fluorescence and single-system dynamics

So far our examples of the quantum-jump approach were limited to the investigation of the photon statistics

of the radiation emitted by a system and of the internal dynamics of a system conditioned on a measurement record of observing the radiation emitted by the system. As a further application of the quantum-jump approach, we would now like to consider the spectrum of resonance fluorescence of a three-level atom in the V configuration, as shown in Fig. 1. This system, whose photon statistics we already discussed in the context of bright and dark periods, exhibits interesting features in the spectrum of resonance fluorescence on the strong $0\leftrightarrow 1$ transition. In the following we will discuss briefly the ensemble behavior of the spectrum and then show how we can understand this behavior from the point of view of the single-system dynamics. We will closely follow the analysis of Hegerfeldt and Plenio (1995b) and Plenio (1994, 1996). We consider the system shown in Fig. 1 and assume that the Rabi frequencies Ω_i of the lasers and the decay constants Γ_{ii} of the two upper levels satisfy the following conditions.

(i) The Rabi frequency of the laser driving the $0\leftrightarrow 2$ transition is weak, that is

$$\Omega_2^2 \ll \frac{1}{4}\frac{16\Delta_2^2\Gamma_{11}^2+(\Omega_1^2+4\Delta_2(\Delta_1-\Delta_2))^2}{\Gamma_{11}^2+(\Delta_1-\Delta_2)^2}, \tag{221}$$

which simplifies for $\Omega_1 \gg \Delta_1, \Delta_2$ to

$$\Omega_2^2 \ll \left(\frac{\Omega_1^2}{2\Gamma_{11}}\right)^2. \tag{222}$$

(ii) Spontaneous emission on the $2\leftrightarrow 0$ transition should be negligible, that is

$$\Gamma_{22} \ll \frac{\Omega_1^2\Omega_2^2\Gamma_{11}}{16\Delta_2^2\Gamma_{11}^2+\{\Omega_1^2+4\Delta_2(\Delta_1-\Delta_2)\}^2}. \tag{223}$$

These conditions have the following interpretation. If Eq. (221) is satisfied, the V system exhibits long bright and dark periods as discussed in Eqs. (194)–(205). If Eq. (223) is satisfied, stimulated transitions from level 2 to level 0 are much more frequent than spontaneous emissions on the same transition. Under the assumption of Eqs. (221)–(223), the spectrum of resonance fluorescence takes on the following approximate analytical form

$$\begin{aligned} S(\Delta) &= \frac{1}{\pi\rho_{11}^{ss}}\mathrm{Re}\int_0^\infty d\tau\langle\sigma_{10}(\tau)\sigma_{01}(0)\rangle_{ss}e^{-i\Delta\tau} \\ &= S_{coh}(\Delta)+S_{Mollow}(\Delta)+S_{peak}(\Delta), \end{aligned} \tag{224}$$

with

$$B = 6\Gamma_{11}^2-2\Omega_1^2-2\Delta_1^2, \tag{225}$$

$$C = \Omega_1^4+2\Omega_1^2\Gamma_{11}^2+9\Gamma_{11}^4+\Delta_1^4+2\Delta_1^2\Omega_1^2-6\Gamma_{11}^2\Delta_1^2, \tag{226}$$

$$D = \Gamma_{11}^2(\Omega_1^2+2\Delta_1^2+2\Gamma_{11}^2)^2, \tag{227}$$

$$A_p = 2\frac{(\Delta_1^2+\Gamma_{11}^2)[(\Delta_1-\Delta_2)^2+\Gamma_{11}^2][(\Omega_1^2-4\Delta_2^2+4\Delta_1\Delta_2)^2+16\Delta_2^2\Gamma_{11}^2]}{\Omega_1^2\Omega_2^2\Gamma_{11}[\Omega_1^2+2\Delta_2^2+4\Delta_1^2-4\Delta_1\Delta_2+4\Gamma_{11}^2]^2}, \tag{228}$$

$$\Gamma_p = \frac{2\Omega_1^2\Omega_2^2\Gamma_{11}(2\Delta_2^2+4\Delta_1^2-4\Delta_1\Delta_2+\Omega_1^2+4\Gamma_{11}^2)}{[(\Omega_1^2-4\Delta_2^2+4\Delta_1\Delta_2)^2+16\Delta_2^2\Gamma_{11}^2](\Omega_1^2+2\Delta_1^2+2\Gamma_{11}^2)}, \tag{229}$$

and

$$\pi S_{coh}(\Delta) = \pi\frac{2(\Delta_1^2+\Gamma_{11}^2)}{4\Gamma_{11}^2+\Omega_1^2+2\Delta_2^2+4\Delta_1^2-4\Delta_1\Delta_2}\,\delta(\Delta), \tag{230}$$

$$\pi S_{Mollow}(\Delta) = \frac{\Gamma_{11}\Omega_1^2(\Omega_1^2+2\Delta^2+8\Gamma_{11}^2)}{2(\Delta^6+B\Delta^4+C\Delta^2+D)}, \tag{231}$$

$$\pi S_{peak}(\Delta) = \frac{A_p\Gamma_p^2}{\Delta^2+\Gamma_p^2}. \tag{232}$$

The contributions Eqs. (230) and (231) just represent the well-known Mollow triplet and the Rayleigh peak (Mollow, 1969, 1972a, 1972b, 1975, 1981). These contributions are expected and are well understood. The third contribution, however, a narrow Lorentzian, is a new feature in the spectrum of resonance fluorescence. In Figs. 26 and 27 we see the spectra for the cases of strong driving of the $0\leftrightarrow 1$ transition and for a medium strong laser on the same transition. One clearly observes the narrow peak, which should not be confused with the Rayleigh peak, in both spectra. In the following we will focus our attention to this new feature and use it to exemplify the application of the quantum-jump approach for spectral information and to illustrate how ensemble properties can be understood better from a single-system point of view. One might, for example, be interested in the following question. What happens if we observe the spectrum of resonance fluorescence in a bright period exclusively? Experimentally this may be measured by triggering the spectrometer with the broadband counter. The spectrometer will be opened if we detect photons in the broadband counter at a sufficiently high rate, and it will be closed when we fail to find photons for a certain time T_0. Using this time constant T_0 we have a means either to observe the spectrum in a bright period ($T_0 \approx 10/\Gamma_{11}$) or to have no restriction on the emission times ($T_0=\infty$), i.e., the ensemble spectrum. Changing T_0, we can continuously switch between the two regimes. The spectrum of resonance fluores-

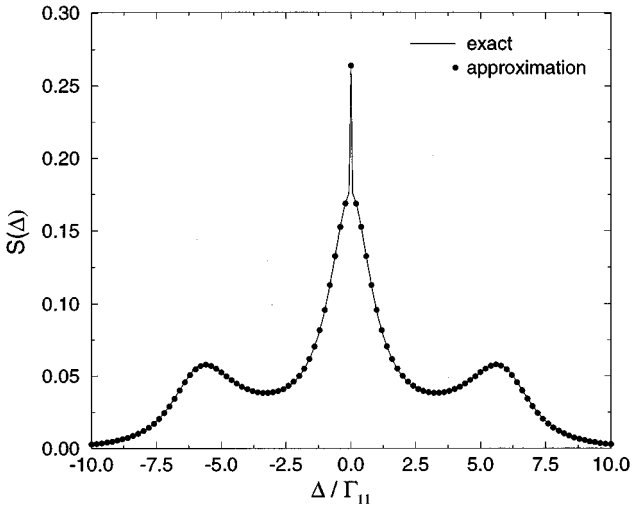

FIG. 26. The spectrum of resonance fluorescence on the $0\leftrightarrow1$ transition. The parameters are $\Omega_1=6\Gamma_{11}$, $\Omega_2=0.4\Gamma_{11}$, and $\Delta_1=\Delta_2=0$. One clearly observes the Mollow triplet and the additional narrow peak in the spectrum. From Hegerfeldt and Plenio (1995b).

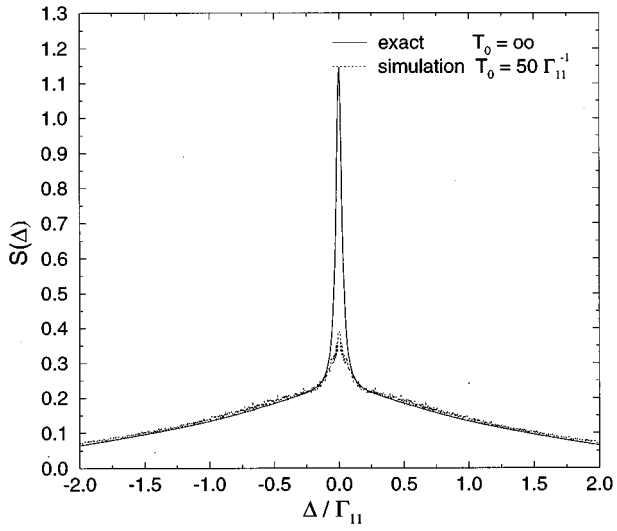

FIG. 28. Simulation of the conditional spectrum of resonance fluorescence for $T_0=\infty$ and $T_0=50\Gamma_{11}^{-1}$. One observes that only the narrow central peak is affected by the conditioning of the photon statistics, while the wings of the spectrum are essentially independent of the choice of T_0.

cence can be simulated using the quantum-jump approach (Hegerfeldt and Plenio, 1996). In Fig. 28 the effect of the change in T_0 is clearly visible. For small T_0 the amplitude of the narrow central peak becomes small. However, only the central part of the spectrum is strongly affected, while the wings of the spectrum are more or less independent of T_0. This is an example of conditional fluorescence spectra, and it shows that spectra can be dependent on the conditions imposed on the photon statistics. Here we have shown the effect for the spectrum of resonance fluorescence, but similar results may be obtained by investigating the absorption spectrum of a weak probe beam on the strongly driven $0\leftrightarrow1$ transition (Plenio, 1996). Again a narrow peak is observed that vanishes if we try to measure the same feature in a bright period of the system. After we have investigated the spectrum of resonance fluorescence of the V system and some of its properties, especially the occurrence of the narrow peak, it is now instructive to see how we can understand this feature from the photon statistics of the single-atom-like system. The photon statistics are provided by the quantum-jump approach. Explicit results have been given in this section in Eqs. (194)–(205).

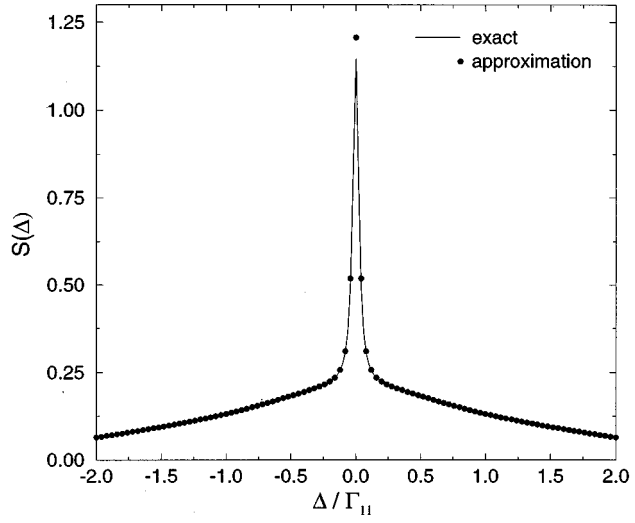

FIG. 27. The spectrum of resonance fluorescence on the $0\leftrightarrow1$ transition. The parameters are $\Omega_1=2\Gamma_{11}$, $\Omega_2=0.2\Gamma_{11}$, and $\Delta_1=\Delta_2=0$. Due to the weaker driving as compared to Fig. 26, the sidebands in the Mollow triplet are no longer resolved. The additional narrow peak is again observable and has a higher relative weight. From Hegerfeldt and Plenio (1995b).

Now that we know that the V configuration exhibits light and dark periods for those parameters for which the narrow peak in the spectrum appears, we proceed with a somewhat simplified model of resonance fluorescence of the V system. We assume that the lengths of light and dark periods obey exactly Poissonian distributions, e.g., the probability density that a light period has the length t is

$$I_L(t)=\frac{1}{T_L}\,e^{-t/T_L}, \tag{233}$$

and for a dark period to have a length of t is

$$I_D(t)=\frac{1}{T_D}\,e^{-t/T_D}. \tag{234}$$

These probability densities have been derived from a rate-equation model of the time evolution by Cook and Kimble (1985). Additionally, we assume that in a bright period the system behaves exactly like a two-level system made up of the two levels 0 and 1. This assumption has to be checked and turns out to be good in the case of

the spectrum of resonance fluorescence treated here. However, it is not always correct, as a careful analysis of the absorption spectrum on the strong $0\leftrightarrow 1$ transition proves, and deviations from this idealized assumption may lead to significant contributions to the absorption spectrum (Plenio, 1996).

It is well known (Loudon, 1983) that the stationary spectrum of resonance fluorescence of such a two-level system is given by

$$S^{(2)}(\Delta)=\lim_{T\to\infty}\frac{C}{T}\int_0^T dt_1\int_0^T dt_2\langle E^{(-)}(t_1)E^{(+)}(t_2)\rangle \times e^{-i\Delta(t_1-t_2)}, \tag{235}$$

where $E^{(-)}(t)$ and $E^{(+)}(t)$ denote the negative- and positive-frequency part of the electric-field operator and C is chosen in such a way that, with

$$E^{(+)}(t)\sim\sigma_{01}(t), \tag{236}$$

one obtains

$$S^{(2)}(\Delta)=\frac{2\Gamma_{11}}{\pi}\,\mathrm{Re}\int_0^\infty d\tau e^{-i\Delta\tau}\langle\sigma_{10}(\tau)\sigma_{01}(0)\rangle_{ss}. \tag{237}$$

For the non-normalized resonance-fluorescence spectrum of the two-level system, one then obtains

$$S^{(2)}(\Delta)=\frac{\Gamma_{11}\Omega_1^2}{\Omega_1^2+2(\Delta_1^2+\Gamma_{11}^2)}\times\left\{\frac{1}{\pi}\frac{\Gamma_{11}\Omega_1^2(\Omega_1^2+2\Delta^2+8\Gamma_{11}^2)}{2(\Delta^6+B\Delta^4+C\Delta^2+D)}+\frac{2(\Delta_1^2+\Gamma_{11}^2)}{\Omega_1^2+2(\Delta_1^2+\Gamma_{11}^2)}\,\delta(\Delta)\right\}, \tag{238}$$

where the constants B, C, and D are given in Eqs. (225)–(227). As the light emitted by the atom switches on and off due to the light and dark periods, we assume that the electric field radiated by the three-level configurations is given by

$$\hat{E}^{(\pm)}(t):=E^{(\pm)}(t)f(t), \tag{239}$$

where $f(t)$ is a two-state jump process with values 0 and 1. The probability density for the length of a period where $f(t)=0$ is given by Eq. (233) and that for $f(t)=1$ is given by Eq. (234). Therefore we have to substitute

$$\hat{\sigma}_{ij}(t):=\sigma_{ij}(t)f(t) \tag{240}$$

in Eq. (237) and expect the spectrum of the three-level configurations to be given by

$$S^{(3)}(\Delta)=\frac{2\Gamma_{11}}{\pi}\,\mathrm{Re}\int_0^\infty d\tau\, e^{-i\Delta\tau}\langle\langle\hat{\sigma}_{10}(\tau)\hat{\sigma}_{01}(0)\rangle\rangle_{ss}, \tag{241}$$

where $\langle\langle.\rangle\rangle$ denotes both the quantum mechanical average as well as the stochastic average over all realizations of the process $f(t)$. This can be simplified to

$$\begin{aligned}S^{(3)}(\Delta)&=\frac{2\Gamma_{11}}{\pi}\,\mathrm{Re}\int_0^\infty d\Delta e^{-i\Delta\tau}\langle\sigma_{10}(\tau)\sigma_{01}(0)\rangle_{ss}\times\langle f(\tau)f(0)\rangle_{stoch.}\\&=\int_{-\infty}^\infty d\Delta' S^{(2)}(\Delta-\Delta')k(\Delta'),\end{aligned} \tag{242}$$

with

$$\begin{aligned}k(\Delta)&=\frac{1}{\pi}\int_0^\infty d\tau e^{-i\Delta\tau}\langle f(\tau)f(0)\rangle_{stoch.}\\&=\frac{T_L}{T_L+T_D}\left\{\frac{T_L}{T_L+T_D}\,\delta(\Delta)+\frac{T_D}{T_D+T_L}\,\mathcal{L}(\Delta)\right\},\end{aligned} \tag{243}$$

where

$$\mathcal{L}(\Delta)=\frac{1}{\pi}\frac{1/T_D+1/T_L}{(1/T_D+1/T_L)^2+\Delta^2}. \tag{244}$$

Because both T_D and T_L, Eqs. (203)–(205), are assumed to be much longer than the mean emission time of a two-level system, which is of the order of Γ_{11}^{-1}, we can deduce from this

$$\begin{aligned}S^{(3)}(\Delta)&\cong\left(\frac{T_L}{T_D+T_L}\right)^2\left\{S^{(2)}(\Delta)+\frac{T_D}{T_L}\,S_{inc}^{(2)}(\Delta)+\frac{T_D}{T_L}\,\mathcal{L}(\Delta)\,\frac{2(\Delta_1^2+\Gamma_{11}^2)}{\Omega_1^2+2(\Delta_1^2+\Gamma_{11}^2)}\right\}\\&=\frac{T_L}{T_D+T_L}\left\{S_{inc}^{(2)}(\Delta)+\frac{T_L}{T_D+T_L}S_{coh}^{(2)}(\Delta)+\frac{T_D}{T_D+T_L}\,\frac{2(\Delta_1^2+\Gamma_{11}^2)}{\Omega_1^2+2(\Delta_1^2+\Gamma_{11}^2)}\,\mathcal{L}(\Delta)\right\}.\end{aligned} \tag{245}$$

This expression has to be compared with the results Eqs. (224)–(232). In fact, inserting Eqs. (203)–(205) into Eq. (245) yields an expression in very good agreement with the spectra of the V system. The width Γ_p of the resulting narrow peak is

$$\Gamma_p=\frac{1}{T_D}+\frac{1}{T_L}. \tag{246}$$

The amplitude A_p of the narrow peak in the normalized spectrum is then given by

$$A_p=\frac{2(\Delta_1^2+\Gamma_{11}^2)}{\Omega_1^2+2(\Delta_1^2+\Gamma_{11}^2)}\,\frac{T_D^2T_L}{(T_D+T_L)^2}. \tag{247}$$

Now the interpretation of the narrow peak is obvious. The stochastic modulation of the resonance fluorescence due to dark periods leads to a partial broadening of the Rayleigh peak. The small width of the additional peak in the resonance-fluorescence spectrum is then understood from the fact that the correlation time τ_c of the random telegraph process $f(t)$, which simulates the light and dark periods, is very large. In fact it is easy to show that

$$\tau_c=\left(\frac{1}{T_D}+\frac{1}{T_L}\right)^{-1}. \tag{248}$$

This results in an extremely narrow distribution in frequency space with a width $\Gamma_p = \tau_c^{-1}$. It is this structure that is observable in the spectrum of resonance fluorescence. It is interesting to note that the narrow peak is not easily interpreted in a dressed-states picture. Indeed, in secular approximation and for $\Delta_1 = \Delta_2 = 0$, one obtains a zero weight for the narrow peak. Even if we tune the laser on the $0 \leftrightarrow 2$ transition to resonance with one of the dressed states, i.e., $\Delta_2 = \pm \Omega_1/2$, the weight of the narrow peak comes out much too small. In fact it would then be predicted to be proportional to Ω_2^2. The narrow peak found here clearly has a different origin than the line-narrowing effects found by others (Narducci, Oppo, and Scully, 1990; Narducci, Scully, *et al.*, 1990; Manka *et al.*, 1993), where the systems do not exhibit bright and dark periods in their resonance fluorescence, but simply a decrease in intensity. The existence of bright and dark periods in the resonance fluorescence leads to a narrow peak in the spectrum, but it should be noted that the converse is not necessarily true. There are situations [e.g., a laser-driven two-level system in a squeezed vacuum (Swain, 1994)] in which the spectrum of resonance fluorescence exhibits narrow peaks but where the photon statistics does not show bright and dark periods. The reason for that can be found in the fact that the photon statistics is governed by the population decay rates, while the spectrum of resonance fluorescence is derived from the $g^{(1)}(t)$ correlation function, which is strongly influenced by the decay rates of the coherences in the system. In the case of a two-level system in squeezed light the coherences have a slowly decaying component, while the population decay rate is still large.

G. Spontaneous emission in quantum computing

As a last application of the quantum-jump approach, we would like to investigate the influence that spontaneous emission has on the function of a quantum computer. Quantum computing is an idea that has attracted enormous interest in the last two years. It was elevated from the obscurity of theoretical idealization to possible practical applications by the discovery of an algorithm by Shor (1994) (see also Ekert and Josza, 1996, and references therein) that allows the factorization of large numbers in polynomial time on a quantum computer, as compared to the exponential time required on a classical computer. However, this achievement in computing speed is only possible due to the massive use of the superposition principle in quantum mechanics. The basic idea is that a qubit (a two-level system) can exist in a superposition of the two values 0 and 1. N qubits can then exist in a superposition of 2^N values. These values can be manipulated by a series of unitary transformations. A final readout can then provide us with information about global properties of the function implemented by the unitary transformation. Such a global property of the function is, for example, its period, which a quantum computer determines by performing a discrete Fourier transform, something which can also be implemented on a quantum computer (Coppersmith, 1994). In the course of its time evolution (computation) the quantum computer evolves into a highly entangled state. However, it is known that any entangled state is very sensitive to dissipation. Therefore one expects that the quantum computer is highly sensitive to spontaneous emission and other sources of dissipation. This is in fact the case, and currently research in quantum error-correction methods has concentrated on attempts to find methods to correct for these errors (Calderbank and Shor, 1996; Shor, 1996; Steane, 1996). The quantum-jump approach is ideally suited for the investigation of this problem because it is able to describe single runs of a quantum computer rather than an ensemble of quantum computers, as in the Bloch-equation description. We will illustrate the problems caused by spontaneous emission in quantum computers by examining the example of the discrete Fourier transform mentioned above. There are two effects contributing to the decoherence of the quantum computer. One is the obvious fact that a spontaneous emission will destroy at least part of the coherence in the quantum computer. The second decohering effect, however, originates from the conditional time evolution between spontaneous emissions (Plenio and Knight, 1997). We have learnt above that this time evolution is actually different from the unit operation because even the nondetection of a photon represents a gain in our knowledge about the system. Therefore the wave function of the system, which represents our knowledge of the system, has to change. This leads to a distortion of the time evolution, which will then affect the result of our calculation. In Figs. 29 and 30 we simulate a quantum computer (we do not go into detail concerning its implementation here) that calculates the discrete Fourier transform of a function that is evaluated at 32 points (Plenio and Knight, 1997). The resulting square modulus of the wave function of the quantum computer is compared to the exact result obtained from an absolutely stable quantum computer. The function on which we perform the discrete Fourier transform is given for definiteness in this example by $f(n) = \delta_{8,(n \bmod 10)}$ for $n = 0,1,\ldots,31$. One can implement the Hamiltonian operators (in the Lamb-Dicke limit) for all the necessary quantum gates in a linear ion trap (Cirac and Zoller, 1995) to realize this discrete Fourier transform. In addition to the coherent time evolution, possible spontaneous emissions from the upper levels of the ions are taken into account, but all other sources of loss are neglected.

In Fig. 29 one emission has taken place during the calculation time of the quantum computer. If we compare the resulting wave function with the correct wave function, we observe a marked difference between the two. In Fig. 30 we show the wave function of an unstable quantum computer that has not suffered a spontaneous emission during the calculation of the discrete Fourier transform. We clearly see that even when no spontaneous emission has taken place, the wave function of the quantum computer differs substantially from the correct result. This difference becomes stronger and stronger the larger the ratio between the computation time T and

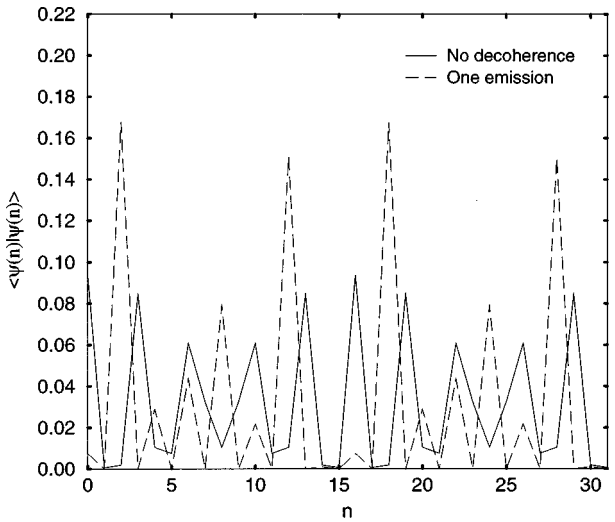

FIG. 29. Results of a discrete Fourier transform of a function $f(n)=\delta_{8,(n \bmod 10)}$ with $n=0,1,\ldots,31$. The solid line is the result for a quantum computer with stable qubits and represents the correct result. The dashed line shows the result of the same computation using a quantum computer with unstable qubits, one of which has suffered a spontaneous emission during the calculation. The results clearly differ and show the impact of a single spontaneous emission on a quantum computation. For the parameters chosen on average, the quantum computer will suffer one emission per discrete Fourier transform, i.e., $\tau_{sp}=T$ in this case. From Plenio and Knight (1997).

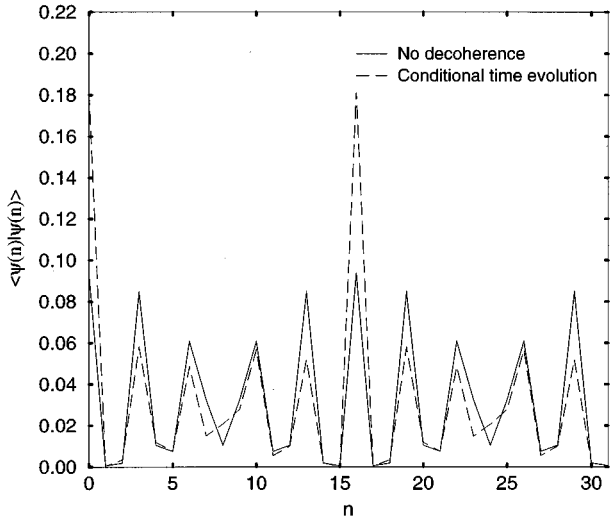

FIG. 30. The same quantum computation as in Fig. 5. The solid line again represents the result using a quantum computer with stable qubits, while the dashed line shows the result using a quantum computer with unstable qubits. This time, however, the unstable quantum computer does not suffer an emission during the whole calculation. Again the results differ, illustrating the impact of the conditional time evolution between spontaneous emissions. From Plenio and Knight (1997).

the spontaneous lifetime τ_{sp} of the quantum computer becomes. Therefore the wave function of the quantum computer will be sufficiently close to the correct result only if the whole computation is finished in a time T that is much shorter than the spontaneous lifetime τ_{sp} of the quantum computer.

The fact that even one spontaneous emission will usually make the result of the quantum computation completely incorrect can then be used to derive stringent upper limits on the numbers that can be factorized on a quantum computer (Plenio and Knight, 1996, 1997). This again shows that knowledge of the single-system behavior gained from the quantum-jump approach gives us useful new insights into important properties of quantum systems.

VI. CONCLUSIONS

Recent work in quantum optics has forced us to reexamine the dynamics of individual quantum systems in which single realizations (single atoms or trapped ions, single cavity-field modes, and so on) are described in quantum mechanics. In these situations, the dynamics is always dissipative and leaves a record of its history accessible in the wider world of the outside environment. If this record is read, so that we acquire specific information, then we can associate a specific quantum trajectory to that conditional record. In this way we "unravel" the dissipative master equation into a family of records.

We have reviewed the new technique developed to describe this unravelling, which goes under the names of quantum jumps, Monte Carlo wave-function simulations, and so on. We have further demonstrated how they can be used to describe entirely nonclassical behavior in a wide range of situations in quantum optics. Future applications will surely emerge from these powerful approaches.

ACKNOWLEDGMENTS

We are grateful to J. Dalibard, B. M. Garraway, G. C. Hegerfeldt, M. S. Kim, R. Loudon, K. Mølmer, D. T. Pegg, I. C. Percival, W. L. Power, R. Reibold, D. Sondermann, J. Steinbach, S. Stenholm, R. C. Thompson, and K. Wódkiewicz for discussions over the years on quantum jumps. This work was supported in part by the UK Engineering and Physical Sciences Research Council, the European Union, and the Alexander von Humboldt Foundation.

REFERENCES

Agarwal, G. S., 1974, *Quantum Statistical Theories of Spontaneous Emission and their Relation to other Approaches*, Springer Tracts in Modern Physics **70** (Springer, Berlin), p. 1.
Agarwal, G. S., S. V. Lawande, and R. D'Souza, 1988a, IEEE J. Quantum Electron. **24**, 1413.
Agarwal, G. S., S. V. Lawande, and R. D'Souza, 1988b, Phys. Rev. A **37**, 444.
Alsing, P., and H. J. Carmichael, 1991, Quantum Opt. **3**, 13.
Arecchi, F. T., A. Schenzle, R. G. De Voe, K. Jungmann, and R. G. Brewer, 1986, Phys. Rev. A **33**, 2124.

Autler, S. H., and C. H. Townes, 1955, Phys. Rev. **100**, 703.
Barchielli, A., 1986, Phys. Rev. A **34**, 1642.
Barchielli, A., 1993, Quantum Opt. **2**, 423.
Barchielli, A., and V. P. Belavkin, 1991, J. Phys. A **24**, 1495.
Bardou, F., J. P. Bouchaud, O. Emile, A. Aspect, and C. Cohen-Tannoudji, 1994, Phys. Rev. Lett. **72**, 203.
Barnett, S. M., and P. L. Knight, 1986, Phys. Rev. A **33**, 2444.
Beige, A., and G. C. Hegerfeldt, 1996a, Phys. Rev. A **53**, 53.
Beige, A., and G. C. Hegerfeldt, 1996b, Quantum Opt. **8**, 999.
Bergquist, J. C., R. B. Hulet, W. M. Itano, and D. J. Wineland, 1986, Phys. Rev. Lett. **57**, 1699.
Bergquist, J. C., W. M. Itano, and D. J. Wineland, 1994, in *Frontiers in Laser Spectroscopy: Proceedings of the International School of Physics "Enrico Fermi," Course CXX*, edited by T. W. Hänsch and M. Inguscio (North-Holland, Amsterdam), pp. 359–376.
Blatt, R., W. Ertmer, P. Zoller, andJ. J. Hall, 1986, Phys. Rev. A **34**, 3022.
Bouwmeester, D., R. J. C. Spreeuw, G. Nienhuis, and J. P. Woerdman, 1994, Phys. Rev. A **49**, 4170.
Brun, T. A., 1997, Phys. Rev. Lett. **78**, 1833.
Brun, T. A., and N. Gisin, 1996, J. Mod. Opt. **43**, 2289.
Brun, T. A., N. Gisin, P. F. O'Mahony, and M. Rigo, 1997, Phys. Lett. A **229**, 267.
Brun, T. A., I. C. Percival, and R. Schack, 1996, J. Phys. A **29**, 2077.
Brune, M., F. Schmidt-Kaler, A. Maali, J. Dreyer, E. Hagley, J. M. Raimond, and S. Haroche, 1996, Phys. Rev. Lett. **76**, 1800.
Burt, T. C., and J. Gea-Banacloche, 1996, Quantum Opt. **8**, 105.
Calderbank, A. R., and P. W. Shor, 1996, Phys. Rev. A **54**, 1098.
Carmichael, H. J., 1993a, *An Open Systems Approach to Quantum Optics*, Lecture Notes in Physics (Springer, Berlin).
Carmichael, H. J., 1993b, Phys. Rev. Lett. **70**, 2273.
Carmichael, H. J., 1994, in *Quantum Optics VI*, edited by J. D. Harvey and D. F. Walls (Springer, Berlin), p. 219.
Carmichael, H. J., S. Singh, R. Vyas, and P. R. Rice, 1989, Phys. Rev. A **39**, 1200.
Castin, Y., J. Dalibard, and K. Mølmer, 1993, in *Atomic Physics 13*, edited by H. Walther, T. W. Hänsch, and B. Neizert, AIP Conf. Proc. No. 275 (AIP, New York), p. 1143.
Castin, Y., and K. Mølmer, 1995, Phys. Rev. Lett. **74**, 3772.
Cirac, J. I., and P. Zoller, 1995, Phys. Rev. Lett. **74**, 4091.
Cohen-Tannoudji, C., and J. Dalibard, 1986, Europhys. Lett. **1**, 441.
Cohen-Tannoudji, C., J. Dupont-Roc, and G. Grynberg, 1992, *Atom-Photon Interactions* (Wiley, New York).
Cohen-Tannoudji, C., B. Zambon, and E. Arimondo, 1992a, C. R. Acad. Sci., Ser. II: Mec. Phys., Chim., Sci. Terre Univers **314**, 1139.
Cohen-Tannoudji, C., B. Zambon, and E. Arimondo, 1992b, C. R. Acad. Sci., Ser. II: Mec. Phys., Chim., Sci. Terre Univers **314**, 1293.
Cohen-Tannoudji, C., B. Zambon, and E. Arimondo, 1993, J. Opt. Soc. Am. B **10**, 2107.
Cook, R. J., 1981, Phys. Rev. A **23**, 1243.
Cook, R. J., 1988, Phys. Scr. **T21**, 49.
Cook, R. J., 1990, Prog. Opt. **28**, 361.
Cook, R. J., and H. J. Kimble, 1985, Phys. Rev. Lett. **54**, 1023.
Coppersmith, D., 1994, IBM Research Report No. RC19642.
Dagenais, M., and L. Mandel, 1978, Phys. Rev. A **18**, 2217.
Dalibard, J., Y. Castin, and K. Mølmer, 1992, Phys. Rev. Lett. **68**, 580.
Davies, E. B., 1969, Commun. Math. Phys. **15**, 277.
Davies, E. B., 1970, Commun. Math. Phys. **19**, 83.
Davies, E. B., 1971, Commun. Math. Phys. **22**, 51.
Davies, E. B., 1976, *Quantum Theory of Open Systems* (Academic, New York).
Dehmelt, H. G., 1975, Bull. Am. Phys. Soc. **20**, 60.
Dehmelt, H. G., 1982, IEEE Trans Instrum. Meas. **IM-31**, 83.
Dehmelt, H. G., 1987, Nature (London) **325**, 581.
Dicke, R. H., 1981, Am. J. Phys. **49**, 925.
Diòsi, L., 1988, J. Phys. A **21**, 2885.
Diòsi, L., 1989, Phys. Rev. A **40**, 1165.
Diòsi, L., N. Gisin, J. J. Halliwell, and I. C. Percival, 1995, Phys. Rev. Lett. **74**, 203.
Dum, R., A. S. Parkins, P. Zoller, and C. W. Gardiner, 1992, Phys. Rev. A **46**, 4382.
Dum, R., P. Zoller, and H. Ritsch, 1992, Phys. Rev. A **45**, 4879.
Ekert, A., and R. Josza, 1996, Rev. Mod. Phys. **68**, 733.
Ekert, A., and P. L. Knight, 1995, Am. J. Phys. **63**, 415.
Erber, T., P. Hammerling, G. Hockney, M. Porrati, and S. Putterman, 1989, Ann. Phys. (N.Y.) **190**, 254.
Erber, T., and S. Putterman, 1985, Nature (London) **318**, 41.
Finn, M. A., G. W. Greenlees, T. W. Hodapp, and D. A. Lewis, 1989, Phys. Rev. A **40**, 1704.
Finn, M. A., G. W. Greenlees, and D. A. Lewis, 1986, Opt. Commun. **60**, 149.
Frerichs, V., and A. Schenzle, 1991, Phys. Rev. A **44**, 1962.
Gardiner, C. W., 1992, *Quantum Noise* (Springer, Berlin).
Gardiner, C. W., 1993, Phys. Rev. Lett. **70**, 2269.
Gardiner, C. W., and A. S. Parkins, 1994, Phys. Rev. A **50**, 1792.
Gardiner, C. W., A. S. Parkins, and P. Zoller, 1992, Phys. Rev. A **46**, 4363.
Garraway, B. M., M. S. Kim, and P. L. Knight, 1995, Opt. Commun. **117**, 560.
Garraway, B. M., and P. L. Knight, 1994a, Phys. Rev. A **49**, 1266.
Garraway, B. M., and P. L. Knight, 1994b, Phys. Rev. A **50**, 2548.
Garraway, B. M., P. L. Knight, and J. Steinbach, 1995, Appl. Phys. B: Photophys. Laser Chem. **60**, 63.
Gell-Mann, M., and J. B. Hartle, 1990, in *Complexity, Entropy, and the Physics of Information*, Santa Fe Institute Studies in the Science of Complexity, v. VIII, edited by W. Zurek (Addison-Wesley, Reading, PA), p. 425.
Gell-Mann, M., and J. B. Hartle, 1993, Phys. Rev. D **47**, 3345.
Ghirardi, G. C., Ph. Pearle, and A. Rimini, 1990, Phys. Rev. A **42**, 78.
Ghirardi, G. C., A. Rimini, and T. Weber, 1986, Phys. Rev. D **34**, 470.
Gisin, N., 1984, Phys. Rev. Lett. **52**, 1657.
Gisin, N., 1989, Helv. Phys. Acta **62**, 363.
Gisin, N., 1993, J. Mod. Opt. **40**, 2313.
Gisin, N., P. L. Knight, I. C. Percival, R. C. Thompson, and D. C. Wilson, 1993, J. Mod. Opt. **40**, 1663.
Gisin, N., and I. C. Percival, 1992, J. Phys. A **25**, 5677.
Gisin, N., and I. C. Percival, 1993a, J. Phys. A **26**, 2233.
Gisin, N., and I. C. Percival, 1993b, J. Phys. A **26**, 2245.
Goetsch, P., and R. Graham, 1993, Ann. Phys. (N.Y.) **3**, 706.
Goetsch, P., and R. Graham, 1994, Phys. Rev. A **50**, 5242.
Goetsch, P., R. Graham, and F. Haake, 1995, Phys. Rev. A **51**, 136.

Granzow, C. M., 1996, Diploma thesis (University of Stuttgart).
Griffiths, R., 1984, J. Stat. Phys. **36**, 219.
Grochmalicki, J., and M. Lewenstein, 1989a, Phys. Rev. A **40**, 2517.
Grochmalicki, J., and M. Lewenstein, 1989b, Phys. Rev. A **40**, 2529.
Haake, F., 1973, in *Statistical Treatment of Open Systems by Generalized Master Equations*, Springer Tracts of Mod. Physics 66 (Springer, Berlin), p. 98.
Haroche, S., and J. M. Raimond, 1984, Adv. At. Mol. Phys. **20**, 347.
Hegerfeldt, G. C., 1993, Phys. Rev. A **47**, 449.
Hegerfeldt, G. C., and M. B. Plenio, 1992, Phys. Rev. A **46**, 373.
Hegerfeldt, G. C., and M. B. Plenio, 1993, Phys. Rev. A **47**, 2186.
Hegerfeldt, G. C., and M. B. Plenio, 1994, Quantum Opt. **6**, 15.
Hegerfeldt, G. C., and M. B. Plenio, 1995a, Z. Phys. B **96**, 533.
Hegerfeldt, G. C., and M. B. Plenio, 1995b, Phys. Rev. A **52**, 3333.
Hegerfeldt, G. C., and M. B. Plenio, 1996, Phys. Rev. A **53**, 1164.
Hegerfeldt, G. C., and D. Sondermann, 1996, Quantum Opt. **8**, 121.
Hegerfeldt, G. C., and T. S. Wilser, 1991, in *Proceedings of the II International Wigner Symposium*, edited by H. D. Doebner, W. Scherer, and F. Schroeck (World Scientific, Singapore), p. 104.
Hendriks, B. H. W., and G. Nienhuis, 1988, J. Mod. Opt. **35**, 1331.
Herkommer, A. M., H. J. Carmichael, and W. P. Schleich, 1996, Quantum Opt. **8**, 189.
Holland, M., and J. Cooper, 1996, private communication.
Holland, M., S. Marksteiner, P. Marte, and P. Zoller, 1996, Phys. Rev. Lett. **76**, 3683.
Horvath, G. Z. K., P. L. Knight, and R. C. Thompson, 1997, Contemp. Phys. **38**, 25.
Imamoglu, A., 1993, Phys. Rev. A **48**, 770.
Imamoglu, A., 1994, Phys. Rev. A **50**, 3650.
Itano, W. M., J. C. Bergquist, and D. J. Wineland, 1988, Phys. Rev. A **38**, 559.
Itano, W. M., D. J. Heinzen, J. J. Bollinger, and D. J. Wineland, 1990, Phys. Rev. A **41**, 2295.
Javanainen, J., 1986a, Phys. Rev. A **33**, 2121.
Javanainen, J., 1986b, Phys. Scr. **T12**, 67.
Javanainen, J., 1986c, J. Opt. Soc. Am. B **3**, 98.
Javanainen, J., 1992, Europhys. Lett. **17**, 407.
Jayarao, A. S., R. D'Souza, and S. V. Lawande, 1990, Phys. Rev. A **41**, 1533.
Kelley, P. L., and W. H. Kleiner, 1964, Phys. Rev. **136**, 316.
Kim, M. S., 1987, Ph.D. Thesis (Imperial College, University of London).
Kim, M. S., F. A. M. de Oliveira, and P. L. Knight, 1989, Opt. Commun. **70**, 473.
Kim, M. S., and P. L. Knight, 1987, Phys. Rev. A **36**, 5265.
Kim, M. S., P. L. Knight, and K. Wodkiewicz, 1987, Opt. Commun. **62**, 385.
Kimble, H. J., R. J. Cook, and A. L. Wells, 1986, Phys. Rev. A **34**, 3190.
Kimble, H. J., M. Dagenais, and L. Mandel, 1977, Phys. Rev. Lett. **39**, 691.
Knight, P. L., and B. M. Garraway, 1996, in *Quantum Dynamics of Simple Systems. Proceedings of the Forty Fourth Scottish Universities Summer School in Physics Stirling*, edited by G.-L. Oppo, S. M. Barnett, E. Riis, and M. Wilkinson (Institute of Physics, Bristol), p. 199.
Knight, P. L., R. Loudon, and D. T. Pegg, 1986, Nature (London) **323**, 608.
Knight, P. L., and P. W. Milonni, 1980, Phys. Rep. **66**, 21.
Knight, P. L., and D. T. Pegg, 1982, J. Phys. B **15**, 3211.
Kochan, P., and H. J. Carmichael, 1994, Phys. Rev. A **50**, 1700.
Köhler, T., 1996, Phys. Rev. A **54**, 4544.
Lawande, S. V., Q. V. Lawande, and B. N. Jagatap, 1989, Phys. Rev. A **40**, 3434.
Lawande, S. V., B. N. Jagatap, and Q. V. Lawande, 1989, Opt. Commun. **73**, 126.
Lawande, Q. V., B. N. Jagatap, and S. V. Lawande, 1990, Phys. Rev. A **42**, 4343.
Lax, M., 1963, Phys. Rev. **129**, 2342.
Lenstra, D., 1982, Phys. Rev. A **26**, 3369.
Lewenstein, M., and J. Javanainen, 1987, Phys. Rev. Lett. **59**, 775.
Lewenstein, M., and J. Javanainen, 1988, IEEE J. Quantum Electron. **24**, 1403.
Ligare, M., 1988, Phys. Rev. A **37**, 3293.
Lindblad, G., 1976, Commun. Math. Phys. **48**, 119.
Loudon, R., 1983, *The Quantum Theory of Light* (Oxford University, New York).
Loudon, R., and P. L. Knight, 1987, J. Mod. Opt. **34**, 1.
Lüders, G., 1951, Ann. Phys. (Leipzig) **8**, 323.
Mahler, G., and V. A. Weberruβ, 1995, *Quantum Networks: Dynamics of Open Nanostructures* (Springer, Berlin).
Mandel, L., 1979, Opt. Lett. **4**, 205.
Manka, A. S., H. M. Doss, L. M. Narducci, P. Ru, and G.-L. Oppo, 1993, Phys. Rev. A **47**, 1378.
Marte, P., R. Dum, R. Taieb, P. D. Lett, and P. Zoller, 1993, Phys. Rev. Lett. **71**, 1335.
Marte, P., R. Dum, R. Taieb, and P. Zoller, 1993, Phys. Rev. A **47**, 1378.
Meekhof, D. M., C. Monroe, B. E. King, W. M. Itano, and D. J. Wineland, 1996, Phys. Rev. Lett. **76**, 1796.
Milburn, G. J., 1991, Phys. Rev. A **44**, 5401.
Milonni, P. W., 1976, Phys. Rep. **25**, 1.
Misra, B., and E. C. G. Sudarshan, 1977, J. Math. Phys. **18**, 756.
Mollow, B. R., 1969, Phys. Rev. **188**, 1969.
Mollow, B. R., 1972a, Phys. Rev. A **5**, 1522.
Mollow, B. R., 1972b, Phys. Rev. A **5**, 2217.
Mollow, B. R., 1975, Phys. Rev. A **12**, 1919.
Mollow, B. R., 1981, Prog. Opt. **XIX**, 3.
Mølmer, K., 1994, in *Lectures Presented at the Trieste Winter School on Quantum Optics 1994* (International Centre for Theoretical Physics, Trieste).
Mølmer, K., and Y. Castin, 1996, Quantum Opt. **8**, 49.
Mølmer, K., Y. Castin, and J. Dalibard, 1993, J. Opt. Soc. Am. B **10**, 524.
Moya-Cessa, H., V. Bužek, M. S. Kim, and P. L. Knight, 1993, Phys. Rev. A **48**, 3900.
Mu, Y., 1994, Opt. Commun. **110**, 334.
Nagourney, W., J. Sandberg, and H. G. Dehmelt, 1986a, Phys. Rev. Lett. **56**, 2797.
Nagourney, W., J. Sandberg, and H. G. Dehmelt, 1986b, J. Opt. Soc. Am. B **3**, 252.
Nakajima, S., 1958, Prog. Theor. Phys. **20**, 948.

Narducci, L. M., G.-L. Oppo, and M. O. Scully, 1990, Opt. Commun. **75**, 111.
Narducci, L. M., M. O. Scully, G.-L. Oppo, P. Ru, and J. R. Tredicce, 1990, Phys. Rev. A **42**, 1630.
Narozhny, N. B., J. J. Sanchez-Mondragon, and J. H. Eberly, 1981, Phys. Rev. A **23**, 236.
Neuhauser, W., M. Hohenstatt, P. Toschek, and H. G. Dehmelt, 1980, Phys. Rev. A **22**, 1137.
Nienhuis, G., 1987, Phys. Rev. A **35**, 4639.
Omnès, R., 1988, J. Stat. Phys. **53**, 893.
Omnès, R., 1989, J. Stat. Phys. **57**, 359.
Omnès, R., 1994, *The Interpretation of Quantum Mechanics* (Princeton University, Princeton, NJ).
Paul, W., 1990, Rev. Mod. Phys. **62**, 531.
Paul, W., O. Osberghaus, and E. Fischer, 1958, *Ein Ionenkäfig* (Forschungsberichte des Wirtschafts- und Verkehrsministeriums, Nordrhein-Westfalen), p. 415.
Pearle, Ph., 1976, Phys. Rev. D **13**, 857.
Pegg, D. T., 1980, in *Laser Physics*, edited by J. D. Harvey and D. F. Walls (Academic, Sydney), p. 33.
Pegg, D. T., and P. L. Knight, 1988a, Phys. Rev. A **37**, 4303.
Pegg, D. T., and P. L. Knight, 1988b, J. Phys. D **21**, 128.
Pegg, D. T., R. Loudon, and P. L. Knight, 1986a, Nature (London) **323**, 608.
Pegg, D. T., R. Loudon, and P. L. Knight, 1986b, Phys. Rev. A **33**, 4085.
Percival, I. C., 1994a, J. Phys. A **27**, 1003.
Percival, I. C., 1994b, Proc. R. Soc. London, Ser. A **447**, 189.
Percival, I. C., 1995, Proc. R. Soc. London, Ser. A **451**, 503.
Percival, I. C., 1997, Phys. World **10**, 43.
Percival, I. C., and W. T. Strunz, 1997, Proc. R. Soc. London, Ser. A **453**, 431.
Piraux, B., R. Bhatt, and P. L. Knight, 1990, Phys. Rev. A **41**, 6296.
Plenio, M. B., 1994, Ph.D. thesis (University of Göttingen).
Plenio, M. B., 1996, J. Mod. Opt. **43**, 753.
Plenio, M. B., and P. L. Knight, 1996, Phys. Rev. A **53**, 2986.
Plenio, M. B., and P. L. Knight, 1997, Proc. R. Soc. London., Ser. A **453**, 2017.
Plenio, M. B., P. L. Knight, and R. C. Thompson, 1996, Opt. Commun. **123**, 278.
Porrati, M., and S. Putterman, 1987, Phys. Rev. A **36**, 929.
Porrati, M., and S. Putterman, 1989, Phys. Rev. A **39**, 3010.
Power, W. L., 1995a, Ph.D. thesis (Imperial College, University of London).
Power, W. L., 1995b, J. Mod. Opt. **42**, 913.
Power, W. L., and P. L. Knight, 1996, Phys. Rev. A **53**, 1052.
Reibold, R., 1992, Physica A **190**, 413.
Reibold, R., 1993, J. Phys. A **26**, 179.
Rempe, G., and H. Walther, 1987, Phys. Rev. Lett. **58**, 353.
Reynaud, S., J. Dalibard, and C. Cohen-Tannoudji, 1988, IEEE J. Quantum Electron. **24**, 1395.
Rigo, M., and N. Gisin, 1996, Quantum Opt. **8**, 255.
Salama, Y., and N. Gisin, 1993, Phys. Lett. A **181**, 269.
Saleh, B., 1978, *Photoelectron Statistics*, Springer Series in Optical Sciences Vol. 6 (Springer, Berlin).
Sauter, T., R. Blatt, W. Neuhauser, and P. E. Toschek, 1986, Opt. Commun. **60**, 287.
Sauter, T., W. Neuhauser, R. Blatt, and P. E. Toschek, 1986a, Phys. Rev. Lett. **57**, 1696.
Sauter, T., W. Neuhauser, R. Blatt, and P. E. Toschek, 1986b, J. Opt. Soc. Am. B **3**, 252.
Schack, R., T. A. Brun, and I. C. Percival, 1995, J. Phys. A **28**, 5401.
Schack, R., T. A. Brun, and I. C. Percival, 1996, Phys. Rev. A **53**, 2694.
Schenzle, A., and R. G. Brewer, 1986, Phys. Rev. A **34**, 3127.
Schenzle, A., R. G. De Voe, andR. G. Brewer, 1986, Phys. Rev. A **33**, 2127.
Schrödinger, E., Br. J. Philos. Sci. III, 1952, August.
Schubert, M., I. Siemers, R. Blatt, W. Neuhauser, and P. E. Toschek, 1992, Phys. Rev. Lett. **68**, 3016.
Shor, P. W., 1994, in *Proceedings of the 35th Annual Symposium on the Foundations of Computer Science, Los Alamitos, California*, edited by S. Goldwasser (IEEE Computer Society, New York), p. 124.
Shor, P. W., 1996, Phys. Rev. A **52**, R2493.
Shore, B. W., and P. L. Knight, 1993, J. Mod. Opt. **40**, 1195.
Sondermann, D., 1995a, J. Mod. Opt. **42**, 1659.
Sondermann, D., 1995b, in *Nonlinear, Deformed and Irreversible Quantum Systems*, edited by H. D. Doebner, V. K. Dobrev, and P. Nattermann (World Scientific, Singapore), p. 273.
Spiller, T. P., and J. F. Ralph, 1994, Phys. Lett. A **194**, 235.
Srinivas, M. D., 1996, Pramana, J. Phys. **47**, 1.
Srinivas, M. D., and E. B. Davies, 1981, Opt. Acta **28**, 981.
Srinivas, M. D., and E. B. Davies, 1982, Opt. Acta **29**, 235.
Steane, A. M., 1996, Phys. Rev. Lett. **77**, 793.
Steinbach, J., B. M. Garraway, and P. L. Knight, 1995, Phys. Rev. A **51**, 3302.
Stratonovitch, R. L., 1963, *Topics in the Theory of Random Noise* (Gordon and Breach, New York), Vol. 1.
Strunz, W. T., 1996a, Phys. Lett. **224**, 25.
Strunz, W. T., 1996b, Phys. Rev. A **54**, 2664.
Swain, S., 1994, Phys. Rev. Lett. **73**, 1493.
Teich, W. G., G. Anders, and G. Mahler, 1989, Phys. Rev. Lett. **62**, 1.
Teich, W. G., and G. Mahler, 1992, Phys. Rev. A **45**, 3300.
Thompson, R. C., 1996, private communication.
Tian, L., and H. J. Carmichael, 1992, Phys. Rev. A **46**, 6801.
Vogel, W., and D.-G. Welsch, 1994, *Lectures on Quantum Optics* (Akademie, Berlin).
von Neumann, J., 1955, *Mathematical Foundations of Quantum Mechanics* (Princeton University, Princeton, NJ).
Weisskopf, V., and E. Wigner, 1930, Z. Phys. **63**, 54.
Wilser, T. S., 1991, Ph.D. thesis (University of Göttingen).
Wiseman, H. M., 1996, Quantum Opt. **8**, 205.
Wiseman, H. M., and G. J. Milburn, 1993a, Phys. Rev. A **47**, 642.
Wiseman, H. M., and G. J. Milburn, 1993b, Phys. Rev. A **47**, 1652.
Wiseman, H. M., and G. J. Milburn, 1994, Phys. Rev. A **49**, 1350.
Yamada, K., and P. R. Berman, 1990, Phys. Rev. A **41**, 453.
Yu, T., 1996, Imperial College preprint TP/95-96/44, gr-qc/9605071.
Zoller, P., and C. W. Gardiner, 1995, *Lecture Notes of the Les Houches Summer School on Quantum Fluctuations* (Elsevier, N.Y.), p. 79.
Zoller, P., M. Marte, and D. F. Walls, 1987, Phys. Rev. A **35**, 198.
Zwanzig, R., 1960, Lect. Theor. Phys. (Boulder) **3**, 106.